europhysicsnews

34/6
2003
November/December 2003
Institutional subscription price:
91 euros per year

MAGNETISM SPECIAL ISSUE

Biomedical aspects of magnetic nanoparticles
Imaging of micro- and nanomagnetic structures
The extraordinary properties of magnetic oxides
The new era of spintronics
Magnetoresistive biochips

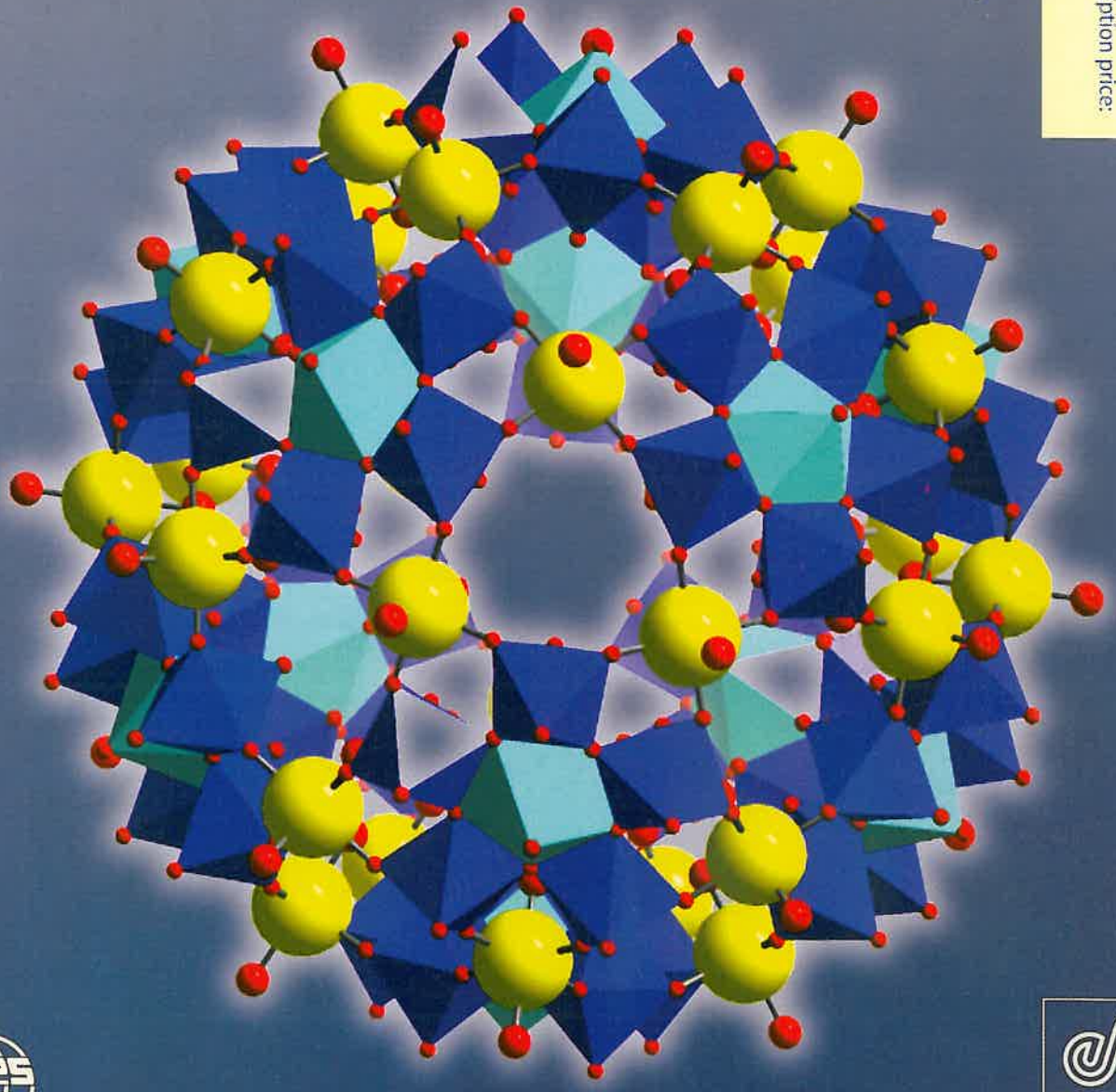

features

European Physical Society

EDP SCIENCES

New Books from Springer

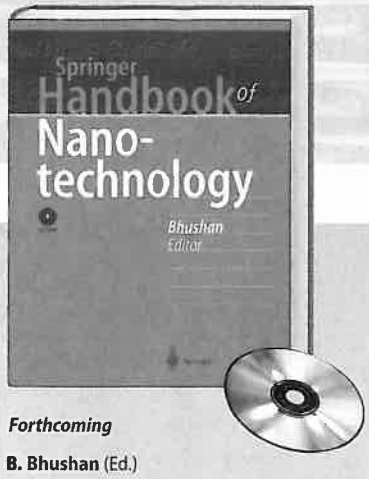

Forthcoming

B. Bhushan (Ed.)

Springer Handbook of Nanotechnology

The "Springer Handbook of Nanotechnology" integrates knowledge from Nanofabrication, Nanomechanics, Materials Science, and Reliability Engineering in just one comprehensive volume. Besides the presentation of Nanostructures, Micro/Nanofabrication, and Micro/Nanodevices, special emphases are on Scanning Probe Microscopy, Nanotribology and Nanomechanics, Molecularly-Thick Films, industrial applications and Microdevice reliability, and on social and ethical implications. The book is organized by an experienced editor with a universal knowledge and written by an international team of distinguished experts (e.g. Nobel prize winner Gerd K. Binnig).

Benefits

- Covers basic concepts, theory, materials, properties, and fabrication.
- Contains over 900 illustrations and numerous comprehensive materials data tables.
- Features exhaustive references to approved data.
- A detailed index and fully searchable CD-ROM guarantee quick acces to data.

2004. Approx. 1300 p., 971 two-color illus. with CD-ROM
Hardcover **€ 249**; sFr 402.50; £ 191.50
ISBN 3-540-01218-4

Prepublication price, valid until 01.03.2004: € 199.95; sFr 323.50; £ 154

Save Money - Order Now!

R. K. Zeytounian TOC

Theory and Applications of Viscous Fluid Flows

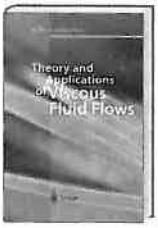

The purpose of this book is to close the gap between standard undergraduate texts on fluid mechanics and monographical publications devoted to specific aspects of viscous fluid flows. This volume complements, but is independent of, Zeytounian`s **Theory and Applications of Nonviscous Fluid Flows.**

2004. XVI, 488 p. 80 illus. Hardcover
€ 89.95; sFr 149.50; £ 69 ISBN 3-540-44013-5

T. K. Bose TOC

High Temperature Gas Dynamics

An Introduction for Physicists and Engineers

A class-tested primer for students, scientists and engineers who would like to have a basic understanding of the physics and the behaviour of high-temperature gases.

2004. XV, 359p. 81 illus Hardcover **€ 69.95**; sFr 116.50; £ 54
ISBN 3-540-40885-1

Y. Hamakawa (Ed.) TOC

Thin-Film Solar Cells

Next Generation Photovoltaics and Its Applications

Covers a wide range of scientific and technological aspects of thin film semiconductors - deposition technologies, growth mechanisms and the basic properties of amorphous and nano-crystalline silicon - as well as the optimum design theory and device physics of high-efficiency solar cells, especially of single-junction and multi-junction solar cells.

2004. XV, 244 pp. 210 figs. (Springer Series in Photonics, Vol. 13) Hardcover **€ 99.95**; sFr 166; £ 77
ISBN 3-540-43945-5

3rd Edition

M. H. Niemz TOC

Laser-Tissue Interactions

Fundamentals and Applications

From the reviews

"... the author has provided a comprehensive background with examples describing the basics of laser-tissue interaction ... an extremely useful reference companion."

Lasers in Surgery and Medicine

3rd enlarged ed. 2004. XVI, 308 p. 175 illus., 33 tabs., 40 Problems and Solutions. (Biological and Medical Physics, Biomedical Engineering) Hardcover
€ 79.95; sFr 133; £ 61.50 ISBN 3-540-40553-4

H. Zappe TOC

Laser Diode Microsystems

Provides the reader with the basic knowledge and understanding required for using semiconductor laser diodes in optical microsystems and micro-optical electromechanic systems.

2004. XXI, 334 p. 167 illus. (Microtechnology and MEMS) Hardcover **€ 79.95**; sFr 133; £ 61.50 ISBN 3-540-40454-6

T. Michely; J. Krug

Islands, Mounds, and Atoms

Patterns and Processes in Crystal Growth Far from Equilibrium

Topics include surface diffusion, nucleation theory, island shapes, mound formation and coarsening, and layer-by-layer growth.

2004. XVIII, 313 p. 134 illus. Including a Foldout Color Plate. (Springer Series in Surface Sciences, Vol. 42) Hardcover **€ 99.95**; sFr 166; £ 77 ISBN 3-540-40728-6

M. Ohtsu; K. Kobayashi

Optical Near Fields

Introduction to Classical and Quantum Theories of Electromagnetic Phenomena at the Nanoscale

The book presents physically intuitive concepts and theories for students, engineers, and scientists engaged in research in nanophotonics and atom photonics.

2004. XI, 205 p. 108 illus. 20 Problems and Solutions (Advanced Texts in Physics) Hardcover **€ 59.95**; sFr 99.50; £ 46
ISBN 3-540-40483-X

TOC

Complete Table of Contents (PDF) available online! Simply visit the Springer website and enter the ISBN number into the search facility. Then click on the title's catalogue entry and go to the "Table of Contents".

springeronline.com

Please order from
Springer · Customer Service
Haberstr. 7
69126 Heidelberg, Germany
Tel.: +49 (0) 6221 - 345 - 0
Fax: +49 (0) 6221 - 345 - 4229
e-mail: orders@springer.de
or through your bookseller

Springer

All Euro and GBP prices are net-prices subject to local VAT, e.g. in Germany 7% VAT for books and 16% VAT for electronic products. Prices and other details are subject to change without notice. d&p · 010403x

europhysicsnews

Volume 34 Number 6
November/December 2003

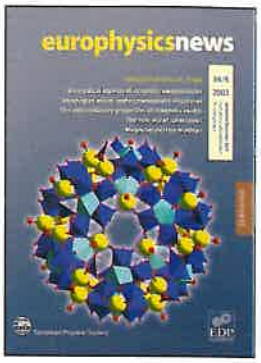

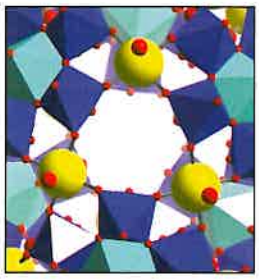

PAGE 214

Molecular magnetism

PAGE 232

Magnetism in nanocrystals

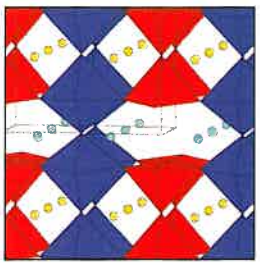

PAGE 238

Extraordinary properties of magnetic oxides

FEATURES

209 **Special issue overview**
M.R. Ibarra

210 **Biomedical aspects of magnetic nanoparticles**
Adam Curtis

211 **Magnetostriction: fundamental principles and novel magnetostrictive materials**
A.del Moral

214 **Molecular magnetism: mesoscopic and nanoscopic structures**
D. Gatteschi

216 **Ferromagnetic semiconductor heterostructures**
Tomasz Dietl

219 **Magnetic materials: from the search of new phases to nanoscale engineering**
D. Givord

222 **Imaging of micro- and nanomagnetic structures**
C. König, F. Kiendl, U. Rüdiger, and G. Güntherodt

224 **Magnetoresistive biochips**
P.P. Freitas, H. Ferreira, D. Graham, L. Clarke, M. Amaral, V. Martins, L. Fonseca, J.S. Cabral

227 **The new era of spintronics**
Albert Fert, Jean-Marie George, Henri Jaffrès, Richard Mattana, and Pierre Seneor

232 **Magnetism in nanocrystals**
A.Hernando

235 **Magnetoresistance and magnetostriction in magnetic contacts**
N. García

238 **The extraordinary properties of magnetic oxides**
B. Raveau and A. Maignan

240 **Optical studies of spin injection and detection at ferromagnet / semiconductor interfaces**
J.A.C. Bland, S.J. Steinmuller, A. Hirohata, W.S. Cho, Y.B. Xu, C.M. Guertler, G. Wastlbauer, A. Ionescu, T. Taniyama and T. Trypiniotis

243 **Strong electron correlations in magnetic systems**
F.Steglich

246 **Magnetoelectrochemistry**
J.M.D. Coey

europhysicsnews

Europhysics News is the magazine of the European physics community. It is owned by the European Physical Society and produced in cooperation with EDP Sciences. The staff of EDP Sciences are involved in the production of the magazine and are not responsible for editorial content. Most contributors to Europhysics News are volunteers and their work is greatly appreciated by the Editor and the Editorial Advisory Board.
Europhysics News is also available online at: **www.europhysicsnews.com**

34/6
2003
November/December 2003
Institutional subscription price:
91 euros per year

Editor David Lee EMAIL: d.lee@uha.fr
Science Editor George Morrison EMAIL: g.c.morrison@bham.ac.uk
Designer Paul Stearn EMAIL: p.stearn@uha.fr
Directeur de la publication Jean-Marc Quilbé, EDP Sciences

Schedule
Six issues will be published in 2003. The magazine is distributed in the second week of January, March, May, July, September, November. A directory issue with listings of all EPS officials is published once a year.

Advertising Manager Susan Mackie
Address 250, rue Saint-Jacques, 75005 Paris, France
Tel +33 155 42 80 51
Fax +33 146 33 21 06
Email mackie@edpsciences.org

Production Manager Agnes Henri
Address EDP Sciences, 17 avenue du Hoggar, BP 112, PA de Courtabœuf, F-91944 Les Ulis Cedex A, France
Tel +33 169 18 75 75
Fax +33 169 28 84 91

Printer Rotofrance, Lognes, France

Dépôt légal: novembre 2003

Subscriptions
Individual Ordinary Members of the European Physical Society receive Europhysics News free of charge. Members of EPS National Member Societies receive Europhysics News through their society, except members of the Institute of Physics in the United Kingdom and the German Physical Society who receive a bimonthly bulletin. The following are subscription prices available through EDP Sciences. **Institutions** 91 euros (VAT included, European Union countries); 91 euros (the rest of the world). **Individuals** 58 euros (VAT included, European Union countries); 58 euros (the rest of the world). Contact subscribers@edpsciences.com or visit www.epdsciences.com

ISSN 0531-7479
ISSN 1432-1092 (electronic edition)

Magnetism: Special issue overview

M.R. Ibarra
Guest Editor and Chairman of the Magnetism section of the Condensed Matter Division of EPS

Since the early days of our civilization, magnetic phenomena were observed due to the existence of natural magnets, the "loadstone". The use of magnetic needles for compasses made navigation one of the most profitable areas of application. An aura of mystery and magic has always surrounded magnetic phenomena. Sir W. Gilbert at the beginning of the XVII century wrote the first scientific compendium "De Magnete, Magneticisque Corporibus, et de Magno magnete tellure; Physiologia nova, plurimis & argumentiis, & experimentis demonstrata. *Londra, Pietro Short, 1600*"

Since then and with relevant historic milestones such as the experimental genius of Michael Faraday and the theoretical compendium of J. Clerk Maxwell, magnetism nowadays is one of the scientific pillars of human knowledge. The theoretical advances and the strong involvement of magnetism in all branches of technological development make this discipline one of the most relevant areas of current research. The present monograph is a consequence of the large activity in this exciting field. The capabilities for materials fabrication with control at the nanoscopic level and the development of new instruments are the basis of an everyday emerging and interdisciplinary magnetism.

Sir William Gilbert.

In this issue, we have tried to cover the most exciting topics in magnetism with articles by relevant specialists in this field.

New advances in the application of magnetic properties in life sciences are of great interest due to the strong social implications related to health problems. The impact of magnetism in diagnosis and therapy constitutes a rapidly developing field, summarized in the A. Curtis and P. Freitas contributions. Other interdisciplinary examples are the contributions from J.M.D. Coey and D. Gatteschi in which the close connection of Magnetism with Chemistry has opened new research fields such as the electrochemical growth of new materials under the influence of an applied magnetic field and research on mesoscopic magnetism based on the spectacular development of molecular chemistry techniques. With regard to the development of new experimental techniques, the emergence imaging possibilities based on the use of magnetic force microscopy opens a new area that will allow a better understanding of magnetism at a micro- and nanoscopic level. The G. Guntherodt and colleagues contribution reports the state of the art in this field. D. Givord describes the wide range of application of magnetic materials in which the control of the change in the coercive field by more than six orders of magnitude allows the design of materials with adequate magnetic properties going from the very soft to the extremely hard. A. Hernando reviews magnetism in nanocrystalline materials showing relevant examples of how nanoscale influences the magnetic properties.

> ... magnetism nowadays is one of the scientific pillars of human knowledge.

Several contributions are devoted to one of the currently most expanding areas of magnetism: "spintronics". This field, lying at the interface between Magnetism and Electronics is of considerable interest given the large demand for novel electronic devices, in which a magnetic field acting on the spin of the electrons can control the electrical current. The description of several phenomena based on the control of the spin in heterostructures such as magnetoresistive magnetic multilayers, magnetic tunnel junctions, and hybrid ferromagnetic-semiconductor are nicely summarized in the A. Fert contribution. The spin injection phenomena at these interfaces are described in the J.A.C. Bland contribution showing a highly efficient spin transport from a semiconductor to a ferromagnet at room temperature, whose origin could be spin-polarized Schottky barriers. Within the former context the deep knowledge of magnetic interactions in diluted magnetic semiconductors supports the existence of ferromagnetism well above room temperature, a subject that is summarized in the T. Dietl contribution. Half-metal ferromagnets are of great interest within the context of spin-polarized transport and many magnetic oxides fall within this category. Among them, an exciting renewal of interest in manganites has been opened up with the discovery of colossal magnetoresistance; B. Raveau and A. Maignan report on these extraordinary properties that are found and expected in magnetic oxides. Also related to possible applications of magnetoresistance in electronic devices, N. Garcia has found huge ballistic magnetoresistance at nanocontacts; this discovery is proposed as the basis for extremely sensitive sensors needed for reading heads in the compacted new Terabit/inch^2 technology. Magnetostriction effects observed by means of atomic force microscopy are also reported; A. del Moral summarizes the effect and the new theoretical aspects and applications based on magnetostriction phenomena. Finally, F. Steglich reports on the strong electronic correlations and describes how they are at the origin of the formation of extremely heavy quasiparticles composed of a local spin part and delocalized charge-carrier contributions. They may form Cooper pairs that are an essential ingredient to explain the coexistence of magnetism and superconductivity.

These selected contributions offer a broad description of relevant aspects of magnetism in the scientific and technological development of today and demonstrate that this old discipline constitutes the background for technological innovation at the beginning of this new century.

Biomedical aspects of magnetic nanoparticles

Adam Curtis
Centre for Cell Engineering, University of Glasgow, UK

Though all the components of the body are either dia-, para, superpara- or ferromagnetic, the magnetic fields required which are likely to produce obvious effects on the body are very large. Even red blood cells with micrograms each of the iron protein haemoglobin are relatively unreactive to large fields or steep field gradients. However, there is sufficient iron present for MRI to be possible without adding iron-rich or other contrast enhancing reagents. Indeed many cell types contain magnetite or other iron oxide nanoparticles—it is not clear whether these are generated by some standard biochemical process or are adventitious particles acquired from the environment.

The other natural iron-containing compounds in the body are haemosiderin, ferritin, transferrin and the cytochromes. The question of whether there are hazards or effects from magnetic fields of the magnitudes normally encountered in the environment even in the 'built' environment acting on these molecules is unlikely though unresolved. But the electromagnetic fields produced by mobile phones may perhaps be large enough to have pathological effects (see Cranfield *et al.* 2003 for a suggestion as to mechanism).

However the most likely exposures to large fields or field gradients arises from therapy or diagnosis. MRI produces images of both hard and soft organs and this is useful in diagnosis and in following the course of therapy. MRI contrast reagents are often used and there are a number of potential compounds for infusion or injection. Basically there are three ways in which a contrast reagent may act. It may not enter or attach to cells and simply act as an indicator of fluid-filled space eg the knee capsule. It may attach to the outside of cells or lastly it may be taken into the cells. Closely related to these biological differences are the routes by which the agent reaches the target area. A wider and wider range of effective contrast agents continue to be developed and perhaps noteworthy amongst these are dendrimer based agents to help image the lymph system (Kobayashi *et al.* 2003), putrescine-Gd-amyloid beta peptides for Alzheimer plaque detection (Poduslo *et al.* 2003).

There are advantages in using strongly magnetic nanoparticle contrast reagents, at least in theory, because there is a possibility that the particles can be localised in the desired region by applying local magnetic field gradients. There is also the possibility of producing localised hyperthermia when an organ loaded with nanoparticles is exposed to electromagnetic radiation. There are, however, potential if not real hazards with the use of superparamagnetic nanoparticles which are discussed below.

The localizability of the particles by applying external small fields is of apparent value in other types of therapy, for instance drug delivery or hyperthermia. It has been usual to suppose that the route or delivery would be by injection either through a vascular route or by localised injection into a tissue. After injection the particles would either remain un-attached to cells and drift around the body fluids. If attachment was reversible particles might move from cell to cell. The next phase would be the endocytosis of the particles into the cells. If the cells remain alive the particles are very unlikely to re-enter the extracellular space. The final localisation of the particles would be intracellular in many cases. Though it is clear from in vitro and some in vivo experiments that cells can survive the presence of such particles in moderate loadings for moderate periods of time, little is known about this. However, data from 'epidemological' sources suggests that carbon nanoparticles particles in the form of soot may present a risk at high exposures. On the otherhand 'natural' garden fires produce carbon nanotubes. Post-mortem samples should be taken from the lungs of people to discover if there is nanoparticle loading in the cells and if so whether it is associated with disease. Magnetite or maghemite particles may present an additional risk because the pH in the endo-lysosomes (see Fig 1a) is low. This final destination is so acidic that ferric ions may be formed which will damage many biochemical processes. Silica coated nanoparticles may be resistant to this effect.

Drug delivery is another perceived use of superparamagnetic particles. The drug would be attached to a surface coating on the particles such as dextran, PVA, polyglycols etc by fairly standard derivatisation chemistry. Again the application of external magnetic fields would be used to 'capture' the particles in the desired site. Besides the localizability of the particles the immobilisation of a signal molecule on the particles may protect it to an extent from degradation and the long term binding to a receptor may lead to that receptor being activated for long periods. Thus use of nanoparticles may prove to be a very efficient method of delivering a drug to a cell. There are two possible events, the one usually reported is the endocytosis of the particles after preliminary capture at the surface of the cell. The other, discovered only recently is that if certain coating proteins are attached to the particle endocytosis is prevented. This requires that the proteins be bound by surface receptors. This is not in itself a disadvantage in many situations as a very large number of drug receptors are located at the cell surface and since one of them can be chosen to bind the particle to a surface receptor irreversibly and another can be attached to the first to be the active drug which will attach to a nearby second receptor. The advantage of this system is that endocytosis does not occur (see Fig 1b) and there is at least the possibility that use of a competing soluble ligand may allow removal of the signal.

So in terms of drug delivery magnetic nanoparticles offer the possibility of use of external magnetic fields to obtain better localisation than could be achieved with non-magnetic particles. But

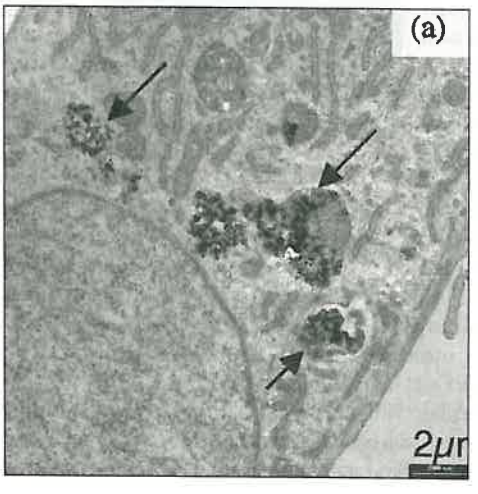

Fig. 1a: Transmission electron micrograph section (TEM) of a cell (h-tert human fibroblast) that has endocytosed uncoated magnetite nanoparticles, Note their location in the phagolyzosome, arrows indicate phagolysosomes.

since magnetic nanoparticles are less easily destroyed or inactivated by cells than many non-magentic ones there is the disadvantage that persistent particles may cause later cell damage and death. The same considerations apply to situations where magnetic nanoparticles are being used for generating hyperthermia by the application of external fields.

Cartmell *et al.* (2003) have suggested that mechanical stimulation could be applied to cells by using an external magnetic field to apply a twisting motion to the particles. Since mechanical stimulation is effective in activating cells this may be a future area for therapeutic developments.

One interesting if rather worrying possibility is that exposure of cells to nanofeatures or nanoparticles can cause large, if perhaps only temporary, changes in gene expression. This would not necessarily be linked solely to the use of magnetic nanoparticles because the work of Dalby *et al.* (2003) shows that nanofeatures on polymer surfaces can cause change in gene expression.

Since excess particles may well be adsorbed onto the surfaces of cells and intercellular material it is appropriate to consider how these adsorbed particles might affect cell behaviour. This has hardly been examined but some recent work (Berry and Curtis 2003) suggests that they may act much as nanofeatured surfaces do.

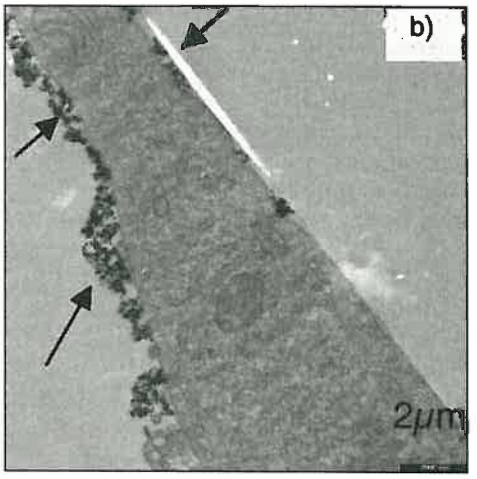

◀ **Fig. 1b:** TEM of a cell (h-tert human fibroblast) exposed to lactoferrin labelled nanoparticles after 24 hours. The particles are on the cell surface or close outside it) see arrows) and none have been endocytosed. Claims have been made in the literature that transferrin-labelled (a related protein) particles are endocytosed but the evidence for this is often based on light microscopy which does not have sufficient resolution to locate the particles precisely. Arrows mark cell surface accumulations.
Figs 1a and 1b courtesy of Dr A.K.Gupta, University of Glasgow.

References

Berry, C and Curtis A. (2003) Applications of Magnetic Nanoparticles in Biomedicine

Journal of Physics D:Applied Physics

Cartmell, S.H. *et al.* (2003) Development of magnetic particle techniques for long term culture of bone cells with intermittent mechanical stimulation. IEEE Transactions in Nanobioscience 1.92-97

Cranfield,C *et al.* (in press) IEEE Transactions in Nanobioscience

Dalby, M.J., *et al.*(2003). Interaction of human and tissue cell types with 95nm high nanotopography. IEEE Transactions in Nanobioscience 1:18-23

Kobayashi, H., *et al.* (2003). Micro-magnetic resonance lymphangiography in mice using a novel dendrimer-based magnetic resonance imaging contrast agent. Cancer Research 63(2): 271-276

Poduslo, J.F. *et al.* (2002). Molecular targeting of Alzheimer's amyloid plaques for contrast-enhanced magnetic resonance imaging Neurobiology of Disease 11, 315-329

The J. Magnetism and Magnetic Materials Volume 194, Issue 1-3, April 1999 published about 40 papers relevant to this area. A title list can be found at http://www.infomag.ru:8082/dbase/J087E/010503-101.txt

Magnetostriction: fundamental principles and novel magnetostrictive materials

A.del Moral
Departamento de Magnetismo, Dpto. Física de Materia Condensada & ICMA, Universidad de Zaragoza & CSIC, 50009 Zaragoza, Spain

Magnetostriction and magnetoelastic coupling

When any magnetic solid acquires a magnetization, $\vec{M}$ under the application of a magnetic field, $\vec{H}$ at the same time its crystalline (or amorphous) lattice is deformed, a phenomenon called *magnetostriction* (MS from hereinafter). Therefore this is a general effect suffered by all solid matter, once it becomes magnetized. It therefore appears for any kind of magnetic materials: diamagnetic, paramagnetic, ferromagnetic, anti-ferromagnetic, ferrimagnetic, superconductors, etc. It does not matter if the solid is a metal or an insulator, what only matters is if the atoms either acquire an induced magnetic moment or they have a permanent one. By Hookes's law the deformation suffered is proportional to the material size, say *l*, and therefore it is convenient to express the deformation by the relative variation $\lambda = \Delta l/l$, called the *linear* MS. In a crystal λ is *doubly anisotropic*: it depends on the crystallographic direction of measurement and on the direction along which the magnetization, $\vec{M}$ is oriented by the applied magnetic field, $\vec{H}$. Because MS depends on the crystalline directions of λ and $\vec{M}$ ($\vec{\beta}$ and $\vec{\alpha}$, respectively) we have to specify MS as $\lambda(\vec{\alpha}, \vec{\beta})$ (Fig.1). But also in a poly-crystalline material, formed by small crystallites more or less randomly distributed, the MS measured along $\vec{H}$, called the parallel MS, $\lambda_{\parallel}$ is quite different from that measured along the perpendicular direction, termed the perpendicular MS, $\lambda_{\perp}$. It can happen that $\lambda_{\perp} \cong -\lambda_{\parallel}/2$, but usually this is not the case and then the volume of the solid changes by the amount $\Delta V / V = \lambda_{\parallel} + 2\lambda_{\perp}$, called the *volume* MS. On the other hand, the shape (or form of the unit cell) of the material is modified if $\lambda_{\parallel} \neq \lambda_{\perp}$, and a measure of this effect is the difference $\lambda_t = \lambda_{\parallel} - \lambda_{\perp}$, called the *shape* MS. Both MS's appear in crystalline, polycrystalline and amorphous solids.

The key questions are: why is this phenomenon so general, and what is the physical mechanism of MS? We know that atoms possess two main sources of magnetic moment: the orbital electronic motion around the nucleus, which gives rise to the *orbital* angular momentum, $\vec{L}$ and the spin, $\vec{S}$. Classically the orbital current produces a magnetic field, $\vec{B}_L$ where the spin magnetic moment, $\vec{m}_S = -\vec{s}\mu_B$ has an energy $-\vec{m}_S \cdot \vec{B}_L$. This is a relativistic

effect, and because $\vec{B}_L \sim \vec{L}$, the energy becomes $E_{SO} = \xi \vec{L} \cdot \vec{S}$, which links the spins to the orbits, e.g. in a ferromagnet. This interaction is called the *spin-orbit coupling*, and is the first ingredient of MS. By it when $\vec{S}$ (or $\vec{M}$) is rotated by the torque $\vec{\Gamma} = \vec{m}_s \times \vec{B}$, $\vec{L}$ is dragged on. In a ferromagnet this is very important because the spins become ordered below the Curie temperature. But there is another equally important ingredient, the interaction which couples the orbit to the lattice, if we want the lattice to deform when their atoms are magnetized.

Let us consider a ferromagnet (FM) or antiferromagnet (AF) in order to fix ideas. For transition metals (TM), notably Fe, Co, Ni and Mn, or their ions (in FM insulators) and for rare earth (RE) metals and insulators, their respective atomic 3d and 4f shells are incompletely filled, and therefore they possess spin and orbital momenta, giving rise to a magnetic moment, $m = m_L + m_S$. In magnetic solids there exists a strongly *inhomogeneous* electric field, called the *crystal electric field* (CEF), whose gradients interact with the ion magnetic electrons, giving rise to a splitting of the ion energy levels while still keeping some degeneracy (CEF energy levels). The splitting is purely dictated by symmetry: e.g. in cubic symmetry the levels are e_g (x2) and t_{2g} (x3). This remaining degeneracy is quite important for MS, because otherwise $\langle L \rangle$ is zero. In the solid, 3d and 4f electrons have orbital wave-functions, φ_{orb}, rather different from those of the free atoms (or ions), as a consequence of the CEF potential which admixes the free atom states $|M_L\rangle$ (M_L is the quantized projection of $\vec{L}$ along some crystal symmetry axis, OZ). So the electronic charge distribution (i.e. $|\varphi_{orb}|^2$) is determined by the symmetry entourage of the ionic site and is very anisotropic. Most importantly is that φ_{orb} changes when $\vec{L}$ rotates, with the result that the CEF energy changes, giving rise to the *magnetocrystalline anisotropy* (MCA), by which the crystal energy changes with the $\vec{M}$ direction. 3d shells are little screened from the CEF ("medium" to "strong" CEF) whereas 4f ones are much more screened ("weak" CEF). For the former, the ground state φ_{orb} is formed by *almost* pure 50% admixtures of $|\pm M_L\rangle$ states and therefore the quantum mechanics expectation value $\langle L_Z \rangle$ is rather weak (an effect called *quenching*). Contrarily for the RE metals quenching is very weak, i.e., $\langle L_Z \rangle$ is weakly reduced. FM or AF order in solids is the result of the exchange interaction between electrons, with energy $E_{ex} = -2J\, S_i \cdot S_j$, which is clearly isotropic. Very important for MS is the fact that J (exchange integral) depends on the atom distance. This interaction gives rise to the spontaneous magnetization, $\vec{M}_S$. Therefore when $\vec{M}_S$ (*or* $\vec{S}$) is *rotated* within the crystal by the $\vec{\Gamma}$ torque, the ionic charge cloud is dragged on and also distorted, with the consequent distortion of the ion entourage: so *the crystal is deformed*. This deformation is the so-called single-ion *CEF magnetostriction* and it requires the *rotation* of $\vec{M}_S$ in some way: either by rigid vector rotation or by domain wall displacements that entrain $\vec{M}_S$ rotation. This happens for 70.5°, 90°, and 109.5° domain walls (DW) in cubic crystals (180° DW displacement can not produce MS, which is the case for uniaxial crystals when they are magnetized along the easy magenetization direction).

In elasticity theory we know that the deformation, or more properly the *strain*, $\in_{ij}$ (a tensor), is the medium response to an external stress, σ_{ij}, the relationship being governed by Hooke's linear law, $\sigma_{ij} = c_{ijkl} \in_{kl}$ (repeated indices summation assumed), c_{ijkl} being the elastic constants. Therefore we can equally think that an *internal magnetoelastic* (MEL) *stress*, B_{ij}, develops under $\vec{L}$ rotation and gives rise to the MS and, in accordance with elasticity theory, the MEL energy gain is given by $F_{ms} = -B_{ij} \in_{ij}$. When the solid deforms under the MEL stress, there is a cost of elastic energy, $E_{el} = (1/2) c_{ijkl} \in_{ik} \in_{jl}$, and an equilibrium MS, for short

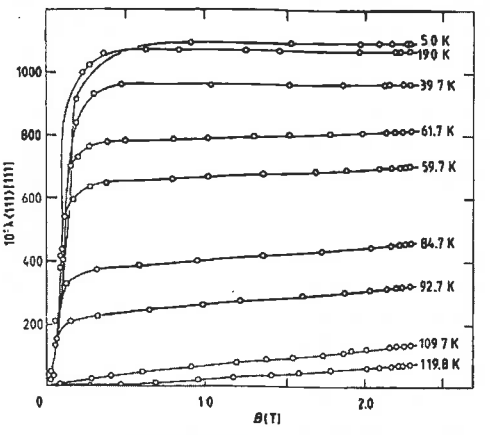

▲ Fig. 1: λ([111], (111)) MS isotherms vs. applied magnetic field for the cubic intermetallic ferromagnet $TbAl_2$ (T_c =115K) [1].

$\lambda = B / c$, is attained when the full energy is minimized. The B_{ij} are also called *MEL constants* and the magnetic moment, m, coupling to the strained lattice, is called *MEL coupling*. The number of strains, and so of MEL constants, is dictated by the crystal symmetry alone. The *irreducible* strains are the minimum number of them, spanning all unit cell deformations compatible with symmetry. They are four for cubic symmetry (see fig. 2): volume dilation $\in^{\alpha}$ (a), tetragonal distortion along a cubic axis $\in^{\gamma}$ (b), orthorhombic deformation of {100} planes $\in^{\gamma}_{2}$ (not shown in Fig. 2), and shear of the <100> axes $\in^{\varepsilon}$ (c).

Invar effect, magnetostrictive superlattices and "giant" magnetostriction materials

There is a second kind of MS due to the spatial dependence of the exchange (EX) interaction, i.e. $\partial J(r)/\partial r$, called *exchange (EX)* MS. Because $J\, S_i \cdot S_j$ is isotropic, EX MS produces just a *volume* deformation (VMS), given by $\omega_{ex} \sim (\partial J(r)/\partial r)/B$, where B is the bulk modulus. Since this VMS shows up *spontaneously* in the thermal expansion (THE) when the temperature approaches from above the Curie temperature, T_c it gives an additional contribution to the lattice THE, that manifests itself as an anomaly of the THE coefficient, $\alpha^{v} = 3\,(1/L)(\partial L/\partial T)$. It also manifests itself in an increase of λ beyond its technical saturation, λ_S, a phenomenon called *forced* MS,where fundamental many-body electron repul-

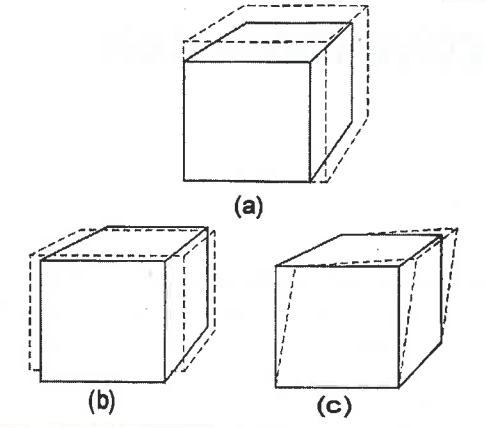

▲ Fig. 2: Three of the possible "irreducible" MS strains for a cubic crystal (the orthorhombic one is not shown) [1].

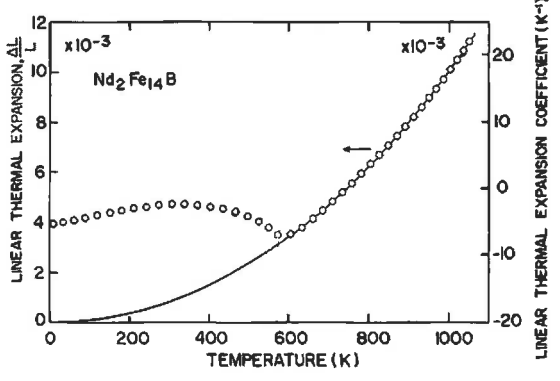

▲ Fig. 3: Invar effect in the thermal expansion (THE) of the tetragonal hard ferromagnet $Nd_2Fe_{14}B$. Also shown is the lattice THE extrapolation (line) [1].

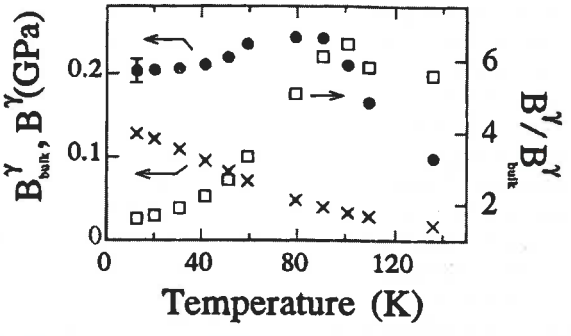

◀ Fig. 4: Tetragonal MEL stress, B^γ vs. temperature (• points) for the ultrathin hexagonal superlattice $(Ho_6/Y_6)_{x\,100}$. The difference from the bulk Ho one, B^γ_{bulk} (x points) is due to interface and non-linear MEL stresses. Also shown is the quotient B^γ/B^γ bulk (€ points) [1].

sion is involved and which varies with H linearly. It can happen that the spontaneous VMS is positive and of such a magnitude that it fully or partially cancels the lattice THE, a phenomenon known as the *invar effect*, and by which the material does not contract below T_c. Obviously this effect has enormous consequences for applications, where materials with "null" effective α are required (watches, optical interferometers, condensers, standards, etc.). Examples of invar materials are the Fe-Ni, Fe-Ni-Cr, Fe-Pt alloys, certain compositions of Fe-Ni-Mn alloys, Ni_3Al, MnSi, amorphous Fe-B and intermetallics $RECo_2$, $RE_2Fe_{14}B$ and Dy_2Fe_{17} (Fig.3). Theoretically it can be shown that $\omega_{mag} \sim T^2$, precisely the same dependence as that for the lattice thermal contraction, ω_{latt} (T). Therefore compensation of the lattice THE takes place, or in other words $\alpha v \approx 0$.

Currently vigorous research is been undertaken on MS in artificially periodic structures known as *multilayers* (ML) and *superlattices* (SL), formed by alternative deposition of thin layers ($\approx$5-10^3 Å) of two magnetic materials. Because of the modification of the electronic structure, an *interface* MS is manifested at the interface (IF) of the two layers (in the SL the layers grow coherently, forming an artficial macroscopic lattice). Usually only one layer is magnetic (m), the m-m exchange being transmitted by the non-magnetic (nm) one. Because ML and SL are grown upon a substrate, this restrains the MS distortion, and therefore experimentally one measures the MEL stress. Néel (1954) showed that the IF MEL stress has the form B_{IF}/t_m, where t_m is the layer thickness. Therefore this stress becomes *as important* as the bulk contribution for very thin m-layers, and can be of opposite sign. When the growth is epitaxial (i.e. the lattice constants $a_m = a_{nm}$ in the SL), which can be achieved using sophisticated fabrication techniques (molecular beam epitaxy, laser ablation and sputtering), the m-layer is under mechanical stress, which induces enormous *misfit* strains (up to $\approx$10%), when the bulk materials have different lattice constants. In such a situation the magnetoelastic coupling becomes *non-linear*, and B_{vol} is modified by a stress of the form $B_{NL} \in_{mf}$ (the MEL free energy is now quadratic in the strain), which can be as substantial as B_{vol}.

The NL MEL coupling is also well manifested in the *elastic constants*, where it gives rise to the appearance of a non-symmetric or *rotational strains*, ω_{ij}, which differ from the usual symmetric ones ($\in_{ij} = \in_{ji}$) in that $\omega_{ij} \neq \omega_{ji}$. These strains give rise to the *rotational invariance* of the MEL energy, in the sense that the MEL anisotropy that originates from the $\vec{M}$ rotation is the same as the one produced by an imposed external rotational deformation of opposite sense. The existence of the three MEL stresses has been experimentally observed in hexagonal symmetry, SL, RE/SP (SP= Y, Lu, Sc) (see Fig.4) and also in SL and ML made of cubic transition metal, such as TM/M, where TM= Fe,Co,Ni and M is a noble metal or Cu. The RE/SP SL are important from a *basic* point of view, because RE magnetic moments are well localized and CEF MS is very amenable to study. However, because RE metals are FM or helically ordered only at rather low temperatures (Gd, Dy, Tb and Ho, although more complex modulated magnetic structures do appear), they are of not much use for applications. Instead the ferromagnetics TM/M ML, with high T_c and weak magnetic anisotropy, may have wide application as MEL transducers (actuators and sensors) within nanostructured devices.

MS in soft transition metals and their alloys is relatively small (expressed in 10^{-6} = 1μst units), with $\lambda_s \equiv \lambda_t \equiv -8, -34$ for Fe and Ni, ~22 for $(FeCo)_{80}B_{20}$, and ~-30 for spinel ferrites ($TM_xFe_{1-x}O_4$, TM = Fe,Ni,Mn). An exception is the Co ferrite that has the very large value $\lambda([100],[100]) \equiv -700$, where all values are at RT. However, for the RE metals and their intermetallic compounds, MS is generally *very large*, up to $\approx$ 1% (thousands of 1 μst) at low temperatures, because of the RE^{3+} ion large quadrupolar electric moment [Q ~ J(J-1/2)], which interacts with the inhomogeneous CEF, albeit this is more more shielded than in TM. The intermetallics, $RETM_2$ (TM=Fe,Co,Ni and Mn) with Laves-phase structure (the RE^{3+} form a diamond lattice), show the *largest* λ_t ever found (the so-called "giant" MS). Among these are, for example: $TbNi_2$ (0.23% at 4.2K), $NdCo_2$ (-0.17% at 77K) and $TbFe_2$, with the largest *room-temperature* λ_t known (0.2%), reaching 0.4 % at 4.2K The problem for use in applications of these inter-

◀ Fig. 5: A Terfenol magnetostrictive device for generation of seismic waves (from Handbook of Giant Magnetostrictive Materials, G. Engdahl, Academic, New York,2000).

features

metallics is the large saturation magnetic field required, of ≈ 1T. However, combining the opposite sign anisotropies of Tb^{3+} and Dy^{3+} in the compound $Tb_{0.27}Dy_{0.73}Fe_2$ (a material commercially known as *Terfenol®*), the saturation field is reduced down to ≈ 2kOe , still with a room temperature MS of 0.12%. This material is currently that most used for MEL transducers, and can be prepared in engineering amounts (Fig.5). But the largest MS ever measured is in $TbMn_2$, where λ_t(40K, H=15T)=0.6% and , which ω_t(20K, H=15T)=−1.6%are certainly *huge values*. But other alloys *not* containing RE also show giant volume MS values of 0.5-1%, at near room temperature and at rather modest fields (≈1-5 kOe), notably FeRh, $FeRh_{1-x}Pt_x$ and $Hf_{1-x}Ta_xFe_{2-y}$, when the applied magnetic field induces an AF to FM transition. This makes them also very promising for applications.

As concluding remarks, we have seen that the most fundamental interactions in solids (exchange, CEF and spin-lattice), taken together with electronic structure, are involved in magnetostriction, and from which fundamental information can be extracted. Magnetostriction is a ubiquitous phenomenon in solid matter, spanning a wide range of values, between $\approx 10^{-8}$ (strongly correlated systems) and $\approx 10^{-2}$ (rare earth and other intermetallics). Applications in sensors and actuators, among many others, is an active reality and their use in nanostructured devices is also promising.

References

[1] A.del Moral, *Magnetostriction;Basic Principles and Applications*, Inst.of Physics Pub.,Bristol,to appear (2004) (references to original papers are given here).

Molecular magnetism: mesoscopic and nanoscopic structures

D. Gatteschi
Department of Chemistry, University of Florence, INSTM

All the magnets currently used are based on metallic or ionic lattices. Since about two decades chemists have started a thorough project of using molecular chemistry techniques to develop new classes of magnets based on molecules rather than on metals or oxides. The idea behind this is the challenge of creating new classes of materials from which new exciting properties may be expected. In a sense this research is the continuation of that which was successfully developed when it was discovered that organic compounds can behave as conductors and superconductors like the classic inorganic materials. In a few years it has been discovered that purely organic magnets are indeed possible, although the critical temperatures are still very low. The most promising results have been obtained using sulfur-nitrogen based organic radicals which behave as weak ferromagnets below 35 K [1]. On the other hand, using a mixture of transition metal ions and organic radicals it has been possible to obtain a room temperature ferrimagnet [2], and similar results have been obtained using derivatives of the old Prussian Blue compounds [3].

Beyond the chemical challenge of assembling new structures using moderately stable building blocks like organic radicals, the factors suggesting that molecular magnetism can indeed provide new interesting classes of materials are:

- The possibility of fine tuning the properties of the materials by using flexible molecular techniques
- The possibility of building a la carte magnetic molecules of increasing size which behave as molecular nanomagnets
- The possibility of obtaining multifunctional materials

An example of the last possibility has been recently reported by Coronado *et al.* [4] They used a hybrid approach, assembling together inorganic building blocks like transition metal oxalato derivatives and organic radicals like the famous BEDT-TTF, well known to form conducting and superconducting materials. They obtained by electrocrystallisation a compound of general formula $[BEDT\text{-}TTF]_3[MnCr(oxalato)_3]$. The structure comprises honeycomb inorganic layers of $[MnCr(oxalato)_3]^-$ separated by stacks of the organic radicals, as shown in Figure 1. The average charge on the BEDT-TTF molecules is +0.34. The inorganic layer is insulating while the organic moiety is a conductor. The magnetic coupling is fairly strong within the inorganic layers and this, coupled to the fact that weak interactions are operative between the layers determined a transition to bulk ferromagnetic behaviour below 5.5 K. Therefore below the critical temperature the material behaves as a ferromagnetic conductor. Although systems like this are well known starting from iron itself, in the molecular derivative the magnetic electrons are different from the conducting electrons, thus offering the possibility of observing new phenomena.

Another important feature of molecular magnets is that they are in general insulators, therefore they are much more transparent to UV—visible light than classic magnets. Therefore it is possible to use light to induce magnetic transitions. This approach has been used by the groups of Verdaguer and Hashimoto for instance.[5,6] Prussian blue derivatives are complex cyanides of general formula ABC(CN). When B= Fe^{2+} and C= Co^{3+} the compound is diamagnetic because both ions are in their low spin, non-magnetic state. By illuminating with red light

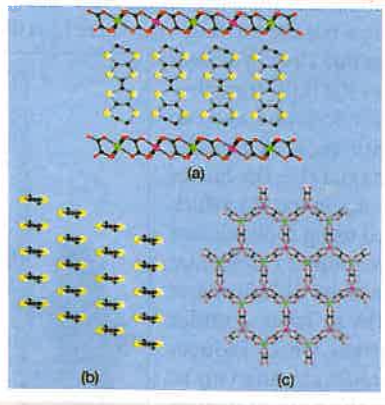

▲ **Fig. 1:** The structure of $[BEDT\text{-}TTF]_3[MnCr(oxalato)_3]$. a) overview of the lattice; b) the organic layers; c) the inorganic layers.

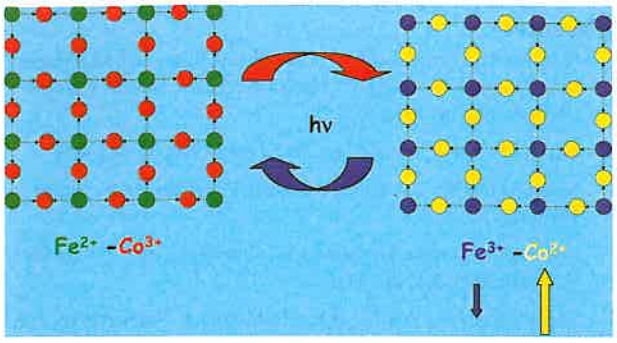

▲ Fig. 2: Scheme of the light induced interconversion of Prussian blue derivatives.

however it is possible to induce an electron transfer in which Fe^{2+} is changed to low spin Fe^{3+}, with one unpaired electron, and Co^{3+} to high spin Co^{2+} with three unpaired electrons:

$$Fe^{2+}\text{-C-N-}Co^{3+} - Fe^{3+}\text{-C-N-}Co^{2+}$$

A schematic drawing of the light induced transformation is shown in Figure 2. The material orders as a bulk ferrimagnet below 50 K. If the irradiation is performed below this temperature we observe a transition to bulk magnetic order induced by light. Therefore these materials can be considered as magnetic switches operated by light. It is also possible to perform the opposite transition by irradiating the Fe^{3+}-Co^{2+} pairs with blue light: the electron is back transferred from cobalt to iron and the system reverts to the diamagnetic state.

The most exciting developments of molecular magnetism of the last few years has been the discovery that some discrete molecules can behave at low temperature as tiny magnets. [7] The archetypal molecule is:

$$[Mn_{12}O_{16}(CH_3COO)_{16}(H_2O)_4].4H_2O.2CH_3COOH,$$

Mn12Ac for short. The structure of the dodecanuclear manganese cluster is shown in Figure 3. It comprises an external ring of eight manganese(III) ions and a tetrahedron of manganese(IV) ions, bridged by oxide bridges, like in a manganite. Acetic acid molecules complete the environment of the metal ions, in fact blocking the growth of the oxide particles. In other terms these clusters can be considered as small particles of manganese oxides, all identical to each other. In this particular case the particles crystallise in a tetragonal space group, and therefore they are also iso-oriented in the lattice. At low temperature the system is in the ground S= 10 state, with the eight S= 2 spins of manganese(III) up and the four S= 3/2 of the manganese(IV) ions down. The clusters have a high Ising type magnetic anisotropy, due to the local anisotropies of the distorted manganese(III) ions. This means that the magnetisation is preferentially oriented parallel to the tetragonal axis of the cluster and to reorient itself it needs a high activation energy. At 2 K the relaxation time of the magnetisation becomes so long that the individual molecules become permanently magnetised, like tiny magnets. They show magnetic hysteresis and in principle information can be stored in one molecule, thus reaching the highest possible level of miniaturisation. But the excitement does not stop here, because Mn12Ac shows a rich range of quantum properties, and it has been proved to be an ideal test ground for theories of quantum effects in magnets. Clear evidence of tunnelling of the magnetisation has been achieved by observing stepped hysteresis. More controversial still is the possibility to observe quantum coherence.

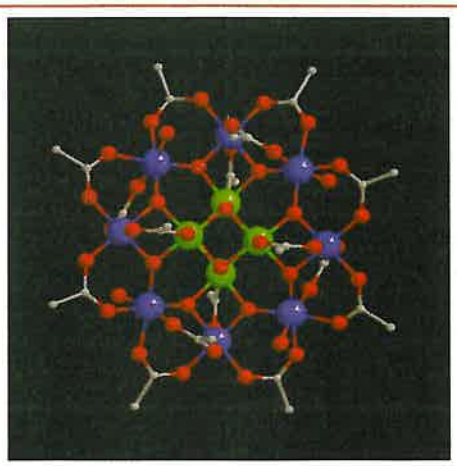

▲ Fig. 3: Sketch of the structure of Mn12Ac.

The advantage of magnetic molecules over other types of magnetic particles is that they are absolutely monodisperse, and that in principle they can be diluted and organised using supramolecular chemistry techniques. Many efforts are currently made to derivatise the magnetic molecules to organise them on suitable supports, like gold or silicon, in order to be able to address them individually. The dream of storing information in one molecule may become reality!

After Mn12 a few other types of single molecule magnets have been discovered and investigated. Among these a cluster containing eight iron(III) ions has been found to show oscillations of the tunnel splitting in the presence of a an applied transverse magnetic field. This is the signature of the Berry phase in magnets which was first reported by Sessoli and Wernsdorfer in 1999. [8]

Recently it has been discovered that similar effects of slow relaxation can be observed in one-dimensional magnets. [9] A compound containing Co^{2+} ions regularly alternating in space with organic radicals behaves as a one dimensional ferrimagnet. Below 20 K the relaxation time of the magnetisation rapidly

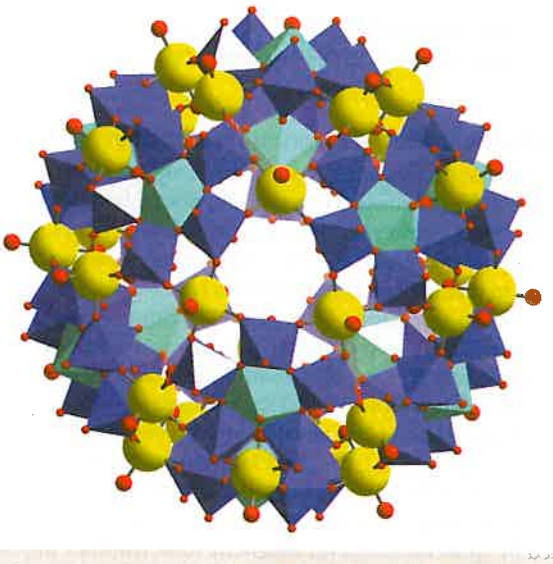

▲ Fig. 4: The structure of [Mo75Fe30] clusters. The yellow circles are iron(III) ions.

increases on decreasing temperature, with a barrier for the re-orientation of the magnetisation larger than 150 K. Also in this case magnetic hysteresis is observed which is associated with a high magnetic anisotropy of the easy-axis type. A semi quantitative explanation has been provided using a model proposed by Glauber in 1963. This opens an exciting perspective, that of allowing the storing of information in segments of a polymer, which therefore behaves like a magnetic nanowire.

Finally I want to mention that magnetic molecules are also interesting in the case of antiferromagnetic behaviour. Perhaps the most significant example is that of a cluster [10] containing 76 Mo^{6+} ions and 30 Fe^{3+}, which has the structure shown in Figure 4. The molybdenum ions are non-magnetic so the magnetic behaviour is associated with the interactions between the iron ions. They are antiferromagnetic, and highly frustrated due to the particular topology which corresponds to an icosidodecahedron. The compound has not shown quantum effects down to the mK region, due to the large degeneracy of the low lying states associated with spin frustration.

Molecular magnets open many new possibilities to observe quantum and classic effects in mesoscopic matter. The field is just at its beginning, but many developments can be anticipated in the next few years. Possible applications may range from quantum computing to new types of contrast agents for magnetic resonance imaging.

References

[1] Banister, A. J.; Bricklebank, N.; Lavender, I.; Rawson, J. M.; Gregory, C. I.; Tanner, B. K.; Clegg, W.; Elsegood, M. R. J.; Palacio, F. *Angew Chem Int Ed Engl* **1996**, *35*, 2533

[2] Miller, J. S. E. A. J. *Angew Chem Int Ed Engl* **1994**, *33*, 385-415.

[3] Ferlay, S.; Mallah, T.; Ouahes, R.; Veillet, P.; Verdaguer, M. *Nature* **1995**, *378*, 701-703.

[4] Coronado, E.; Galan-Mascaros, J. R.; Gomez-Garcia, C. J.; Laukhin, V. *Nature* **2000**, *408*, 447-449.

[5] Sato, O.; Iyoda, A.; Fujishima, K.; Hashimoto, K. *Science* **1996**, *272*, 704.

[6] Verdaguer, M.; Bleuzen, A.; Marvaud, V.; Vaissermann, J.; Seuileman, M.; Desplanches, C.; Scuiller, A.; Train, C.; Garde, R.; Gelly, G.; Lomenech, C.; Rosenman, I. V. P.; Cartier, C.; Villain, F. *Coord. Chem. Rev.* **1999**, *190-192*, 1023-1047

[7] Gatteschi, D.; Sessoli, R. *Angew. Chem. Int. Ed. Engl.* **2003**, *42*, 268-297.. Friedman, J. R Sarachik, M.P. Tejada J. Ziolo R., *Phys. Rev. Lett.* **1996**, *76*, 3830 ; Thomas, L. ; Lionti, F. Ballou, R. Gatteschi, D. Sessoli R. Barbara B., *Nature* **1996**, *383*, 145.

[8] Wernsdorfer, W.; Sessoli, R. *Science* **1999**, *284*, 133-135.

[9] Caneschi, A.; Gatteschi, D.; Lalioti, N.; Sangregorio, C.; Sessoli, R.; Venturi, G.; Vindigni, A.; Rettori, A.; Pini, M. G.; Novak, M. A. "Cobalt(II)-Nitronyl Nitroxide Chains as Molecular Magnetic Nanowires" *Angew. Chem. Int. Ed.*, **2001**, *40*, 1760-1763.

[10] Müller, A.; Luban, M.; Schröder, C.; Modler, R.; Kögerler, P.; Axenovich, M.; Schnack, J.; Canfield, P.; Bud'ko, S.; Harrison, N. *Chemphyschem* **2001**, *2*, 517-+.

Ferromagnetic semiconductor heterostructures

Tomasz Dietl, Institute of Physics, Polish Academy of Sciences al. Lotników, 32/46, PL-02668 Warszawa, Poland

Introduction: diluted magnetic semiconductors

As discussed in accompanying papers, today's research on spin electronics involves virtually all material families, the most mature being studies on magnetic metal multilayers, in which spin-dependent scattering and tunnelling are being successfully applied in reading heads of high density hard-discs and in magnetic random access memories (MRAM). However, in the context of spintronics [1] particularly promising are ferromagnetic semiconductors [2] since they combine complementary resources of ferromagnetic and semiconductor material systems. One of the relevant questions is to what extend the powerful methods developed to manipulate the carrier concentration and spin polarisation in semiconductor quantum structures could serve to tailor the magnitude and orientation of magnetisation produced by spins localized on magnetic ions. Another important issue concerns the elaboration of methods of injecting and transporting spin currents, which may ultimately lead to control over single spins in solid state environment.

Already early studies of Cr spinels as well as of rock-salt Eu- and Mn-based chalcogenides led to the observation of a number of outstanding phenomena associated with the interplay between ferromagnetic cooperative phenomena and semiconducting properties [2]. A strong spin-dependent (exchange) coupling between the band carriers and spins localized on the magnetic atoms accounts for outstanding properties of these materials. This coupling gives rise to strong indirect exchange interactions between the localized moments as well as to giant spin-splittings of the electronic states, which is proportional to magnetisation of the spins. The discovery of ferromagnetism in Mn-based zinc-blende III-V compounds [3], such as (Ga,Mn)As, followed by the prediction [4] and observation of ferromagnetism in p-type II-VI materials [5,6], such as (Zn,Mn)Te:N, allows one to explore the physics of previously not available combinations of quantum structures and ferromagnetism in semiconductors. This aspect of ferromagnetic III-V and II diluted magnetic semiconductors (DMS) will be outlined here together with indications of models aiming at explaining the nature of ferromagnetism in these materials.

Carrier-controlled ferromagnetism

It is well established that Mn is divalent in II-VI compounds and assumes the high spin d^5 configuration characterized by $S = 5/2$. Here, Mn ions neither introduce nor bind carriers, but give rise to the presence of localized spins. For low carrier densities, II-VI DMS are paramagnetic but neighbour Mn-Mn pairs are antiferromagnetically blocked owing to short-range super-exchange interactions. However, this antiferromagnetic coupling can be overcompensated by ferromagnetic interactions mediated by band holes [4-6]. In III-V compounds, Mn atoms when substituting trivalent metals supply both localized spins and holes, so

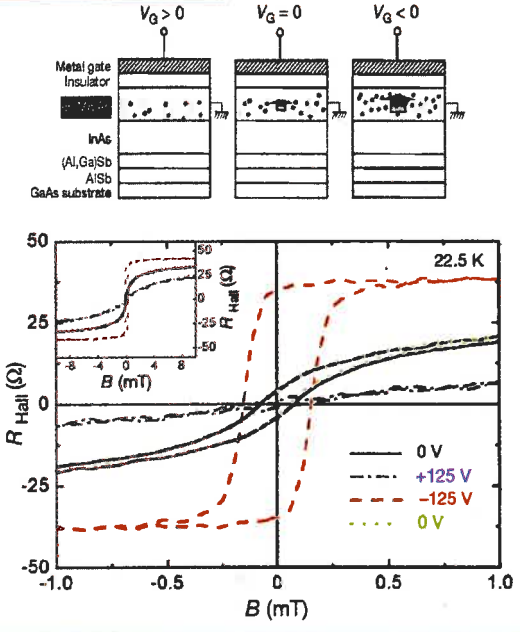

▲ **Fig. 1:** Magnetisation hysteresis loops determined by measurements of anomalous Hall effect at constant temperature of 22.5 K for various gate voltages in field-effect transistor structure with (In,Mn)As channel. (after Ohno *et al.* [9]).

that extrinsic co-doping is not necessary to generate the carrier-mediated spin-spin interaction [1,3,7].

The role of band carriers in promoting ferromagnetic ordering between localized spins was already noted by Zener in the '50s in the context of magnetic metals. This ordering can be viewed as driven by the lowering of the carriers energy associated with their redistribution between spin subbands, split by the exchange coupling to the localised spins. A more detail quantum treatment indicates, however, that the sign of the interaction between localised spin oscillates with their distance according to the celebrated Ruderman-Kittel-Kasuya-Yosida (RKKY) model. Because of the large density of states and spin-dependent hybridisation between anion p and magnetic d states, the carrier-mediated spin-spin interaction is particularly strong in the presence of the holes in tetrahedrally coordinated DMS. Interestingly, this carrier-mediated Zener/RKKY ferromagnetism is enhanced by exchange interactions within the carrier liquid, so that the Stoner mechanism contributes to the magnitude of the Curie temperature in these systems.

Manipulations of magnetisation

Since magnetic properties are controlled by band holes, an appealing possibility is to influence the magnetic ordering isothermally, by light or by the electric field, which affect the carrier concentration in semiconductor structures. Such tuning capabilities of the materials systems in question were put into the evidence in (In,Mn)As/(Al,Ga)Sb [8,9] and modulation doped p-(Cd,Mn)Te/(Cd,Mg,Zn)Te [5,10] heterostructures, as depicted in Figs. 1 and 2. Actually, these findings can be quantitatively interpreted by considering the effect of the electric field or illumination on the hole density under stationary conditions and, therefore, on the Curie temperature in the relevant magnetic layers. Interestingly, according to experimental findings and theoretical modelling, photocarriers generated by above barrier illumination destroy ferromagnetic order in the magnetic quantum well residing in an undoped (intrinsic) region of a p-i-p structure [5,10] but they enhance the magnitude of spontaneous magnetisation in the case of a p-i-n diode [10], as shown in Fig. 2.

For the valence band states, whose periodic part of the Bloch functions contain spin components mixed up by the spin-orbit interaction, the exchange splitting does not depend only on the product of the p-d exchange integral and the Mn magnetisation but also on the magnitude and direction of the hole wave-vector, confinement, and strain. In particular, both experimental and theoretical results demonstrate that the orientation of the easy axis in respect to the film plane depends on whether the epitaxial strain is compressive or tensile [7]. Hence, magnetic anisotropy and thus easy axis direction and domain structure [11], can be manipulated by appropriate layout of the layer sequence, as epitaxial growth of DMS films in question is usually pseudomorphic. Furthermore, magnetic anisotropy at given strain is predicted to vary with the degree of the occupation of particular hole subbands. This, in turn, is determined by the ratio of the valence band exchange splitting to the Fermi energy, and thus, by the magnitude of spontaneous magnetisation, which depends on temperature. Such a temperature-induced switching of the easy axis direction has recently been detected in samples with appropriately low hole densities [12]. A related sensitivity of the easy axis direction to the carrier concentration constitutes a novel method enabling control of the magnetisation direction locally by a system of electrostatic gates.

Spin injection

A number of groups is involved in the development of devices capable of injecting spins into a non-magnetic semiconductor. Obviously, owing to a high degree of spin polarisation and resistance matching, ferromagnetic semiconductors constitute a natural material of choice here. Typically, a p-i-n light emitting diode structure is employed , in which the p-type spin injecting electrode is made of a ferromagnetic semiconductor. Experimental results obtained for the (Ga,Mn)As/GaAs/(In,Ga)As/n-GaAs diode are shown in Fig. 4. In this particular experi-

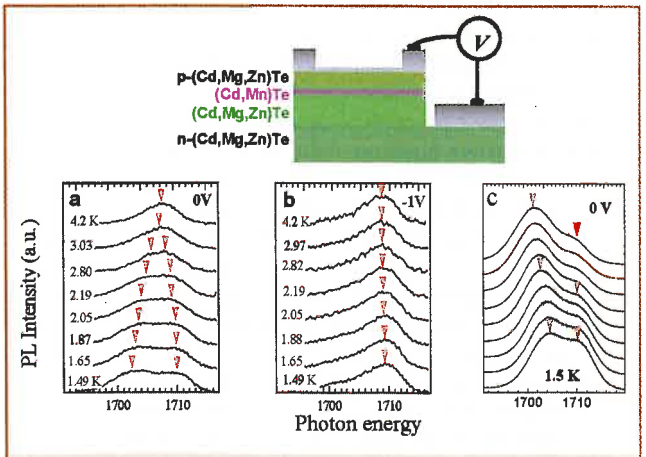

▲ **Fig. 2:** Effect of temperature (a), bias voltage (b), and illumination (c) on photoluminescence of structure consisting of modulation doped p-(Cd,Mn)Te quantum well and n-type barrier. Zero-field line splitting (marked by red arrows) and shift on lowering temperature witness the appearance of a ferromagnetic ordering at low temperatures (a), which does not show up if the quantum well is depleted from the holes by reverse bias of the p-i-n diode (b). The low-temperature splitting is enhanced by additional illumination by white light which increases the hole concentration in the quantum well (after Boukari *et al.* [10]).

features

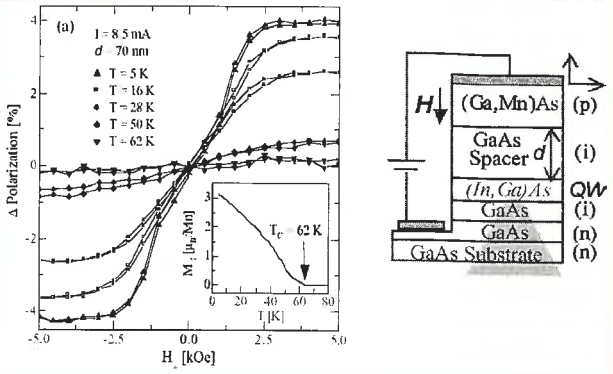

▲ **Fig. 3:** Degree of circular polarisation of light emitted by a (In,Ga)As quantum well located in a p-i-n diode biased in the forward direction and containing (Ga,Mn)As as the p-type electrode. An external magnetic field is applied along the hard axis, that is perpendicularly to the interface plane. The degree of circular polarisation and the (Ga,Mn)As magnetisation depend similarly on the magnetic field and temperature, which together with the lack of photoluminescence polarisation for excitation by linearly polarised light, point to the existence of the hole spin injection from ferromagnetic (Ga,Mn)As to non-magnetic (In,Ga)As via a non-magnetic GaAs (afterYoung *et al.* [13]).

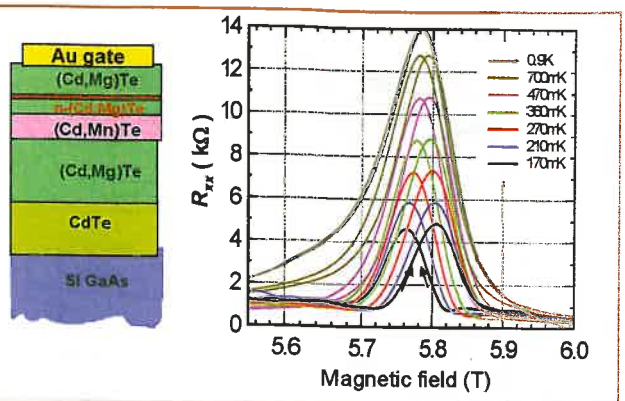

▲ **Fig. 4:** Quantum Hall resistances in modulation doped p-(Cd,Mn)Te quantum well containing a metal gate for changing electron concentration. Resistance spike at 5.8 T occurs at the crossing of ground and excited Landau levels with opposite spin orientations ($0\uparrow$ and $1\downarrow$). The presence of the spike and its hysteretic behaviour signalises ferromagnetic ordering of the electrons residing in partly filled overlapping Landau levels (after Jaroszynski *et al.* [15]).

ment [13], the degree of circular polarisation is examined for light emitted in the growth direction. In this Faraday configuration, simple selection rules are obeyed for radiative recombination between the electron and heavy hole ground state subbands. Since the easy axis is in plane, a field of a few kOe is necessary to align the magnetisation and thus to produce a sizable degree of light polarisation. Importantly, the injection of spin polarised electrons, using Zener or Esaki tunnelling from p-type (Ga,Mn)As electrode into n-type GaAs, was also realized.

Quantum Hall ferromagnet

The above results demonstrate rather convincingly the decisive role of the valence band holes in setting on the ferromagnetic ordering in these systems, a conclusion corroborated by studying the Curie temperature T_C as a function of compensation in epitaxial films of (Ga,Mn)As and as a function of the acceptor concentration in p-(Zn,Mn)Te. At the same time, in agreement with theoretical predictions, no ferromagnetic ordering was detected above 1 K in heavily doped n-type (Zn,Mn)O [14]. However, according to experimental results presented in Fig. 3, for an appropriate combination of an external magnetic field and gate voltage that controls electron concentration, an Ising ferromagnetic ground state with T_C up to 2 K can be observed in high-quality modulation-doped n-(Cd,Mn)Te/(Cd,Mg)Te heterostructures [15]. The quantum Hall ferromagnetism shows up when two partly filled Landau levels with opposite spin directions are brought into a coincidence. This Stoner-like instability of the carrier liquid appears due to the enhancement of the density of states in two-dimensional systems in quantising magnetic fields. Incidentally, Landau level crossings occur in such structures due to the enlargement of electron spin-splitting by the s-d exchange interaction with the Mn spins.

Summary and outlook

Extensive studies of ferromagnetic semiconductor heterostructures have lead to the observation of a number of spin phenomena. Some of them, such as spin injection as well as giant and tunnelling magnetoresistance, are familiar from parallel studies of magnetic multilayers. Other effects, like isothermal driving of the system between ferromagnetic and paramagnetic phases by the electric field or by the photon flux in the direction that can be selected by an appropriate design of the structure, appear unique to ferromagnetic semiconductors. These striking effects offer new tools for patterning magnetic nanostructures as well as for information writing and processing, beyond the heating effects of light exploited in the existing magneto-optical memories. Obviously, however, while the potential of ferromagnetic semiconductors can already be exploited for the development of quantum information hardware, their practical applications in classical information systems have to be preceded by progress in the synthesis of a functional material with T_C surpassing comfortably the room temperature. Following the theoretical suggestion [7], a number of oxide and nitride-based DMS, containing Mn or other magnetic elements, has been obtained, which indeed show indications of ferromagnetism at room temperature [16]. However, a further progress in this field requires development of growth and characterization methods that enable a better control over solubility limits, self-compensations, phase segregations, and precipitations of other compounds.

On the theoretical side, it appears that double- and super-exchange, rather than the Zener/RKKY mechanism, may account for ferromagnetism is systems containing magnetic elements other than Mn. Since ferromagnetic DMS combine intricate properties of charge-transfer insulators and strongly correlated disordered metals with the physics of defect and band states in heavily doped semiconductors, despite important advances in theoretical understanding of these systems, their description from first principles may take some time. Without any doubt, the search for functional ferromagnetic semiconductor nanostructures and their theoretical modelling has evolved into an important branch of today's materials science and condensed matter physics.

Acknowledgements

The author thanks his co-workers listed in the references for fruitful interactions. Author's research in Germany is supported by Alexander von Humboldt Foundation, while the work in Poland by State Committee for Scientific Research, by FENIKS and AMORE EC projects as well as by Ohno Semiconductor Spintronics ERATO Project of Japan Science and Technology Corporation.

References

[1] For general reviews on spintronics, see, A. Fert, this issue; H. Ohno, F. Matsukura, and Y. Ohno, JSAP International **5**, 4 (2002) (www.jsapi.jsap.or.jp/); T. Dietl, Acta Phys. Polon. A **100** (Suppl.), 139 (2001), cond-mat/0201279; S. Wolf, D. D. Awshalom. R. A. Buhrman, J. M. Daughton, S. von Molnár, M. L. Roukes, A. Y. Chtchelkanova, and D. M. Treger, Science **294**, 1488 (2001); topical issue of Semicon. Sci. Technol. **17**, No4 (2002), ed. H. Ohno.

[2] For reviews on ferromagnetic semiconductors, see, T. Dietl, Semicond. Sci. Technol. **17**, 377 (2002); F. Matsukura, H. Ohno, T. Dietl; III-V Ferromagnetic Semi-conductors, in: Handbook of Magnetic Materials, vol. 14, ed. K.H.J. Buschow (Elsevier, Amsterdam, 2002) pp. 1-87; T. Story, Acta Phys. Polon. A **91**, 173 (1997).

[3] H. Ohno, H. Munekata, T. Penney, S. Von Molnár, L.L. Chang, Phys. Rev. Lett. **68**, 2664 (1992); H. Ohno, A. Shen, F. Matsukura, A. Oiwa, A. Endo, S. Katsumoto, Y. Iye, Appl. Phys. Lett. **69**, 363 (1996).

[4] T. Dietl, A. Haury, and Y. Merle d'Aubigné, Phys. Rev. B **55**, R3347 (1997).

[5] A. Haury, A. Wasiela, A. Arnoult, J. Cibert, S. Tatarenko, T. Dietl, Y. Merle d'Aubigné, Phys. Rev. Lett. **79**, 511 (1997).

[6] D. Ferrand, J. Cibert, A. Wasiela, C. Bourgognon, S. Tatarenko, G. Fishman, T. Andrearczyk, J. Jaroszy_ski, S. Kole_nik, T. Dietl, B. Barbara, and D. Dufeu, Phys. Rev. B **63**, 085201 (2001).

[7] T. Dietl, H. Ohno, F. Matsukura, J. Cibert, and D. Ferrand, Science **287**, 1019 (2000); T. Dietl, H. Ohno, and F. Matsukura, Phys. Rev. B **63**, 195205 (2001).

[8] S. Koshihara, A. Oiwa, M. Hirasawa, S. Katsumoto, Y. Iye, C. Urano, H. Takagi, H. Munekata, Phys. Rev. Lett. **78**, 4617 (1997).

[9] H. Ohno, D. Chiba, F. Matsukura, T. Omiya, E. Abe, T. Dietl, Y. Ohno, and K. Ohtani, Nature **408**, 944 (2000).

[10] H. Boukari, P. Kossacki, M. Bertolini, J. Cibert, S. Tatarenko, D. Ferrand, A. Wasiela, J.A. Gaj, and T. Dietl, Phys. Rev. Lett. **88**, 207204 (2002).

[11] T. Dietl, J. König, and A.H. MacDonald, Phys. Rev. B **64**, 241201(R) (2001).

[12] M. Sawicki, F. Matsukura, A. Idziaszek, T. Dietl, G.M. Schott, C. Ruester, G. Karczewski, G. Schmidt, and L.W. Molenkamp, cond-mat/0212511.

[13] D.K. Young, E. Johnston-Halperin, D.D. Awschalom, Y. Ohno, and H. Ohno, Appl. Phys. Lett. **80**, 1598 (2002).

[14] T. Andrearczyk, J. Jaroszynski, M. Sawicki, Le Van Khoi, T. Dietl, D. Ferrand, C. Bourgognon, J. Cibert, S. Tatarenko, T. Fukumura, Z. Jin, H. Koinuma, and M. Kawasaki, in: *Proceedings 25th Intl. Conf. on Physics of Semiconductors*, Osaka, Japan, 2000, eds. N. Miura, T. Ando (Springer, Berlin, 2001) p. 235.

[15] J. Jaroszynski, T. Andrearczyk, G. Karczewski, J. Wróbel, T. Wojtowicz, E. Papis, E. Kaminska, A. Piotrowska, Dragana Popovic, and T. Dietl; Phys. Rev. Lett. **89**, 266802 (2002).

[16] S.J. Pearton, C.R. Abernathy, M.E. Overberg, G.T. Thaler, D.P. Norton, N. Theodoropoulou, A.F. Hebard, Y.D. Park, F. Ren, J. Kim, and L.A. Boatner, J. Appl. Phys. **93**, 1 (2003).

About the author

Tomasz Dietl is a professor and a head of Nanostructure Laboratory at the Institute of Physics, Polish Academy of Sciences. His current research interests are focused in the development of material systems and device concepts for spintronics of ferromagnetic semiconductors and of hybrid metal/semiconductor nanostructures. He is recipient of Maria Curie-Sklodowska Award in Poland (1997) and of Alexander von Humboldt Research Award in Germany (2003).

[1] Address in 2003: Institute of Experimental and Applied Physics, Regensburg University, Universitaetsstr. 31, D-93040 Regensburg, Germany, Tel: +49.941.943-1617, fax: +49.941.943-3196, email: tomasz.dietl@physik.uni-regensburg.de

features

Magnetic materials: from the search of new phases to nanoscale engineering

D. Givord, Laboratoire Louis Néel, C.N.R.S., Grenoble, France

From soft to hard magnetic materials

There is a category of materials, of which the magnetisation is used as a source of a magnetic field or of a magnetic flux. All these materials are Fe, Co or Ni based (transition metal elements, M) and their spontaneous magnetisation, M_s, have similar typical values. Yet, they may exhibit extremely different applicative properties. This is due to differences in the strength of their coercivity, i.e. their ability to resist an applied magnetic field, $\mu_0 H_{app}$, which tends to change the orientation of the magnetisation. From extremely soft to extremely hard materials, the coercive field, $\mu_0 H_c$, at which the magnetisation finally follows the applied field, increases by more than 6 orders of magnitude (see Figure 1). Soft materials are used in magnetic circuits, transformers or sensors; hard materials are used to make motors, actuators or generators; materials with medium coercivity are used as storage media [1]. Coercivity depends on material intrinsic magnetic properties (temperature below which ferromagnetism is stable, magnetisation and anisotropy energy (see below)). It depends also on extrinsic properties (grain size, grain orientation, grain separation, etc...), which define the material microstructure.

During the last 50 years, an impressive development has occurred in the field of magnetic materials, stimulated by the better understanding of the characteristic behaviours of the different types of magnetic elements. More recently, the discovery of behaviours which are specific to nanomaterials, has open a new period. At the nanoscale, the distinction between intrinsic properties, characteristic of a given magnetic phase, and extrinsic properties, related to the detail of the microstructure, disappears.

Interactions involved and fundamental processes

The typical equilibrium magnetization configuration of a ferromagnetic material is made of micron-size domains. Within a given domain, the moments are parallel as required by exchange interactions and they are aligned along a particular direction, the easy magnetisation direction, as required by magnetocrystalline anisotropy. From one domain to the next, the magnetisation direction alternates. Globally, the magnetisation is zero; exchange and anisotropy energies are minimized, as they are in the single domain state, except within small regions, the domain walls, which constitute the transition regions between two magnetic

domains. Additionally, magnetic domain formation allows the weaker long-range dipolar interactions to be strongly reduced with respect to their value in the single-domain state.

Under an applied field, a bulk magnetisation tends to develop to minimize Zeeman energy. In an ideally homogeneous material, the domain wall energy does not depend on the wall position. The magnetisation increases by free domain wall motion, such that the domains in which the magnetisation is along the applied field grow at the expenses of the others. Such materials are magnetically soft (Figure 2). The induced magnetisation is in turn the source of a magnetic field or of a magnetic flux. When the applied field is time dependent, the magnetisation is time-dependent as well. A voltage results, which constitutes the signal exploited in transformers or sensors.

When the applied field is further increased, one reaches ultimately a state in which only one domain remains. The magnetisation is saturated. Assuming that a field is applied again, but of reversed sign, magnetisation reversal requires that a domain of reversed magnetisation is nucleated. The value of the nucleation field is closely linked to that of the anisotropy energy. This can be understood by considering that a moment that participates in the magnetisation processes necessarily assumes an intermediate transitory position in which it is perpendicular to the easy magnetisation direction. In this unfavoured orientation, the magnetocrystalline anisotropy energy is at a maximum. Permanent magnets are based on high anisotropy materials (Figure 2). A potential energy can be stored in a field, which is antiparallel to the magnetisation. Motors or actuators transform this potential energy into mechanical energy.

The two states of saturated magnetisation, up and down, may constitute the two elementary bits of information, 0 and 1. Materials used for information storage have medium coercivity: the magnetisation-saturated states must be stable enough for the information not to be lost; at the same time, the writing process must be realised in a not too high magnetic field. Exchange decoupling between the constituent grains is a specific feature of these materials. It allows each bit of information to be written independently of the others (Figure 2).

Which Materials?

Ferromagnetism above room temperature is a unique property of the 3d transition metals (M= Fe, Co or Ni), their alloys or compounds [1]. It results from large exchange interactions existing between the magnetic 3d electrons. In general, alloys and metallic compounds have higher magnetisation than insulating compounds. At room temperature, pure Fe metal has the largest magnetisation of all known elements ($\mu_0 M_s = 2.2\ T$).

Materials where 3d magnetism only is involved tend to have low magnetic anisotropy and often show soft magnetic behaviour. In the best of these materials, the permeability, which represents the ratio between the induced magnetisation and $\mu_0 H_{app}$, may be as high as 10^5. Most of these materials have been known for many years. This is in particular the case of the Fe-Si alloys in which 3-5 % Si is substituted for Fe [1]. The magnetisation is approximately 10 % less than that of pure Fe metal. Other properties (mechanical properties, resistivity, corrosion resistance, etc...) are decisively improved with respect to those of the pure metal. Fe-Si sheets constitute the core of all transformers used for energy transportation. Soft magnetic materials are mostly used under AC exciting fields. At high frequency, eddy-current losses develop in metallic systems. Insulating ferrites are used in electronics (AC-DC converters, inductances, etc...) at frequencies from typically 1 kHz to 1 GHz. At even higher frequencies, rare-earth garnets are used in non-reciprocal devices, for telecommunication applications.

The hard ferrites are the first magnets that exploited the link existing between coercivity and magnetocrystalline anisotropy [2]. These materials are used in the fabrication of small motors used in the automotive industry and for home appliances. In the 1960's, extremely large anisotropies were discovered in the rare-earth metals (R = rare-earth), the second series of magnetic elements in the periodic table. The R elements are heavy elements, and the magnetic 4 f electrons are characterised by large spin-orbit coupling. By this mechanism the moment orientation is tightly linked to the crystal structure, i.e. the magnetocrystalline anisotropy is large. The interatomic 4f-4f exchange interactions are weak and magnetism in the R metals is only stable at low temperature. In the R-M compounds, strong 4f-3d interactions exist, mediated by the rare-earth 5d electrons. Rare-earth magnetism is preserved above room temperature and, with it, compounds with very large anisotropies may be obtained. Magnets based on the $SmCo_5$ phase, with typical composition $Sm(Fe,Co,Cu,Zr)_{7-8}$, are of particular interest for high-temperature applications [2]. The fabrication of magnets based on the $Nd_2Fe_{14}B$ phase constituted a decisive breakthrough in the development of rare-earth based magnets [3]. These magnets associate outstanding magnetic properties ($\mu_0 M_s = 1.2\text{-}1.4\ T$, $\mu_0 H_c\ 1\text{-}2\ T$) with much lower cost than the $SmCo_5$ magnets. They are used in particular in compact high performance motors, such as the voice coil motors of all hard-disk drives.

Pd or Pt, alloyed with M metals, may also be the source of high anisotropy. In these heavy elements, the magnetic electrons are the 4d or the 5d ones. The equiatomic $L1_0$ Fe-Pt phase has extremely large anisotropy. High performance materials have been prepared in thin film forms. Magnets inserted in microsystems could find application, despite the high cost of Pt.

The coercive field required in materials for magnetic storage is approximately an order of magnitude smaller than the coercive field of hard magnets, $\mu_0 H_c \approx 0.05 - 0.4\ T$. Such coercive field values can be obtained in materials, which show shape anisotropy: the moments tend to align along the long dimension of elongated particles. The γ-Fe_2O_3 particles, which constitute the most common material used in magnetic tapes, exploit this property. More recently, elongated Fe metallic particles, which have higher magnetisation and coercivity, have been developed for the same purpose.

The materials used in Hard Disk Drives (HDD) are Co-based alloys, which contain additive elements such as Cr, Pt and B [4]. The magnetic grains are coated with a non-magnetic Cr-rich layer, which ensures exchange-decoupling. Their coercivity is related to

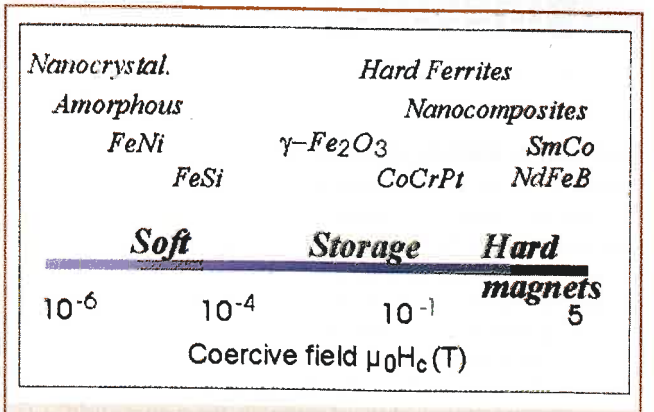

▲ **Fig. 1:** Magnetic materials according to their coercivity.

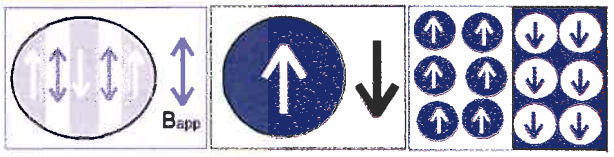

▲ Fig. 2: Magnetic materials of different kinds (a) Soft materials exploit the magnetisation variation with the applied field (b) Hard magnets exploit their ability to resist to a reversed magnetic field (c) in materials for information storage, the magnetisation is stable to keep the information stored and it can be reversed to change this information.

magnetocrystalline anisotropy. The grains being very small, a significant fraction of the atoms are surface atoms. These are known to potentially show larger anisotropy than bulk atoms.

Amorphous alloys, which associate R elements (Gd, Tb) to M elements (Fe, Co) have been developed for perpendicular magneto-optical recording [5]. The R and M moments are coupled antiparallel and the chemical composition is such that, at room temperature, the global magnetisation is almost zero. This allows the magnetisation to lie perpendicular to the substrate surface. To first order, the rare-earth elements do not contribute to the magneto-optical reading signal, which is approximately proportional to the transition metal magnetisation.

To the nanoscale

The understanding of the magnetism of matter is such that it appears unlikely that new alloys and compounds with significantly improved intrinsic properties may be discovered. Tailoring the magnetic properties at the nanoscale offers much more perspective. At this scale, new properties emerge because the dimensions are below the characteristic length-scales of magnetic interactions or magnetic phenomena [6].

Let us consider an assembly of exchange-coupled randomly-oriented nanocrystals. At small scale, the dipolar interactions need not to be considered. Exchange favours parallel coupling of the moments over the whole sample. Anisotropy favours moment alignment along the local easy magnetisation direction of each nanocrystal. One expects in general that exchange energy is much higher than anisotropy energy. However, the nanocrystals are coupled through their surface and thus the exchange energy intervenes as a surface term, whereas anisotropy energy is a volume term as usual. Due to the interplay between these 2 terms, a certain correlation volume must exist over which the moments can be considered as fully aligned. This volume may be expressed as $V \approx A^6/K^6 v^3$, where A ($\approx 10^{-12}$ J/m) is the exchange constant between nanocrystals, K is the nanocrystal anisotropy constant and v is the nanocrystal volume [7]. The number of crystallite in V is not infinite and a resultant anisotropy energy exists at the scale of V, determined by statistics. This energy, normalised to one nanocrystal, is expected to be proportional to $1/\sqrt{N}$, where N is the number of nanocrystals within the correlation volume.

Fe-based ultra-soft nanomaterials (such as FeSiBNbCu or FeZrB) are formed of α-Fe nanocrytals (10-15 nm in diameter) embedded into an amorphous magnetic matrix (Figure 3) [8]. For these systems, $K \approx 10^{-4}$ J/m^3, the correlation volume thus derived is of macroscopic size. The moments being aligned over macroscopic dimensions, the global magnetic anisotropy is averaged over a very large number of grains and it is vanishingly small. This explains the ultra-soft behaviour obtained. These nanomaterials are used to make transformers for electronic applications.

In R-M intermetallics, the anisotropy constant $K \approx 10^{-7}$J/m^3. The correlation volume deduced is of the order of 10^3 nm^3, i.e. of the order of or smaller than the nanocrystal size. To first approximation, the moments are aligned along the local easy magnetisation direction. In this configuration, the anisotropy is not averaged out. This is in agreement with the existence of large coercivity in NdFeB nanostructured alloys [9]. In order to minimize exchange, the moments close to the interface between two nanocrystals, tend to orientate along some intermediate direction between the 2 local easy magnetisation directions. It results that the magnetisation is higher than the value $M_s/2$ expected for perfect alignment along the individual easy magnetisation directions of an assembly of uniaxial randomly-oriented nanocrystals. This is the phenomenon of remanence-enhancement [10].

Hard nanocomposites include soft and hard exchange-coupled nanocrystals, in which the soft nanocrystals show coercivity (Figure 3) [11]. To explain this, let us assume that the applied field is weaker than the hard nanocrystal coercive field, so that the corresponding magnetization is frozen. Due to exchange coupling at the interface, soft phase magnetisation reversal requires the formation of a moment configuration within the soft phase, which is very reminiscent of a domain wall. However, this wall is constrained to the size of the soft nanocrystals. It is much narrower than it would be in the bulk and its energy is 1-2 orders of magnitude higher. Thus, the soft phase resists reversal [12]. The most common of these materials associate hard $Nd_2Fe_{14}B$ nanocrystals and soft α-Fe or Fe_3B ones; $\mu_0 H_c$ values up 0.7 T are obtained. When these materials were discovered [11], it was hoped that new high performance materials could be produced by associating a

▶ Fig. 3: Three different types of nanostructured magnetic materials (a) FeSiBNbCu ultra-soft magnetic materials (b) NdFeB hard nanocomposites (c) CoCrPtB magnetic films for storage. In (a), the soft magnetic properties directly result for exchange coupling between the grains. In (b), exchange coupling between soft and hard grains is at the origin of the global coercivity obtained In (c), exchange decoupling between grains is characteristic of materials for magnetic recording so that the magnetisation of any given region may be reversed, without influencing others.

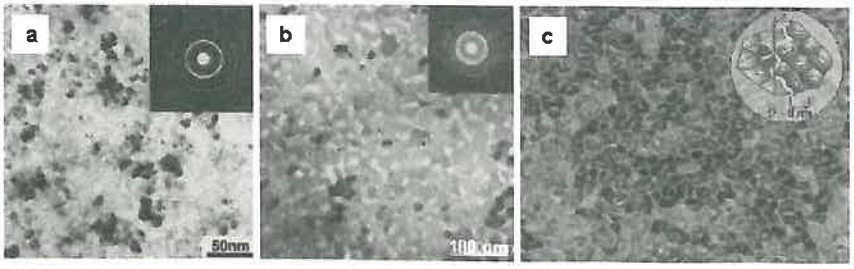

features

coercive hard magnetic phase with large magnetisation soft phases. To date, the properties obtained do not merit large industrial development. The recent successful preparation of anisotropic nanocomposites may open new perspectives [13].

Storage media consist of exchange-decoupled randomly-oriented grains. The transition region from one bit to the next must be sharp. This implies that each bit is made of a large number of grains, typically 100-1000. The recording density envisaged with magnetic tapes is of the order of 5 Gbits/in^2. The corresponding particle volume is around 10^5 nm^3. In modern HDD, the recording density approaches 100 Gbits/in^2. At this density, the bit size is 0.2 μm x 0.1 μm and the particle volume is around 100 nm^3. Thus, magnetic storage necessarily involves nanomaterials (Figure 3) [4].

At such small particle sizes, the phenomenon of superparamagnetism must be considered [1]. The total anisotropy energy of one nanoparticle, Kv, must be compared to the energy brought by thermal activation at the temperature T, of the order of $25k_BT$. Setting $Kv = 25k_BT$, gives $K = 10^6$ J/m^3 which represents a very significant anisotropy. In materials with lower anisotropy value, the magnetisation will fluctuate spontaneously under the effect of thermal activation. This effect is thought to set a limit for magnetic recording density and this limit will be reached before the year 2005. Various approaches are being examined to push superparamagnetism to higher temperature values. These include the growth of pillars, such that the particle volume is increased but the storage density is not affected [14]. In other approaches, the ferromagnetic film, in which the information is stored, is antiferromagnetically coupled to another ferromagnetic layer [15] or the ferromagnetic particles are embedded within an antiferromagnetic matrix [16].

The above discussion concerned longitudinal recording. The particle magnetisation lies in the plane of the substrate. Perpendicular recording is an alternative, which will allow the recording density to be pushed forward by a factor of 4 approximately. Even more promising, is the development of "quantum bits" in which each bit of information is a unique magnetic object. Approaches towards this include film deposition on structured substrates or the direct self-organisation of magnetic nanoparticles prepared by chemistry. Spectacular results in this field have been obtained with FePt nanoparticles [17].

References

[1] R. C. O'Handley, Modern Magnetic Materials: Principles and Applications, John Wiley and Sons, New York, (2000)

[2] R. Skomski and J.M.D. Coey, Permanent Magnetism, IOP (1999)

[3] Rare-Earth Iron Permanent Magnets, J.M.D. Coey (Editor), Clarendon Press, Oxford, 1996

[4] M. Futamoto, N. Inaba, Y. Hirayama, K. Ito and Y. Honda, J. Magn. Magn. Mater. 193 (1999) 36; D. Speliotis, J. Magn. Magn. Mater. 193 (1999) 29

[5] Magneto-Optical Recording Materials R.J. Gambino and T. Suzuki (Editors), IEEE Computer Society, 1999

[6] M.E. Mc Henry and D.E. Laughlin, Acta Mater. 48 (2000) 223

[7] G. Herzer, in Handbook of Magnetic Materials, ed; K.H.J. Buschow, vol. 10, chap.3 (1997) 415, Elsevier Science, Amsterdam

[8] K. Hono, A.Inoue and T. Sakurai, Appl. Phys. Lett., 58 (1991) 2180

[9] J.J. Croat, J.F. Herbst, R.W. Lee and F.E. Pinkerton, Appl. Phys. Lett. 44 (1984) 148

[10] A. Manaf, R.A. Busckley, H.A. Davies, M. Leonowicz, J. Magn. Magn. Mater. 101 (1991) 360

[11] R. Coehoorn, D.B. de Mooij, J.P.W.B. Duchateau and K.H.J. Buschow, J. de Phys. C8 49 (1988) 669

[12] E.F. Kneller and R. Hawig, I.E.E.E. Trans. Magn. 27 (1991) 3588

[13] D. Lee, J.S. Hilton, S. Liu, Y. Zhang, G.C. Hadjipanayis and C.H. Chen, I. E.E.E. Trans. Mag. (to appear)

[14] O. Fruchart, M. Klaua, J. Barthel et J. Kirschner, Phys. Rev. Lett. 83 (1999) 2769

[15] E. N. Abarra, A. Inomata, H. Sato, I. Okamoto, and Y. Mizoshita, Appl. Phys. Lett., 77 (2000) 2581

[16] V. Skumryev, S. Stoyanov, Y. Zhang, G. Hadjipanayis, D. Givord and J. Noguès, Nature 850 (2003) 423

[17] S. Sun, C.B. Murray, D. Weller, L. Folks and A. Moser, Science 287 (2000) 1989

Imaging of micro- and nanomagnetic structures

C. König, F. Kiendl, U. Rüdiger, and G. Güntherodt*
II. Physikalisches Institut, Aachen University, Aachen, Germany
**Fachbereich Physik, Konstanz University, Konstanz, Germany*

There is a great interest in understanding the micromagnetic behavior of thin ferromagnetic layers, driven by their technological exploitation in magnetic field sensors and magnetic random access memory devices (MRAM). As a high storage density is a key goal in the design of such memory devices, recent research has been concentrating on the investigation of ferromagnetic elements with submicrometer lateral dimensions. For a magnetic storage cell to define a bit (0 or 1), it must have two stable remanent magnetization states that are uniformly magnetized, i.e. form a single magnetic domain, independent of its magnetic history.

Apart from other powerful magnetic imaging techniques, we focus on two particular techniques to investigate the magnetic domain configurations of micro- and nanomagnetic structures: Magnetic Force Microscopy (MFM) [1,2] and Scanning Near-Field Optical Microscopy (SNOM) [3,4].

MFM

The MFM detects the magnetic stray fields (blue arrows in Figure 1) which are generated at the edges of magnetic elements

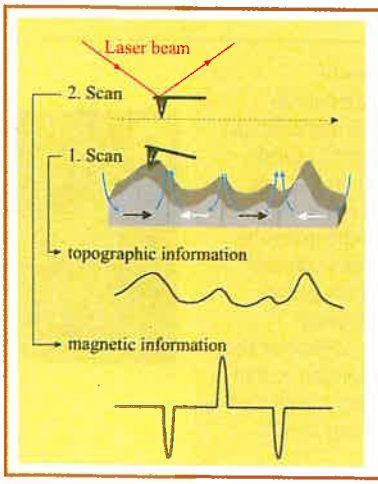

Fig. 1: Imaging mechanism of a Magnetic Force Microscope.

(bits) or in domain walls. For this purpose a small magnetic needle (tip) which is magnetized along the needle axis is attached to the end of a cantilever. This tip is being attracted or repelled by the magnetic stray fields pointing into or out of the surface of the magnetic element (bit), respectively. The deflection of the cantilever resulting from this dipole-dipole-interaction is detected by a laser beam which is reflected at the upper side of the cantilever and hits a four-segment detector. Figure 1 shows schematically how the magnetic information is extracted from this signal. To avoid a cross talk by "atomic force" information the MFM first scans the topography.

The magnetic information is subsequently recorded by lifting the tip to a height of approximately 90 nm and scanning along the topographic profile obtained in the first scan. This method yields the typical MFM images with "dark and bright contrast" depending on direction and strength of the magnetic stray fields.

Figure 2 shows an MFM image of microstructured Fe(110) ellipsoid-shaped elements with lateral dimensions of 1.5 µm 500 nm. Starting with a 25 nm thick iron film with (110) orientation these elements have been fabricated by using electron beam lithography and argon ion etching [6]. After applying a magnetic field of 1 Tesla perpendicular to the long axis of the elements - i.e. along the magnetic hard axis - the MFM image exhibits three different remanent magnetic states for zero magnetic field (see white frame in Figure 2).

If the bright contrast represents an attractive interaction between the tip and the stray fields the upper element in the white frame shows a single domain state (or dipole state) with the magnetization pointing to the right side as illustrated in the upper left inset in Figure 2. According to this the magnetization of the lower element in the white frame is pointing to the right. The element in the middle shows a less pronounced magnetic contrast. This is an evidence for a multi domain state (or demagnetized state). By forming such a state the stray fields are minimized by closing the magnetic flux within the element (see the upper right inset in Figure 2).

SNOM

When a magnetic sample is illuminated with polarized light, it rotates the polarization of the transmitted (Faraday effect) and reflected (Kerr effect) light by an amount proportional to its magnetization. Therefore, a pattern of differently magnetized domains produces a contrast in a polarization-sensitive magneto-optical (MO) microscope. For this microscopy to work, neither a vacuum nor atomically clean surfaces are required. It can be used in an external magnetic field to probe the dependence of the

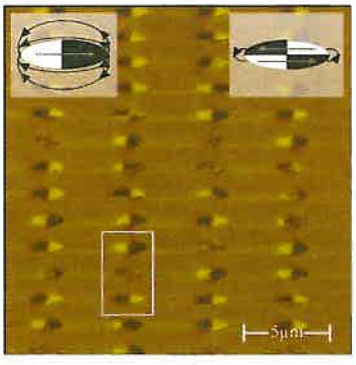

◀ Fig. 2: MFM image of microstructured ellipsoid-shaped Fe(110) elements [5].

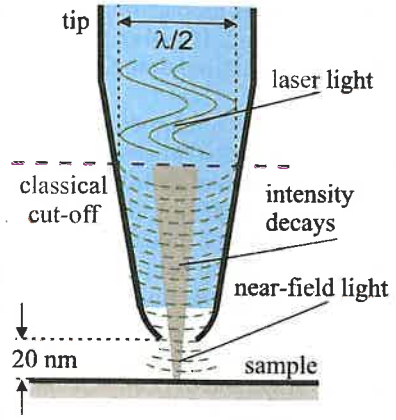

▶ Fig. 3: Imaging mechanism of a scanning near-field optical microscope.

domain pattern on the field. Also, unlike in MFM, there is no danger that the domain pattern is altered by the imaging process itself. Any optical microscopy, however, is limited in its resolution by diffraction. Every illuminated spot on the sample produces its own diffraction pattern, which cannot be distinguished from the diffraction pattern of another spot located less than λ/2 away, where λ is the light's wavelength. Smaller structures therefore cannot be resolved.

Scanning near-field optical microscopy (SNOM) eliminates the need to distinguish diffraction patterns from one another. In the most common "aperture configuration" (Figure 3), a probe with an aperture much smaller than l illuminates only one small spot on the sample at a time. No matter how the light is being diffracted, it is known which spot on the sample it corresponds to. A complete image of the sample is generated by scanning the probe across a grid of spots and assembling the information from all spots by computer.

How is it that light can be emitted from such a small aperture at all? Isn't there a cut-off diameter of λ/2 below which an aperture is not transparent? That depends on how close to the aperture you look. Light is actually transmitted through the aperture, but it is strongly (exponentially) damped as soon as the tip gets narrower than λ/2. Its intensity decreases by a factor of 1/*e* every 20 nm. The light is therefore called evanescent or near-field light, and for it to interact with the sample at all, the aperture must be brought to

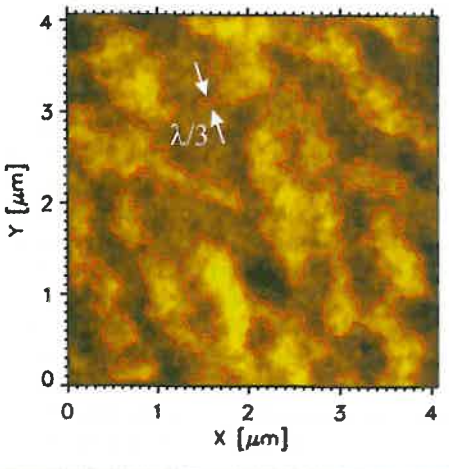

▲ Fig. 4: Magneto-optical SNOM image of a Co/Pt multilayer film.

within 20 nm of the sample surface. Part of the light is converted back into normal, propagating light by the sample and can therefore be detected. If polarized light is used (MO-SNOM), differently magnetized domains produce a contrast in the image as usual.

Figure 4 shows a magneto-optical image produced with our magneto-optical SNOM set-up [7,8] on a Co/Pt multilayer film. The magnetization of such a film is stable when it is perpendicular to the film plane, pointing either out of it ("up") or into it ("down"). Before the image was taken, the film was exposed to a high (2 T) magnetic field in the film plane. When the field was switched off, there was nothing to keep the magnetization in this unstable orientation, so it relaxed into a random pattern of domains magnetized either "up" or "down". These domains appear as bright and dark areas in the image; the domain boundaries are marked by red lines. Rotating the detection set-up reversed the image contrast, proving its magneto-optical origin. The smallest domains visible in Figure 4 are about $\lambda/3$ in size, using an aperture of about 100 nm in diameter and laser light with wavelength λ=488 nm.

References

[1] Y. Martin and H. K. Wickramasinghe, Appl. Phys. Lett. **50**, 1455 (1987)

[2] J. J. Sáenz, N. García, P. Grütter, E. Meyer, H. Heinzelmann, R. Wiesendanger, L. Rosenthaler, H. R. Hidber, and H.-J. Güntherodt, J. Appl. Phys. **62**, 4293 (1987)

[3] D. Pohl, European patent application No. 0112401, Dec. 27 (1982); US patent 4,604, Dec. 20 (1983)

[4] A. Lewis, A. Harootunian, M. Isaacson, E. Kratschmer, Biophys. J. **49**, 269 (1983)

[5] C. König, M. Sperlich, R. Heinesch, R. Calarco, J. O. Hauch, U. Rüdiger, S. Kirsch, B. Özyilmaz, A. D. Kent, and G. Güntherodt, Appl. Phys. Lett. **79**, 3648 (2001)

[6] J. Yu, U. Rüdiger, A. D. Kent, L. Thomas, and S. S. P. Parkin, Phys. Rev. B **60**, 7352 (1999)

[7] G. Eggers, A. Rosenberger, N. Held, A. Münnemann, G. Güntherodt, P. Fumagalli, Ultramicroscopy **71**, 249 (1998)

[8] P. Fumagalli, A. Rosenberger, G. Eggers, A. Münnemann, N. Held, G. Güntherodt, Appl. Phys. Lett. **72**, 2803 (1998)

Magnetoresistive biochips

P.P. Freitas[1,2], H. Ferreira[1,2], D. Graham[1], L. Clarke[3], M. Amaral[3], V. Martins[4], L. Fonseca[4], J.S. Cabral[4]

[1] *INESC-MN, R.Alves Redol, 9 , 1000 Lisbon, Portugal*

[2] *Physics Department, Instituto Superior Tecnico, R.Rovisco Pais, 1000 Lisboa*

[3] *Biology Department, FCUL, Campo Grande, 1000 Lisboa*

[4] *Bioengineering Department, Instituto Superior tecnico, R. Rovisco Pais, 1000 Lisboa*

Detection of biomolecular recognition has been playing an ever important role when applied to DNA-DNA hybridisation (genetic disease diagnostic, mutation detection, gene expression quantification) and antibody-antigen interaction (micro-organism detection, biological warfare agent detection, etc...). A typical DNA biochip will consist of an array of probes (for example gene specific oligonucleotides that were immobilized onto the functionalised chip surface through microspotting), an hybridisation chamber (normally a microfluidic channel arrangement) together with an optional target arraying mechanism (electric fields for charged molecules such as DNA), the target biomolecules (eg, a complementary DNA strand to the immobilized DNA probe), the label (a fluorescent molecule that can be attached to the target), and a hybridization detection mechanism that can be either integrated on the chip or external to the chip (for instance, in the case of fluorophore labels, detection is done by an external laser-based fluorescence scanner) [1,2]. An hybridisation detection experiment (see Fig.1a) occurs through four phases, respectively 1) probe immobilization on chip surface, 2) target labelling, 3) target arraying, hybridization and washing, 4) detection. Requirements on the detection scheme depend on the particular biological assay.

For *gene expression* chips, where the relative amount of a certain gene must be quantified and compared between different patient samples, the detection scheme must lead not only to the knowledge of the presence of the particular gene (Yes or No) but also to a quantitative analysis (present in what percentage). For *Single Nucleotide Polymorphism* chips (SNP), where single DNA base pair changes are being identified, the simple (Yes or No) answer is sufficient. In both cases, the chip should be able to discriminate against false positives (non-specifically bound molecules). A recent example of this technology are DNA microarray chips fabricated by Nanogen [3], where charged target biomolecules are moved over immobilized probes. Electric fields are used for hybridization enhancement and stringency control.

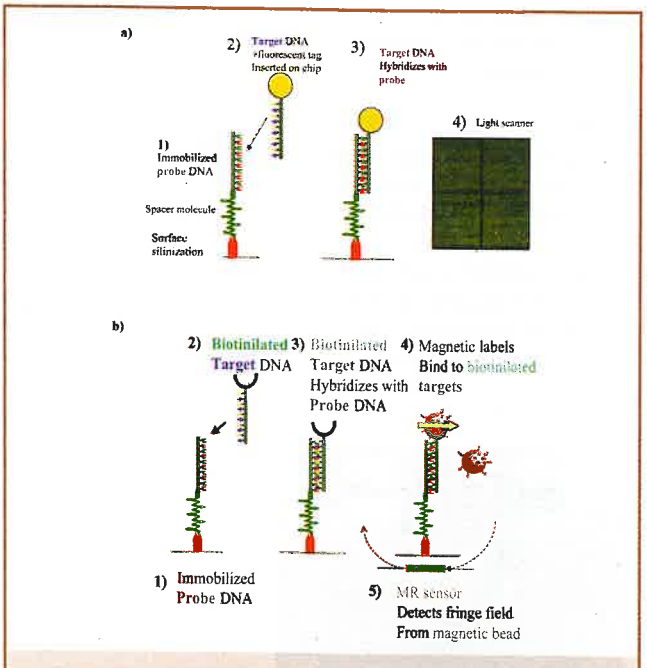

▲ Fig. 1: a) Conventional hybridisation detection using fluorescent labels attached to biological targets, and an external laser-based fluorescent scanner for detection.
b) magnetoresistive-based hybridization detection using magnetic labels, and an integrated magnetoresistive sensor array for detection.

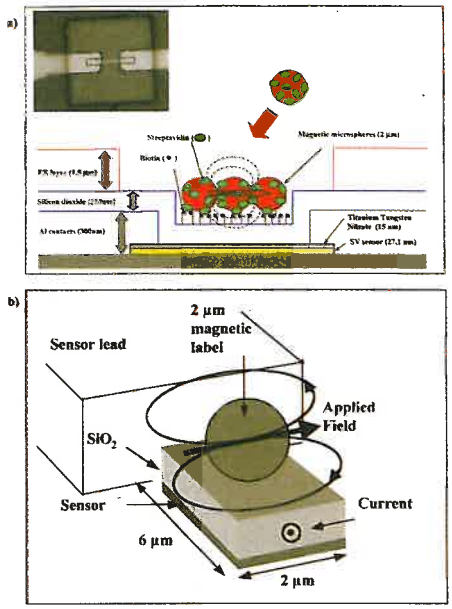

▲ Fig. 2: a) Cross-section of a MR-biochip, showing the spin valve sensor, the leads, the 2000Å thick SiO_2 functionalized passivation layer, the immobilized probes (in this case biotin), and the hybridized targets (streptavidin) coating the magnetic labels. The inset shows the top-view of the probe-pad. b) Detection geometry: a 150e in-plane field magnetizes the superparamagnetic labels, and in turn, these produce a transverse in-plane field in the spin valve).

Detection is external to the chip, done by a laser-based fluorescence scanner. Fluorescence-based systems suffer from gradual loss of label fluorescent emission upon light excitation (photobleaching), and require careful background signal subtraction. Alternative approaches are being pursued in various labs to incorporate other labels (or no labels at all), in order to fully integrate the detection mechanism, aiming at a fully electronic and microfluidic portable and cheap apparatus, of widespread use.

MR-Biochips

Magnetoresistive-based biochips were first introduced in 1998 [4,5]. Fluorophore labels are replaced by magnetic labels (superparamagnetic particles), and detection is done using an integrated magnetic field sensor (GMR multilayer [6], spin valve [7], AMR ring [8], Hall effect cross [9]). The hybridization detection process is shown in Fig.1b. Since the magnetic labels used so far have been relatively large (from 100nm up to 2 μm in diameter) [10],and may hinder the hybridization process if previously attached to the targets, hybridization occurs between the immobilized probe and a biotinylated complementary target (no label, step 3). Streptavidin coated labels are added in a post-hybridization step (4), and detection is done in real-time. The use of magnetic labels allows the use of magnetic fields for stringency control, as well as for arraying (if previously attached to targets). Since magnetic material is usually not present in biomolecules, background signal subtraction is greatly simplified. Fig.2a) represents the cross-section of the MR-biochip at the sensor area.

The MR sensor is passivated by a 0.2μm oxide or nitride layer (required to prevent sensor damage by salt solutions during immobilization, hybridization and washing).

The MR sensor directly measures the in-plane transverse field created by the magnetized label. For applied fields of 15 Oe, 2um Micromod particles (15% FeOx content) have a moment of 10^{-12} emu, creating a maximum transverse bead field of about 1 Oe on the sensor. Fig.2b) shows the detection geometry when using an in-plane field to magnetize the beads, and spin-valve sensors for detection. Depending on the biological assay, the sensor architecture must be designed for its particular application. For example consider μm size labels. If a linear response to the number of labels (up to few hundred) is required, as for example in a *gene expression* chip, the sensor can be made of a spin valve or GMR material in a meander configuration occupying most of the area under the probe pad [6,11]. The output is proportional to the area of the sensor excited by the particles fringe fields. For a spin valve sensor [12], the linear range can be easily tuned from 10 Oe to few hundred Oe either by reducing sensor height and increasing the demagnetising field, or implementing a longitudinal exchange bias field H_{bias} onto the free layer. The dynamic range for these sensors allows measurements from few to few hundred particles. If on the other hand, a *SNP* chip is envisaged, the spin valve sensor dimension can be tuned to that of the particle, and single labels with moments as low 10^{-14} emu should be detected. This minimum detectable moment (field) is limited by the sensor noise [10], and measuring electronics setup (DC vs lock-in detection). MR sensors are normally used in a Wheatstone bridge configuration in order to minimize thermal offsets and to null bridge response in the absence of particles. Fig.3a) shows a typical SNP spin valve sensor biochip , emphasizing the differential detection scheme, while Fig.3b) shows the picture of a packaged device,

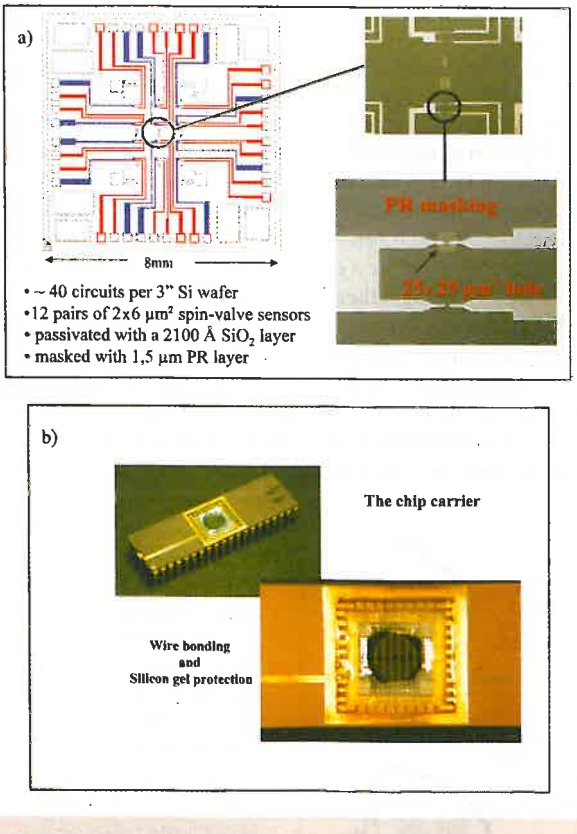

▲ Fig. 3: a) Schematics of one of the MR biochips, using differential detection, with one active sensor and one reference sensor as two arms of a Wheatstone bridge configuration. b) Packaged MR biochips ready for biological assaying.

features

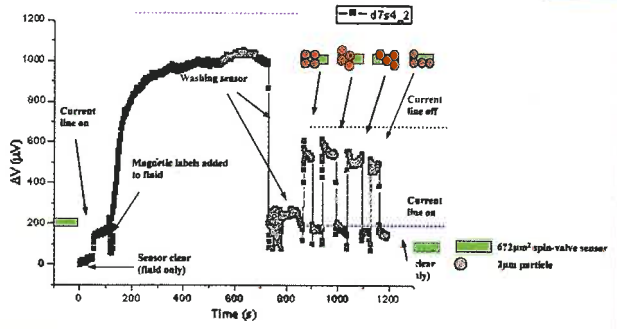

▲ **Fig. 4:** Bead detection using spin valve sensors. After sensor saturation (1mV) , beads are washed away, and repeatidly brought over the sensor. Number of beads is checked by optical microscopy. The sensor signal reproduces clearly the bead immobilization onto and release from the sensor.

ready for biological assaying.

Fig.4 Shows detection signals for few (1-4) 2μm particles over a 6×2μm² spin valve sensor with an MR signal of 8%. For sensor linearization, the sense current is set at 8mA.

An in-plane transverse field of 15Oe is used to magnetize the superparamagnetic beads. A simple DC method was used to measure the sensor output(10μV noise level). For this experiment, the labels were controllably moved across the sensor using field gradients created by auxiliary current lines. Typical signals for single beads are of the order of 150uV/bead.

DNA-cDNA hybridization detection: cystic fibrosis CFTR gene recognition

As an example of DNA-cDNA hybridization recognition using the MR biochip a cystic fibrosis specific 50mer (50 base pairs) oligonucleotide corresponding to a particular strand of the CFTR gene was immobilized onto the 2000 Å thick, sputtered SiO_2 probe pad, covering the MR sensor area. The goal is to detect whether a complementary target will bind or not. Prior to probe immobilization, SiO_2 functionalization was achieved by surface silinization followed by a cross linker placement. Hybridization was attempted using either complementary or non-complementary biotinylated DNA target sequences. After hybridization and washing to remove non-specifically bound DNA targets, streptavidin functionalized magnetic labels are introduced in solution. These attach to the bound, biotinilated complementary DNA targets. Real time measurement of the sensor output during multiple label injection and washing cycles show (see Fig.5a) that where

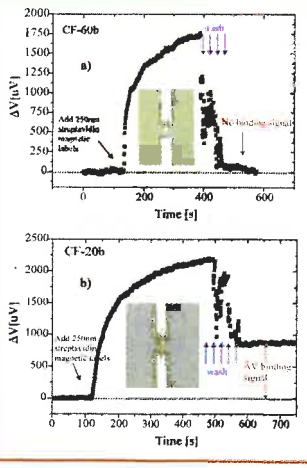

◀ **Fig. 5:** a) Detection of DNA recognition using streptavidin coated 250nm labels, and a biotinylated complementary target. After washing to eliminate non-specifically bound molecules, a strong remnant signal remains, from the bound complementary targets. b) When a non-complementary target is used, after washing, no remnant signal is observed.

hybridization has occurred, MR sensor remnant signals of 1mV are observed, corresponding to about 100 nanoparticles (250nm) bound. Direct optical analysis confirms the MR signal results. When a non-complementary DNA strand is used (Fig.5b), no remnant signal is observed.

Conclusion

MR technology is being successfully applied to biomolecular recognition in different contexts. Advances are required in the development of biocompatible magnetic labels with higher moments (eg, pure Co, Fe, NiFe particles), and nanometric dimensions (< 100nm) providing clustering can be avoided and biocompatibility assured. Developments in the sensing technology are required to allow measurements of single nm-sized labels with moments at the 10^{-15} emu level. Developments are required in the use of magnetic and electric fields for arraying, hybridization enhancement, and force discrimination of non-specifically bound biomolecules. MR technology has shown the potential for single molecule process detection, a target not usually within the reach of most of the competing technologies.

References

[1] "Fundamentals of DNA hybridisation arrays for gene expression analysis", W.M.Freeman, D.J.Robertson, K.E.Vrana, BioTechniques vol.29, pp.1042-1055, 2000

[2] "cDNA microarray technology and its applications", C.Xiang and Y.Chen, Biotechnology Advances vol.18, pp.35-46, 2000

[3] http://www.nanogen.com

[4] "A biosensor based on magnetoresistive technology", Biosens.Bioelectr. vol.13, pp.731-739, 1998

[5] "Biosensor using magnetically detectable label", US Patent 5,981,297, Nov.9,1999

[6] "A DNA array sensor utilizing magnetic microbeads and magnetoelectronic detection", M.M.Miller, P.E.Sheehan, R.L.Edelstein, C.R.Tamanaha, L.Zhong, S.Bounnak, L.J.Whitman, R.J.Colton, J.Magn.Magn.Mater., vol.225, pp.138-144, 2001

[7] "Single magnetic microsphere placement and detection on-chip using current line designs with integrated spin-valve sensors: biotechnological applications", D.L.Graham, H.A.Ferreira, J.Bernardo, P.P.Freitas, J.M.S.Cabral, J.Appl.Phys., vol.91, pp.7786-7788, 2002

[8] "Detection of a micron-sized magnetic sphere using a ring.shaped anisotropic magnetoresistance based sensor: a model for a MR based biosensor", M.M.Miller, G.A.Prinz, S.F.Cheng, S.Bounnak, Appl.Phys.Lett., vol.80, pp.4199-4201, 2002

[9] "Detection of single magnetic microbead using a miniaturized silicon Hall effect sensor", P.A.Besse, G.Boero, M.Demierre, V.Pott, R.Popovic, Appl.Phys.Lett., vol.80, pp.4199-4201, 2002

[10] "Biodetection using magnetically labelled biomolecules and arrays of spin valve sensors", H.A.Ferreira, D.L.Graham, P.P.Freitas, J.M.S.Cabral, J.Appl.Phys., vol.93, pp.7281-7286, 2003

[11] " A biochip based on a magnetoresistive sensor", J.Schotter, P.B.Kamp, A.Becker, A.Puhler, D.Brinkmann, W.Schepper, H.Bruckl, G,Reiss, IEEE Trans.Magn., vol.38, pp.3365-3367, 2003

[12] "Spin valve sensors", P.P.Freitas, F.Silva, N.J.Oliveira, L.V.Melo, L.Costa, and N.Almeida, Sensors and Actuactors A, vol.81, pp.2-8, 2000

The new era of spintronics

Albert Fert, Jean-Marie George, Henri Jaffrès, Richard Mattana, and Pierre Seneor, Unité Mixte de Recherche CNRS-Thales (Associée à l'Université Paris-Sud), Orsay, 91404, France.

Spintronics, at the interface between magnetism and electronics, is a new field of research in considerable expansion [1]. The basic concept of spintronics is the manipulation of spin currents, in contrast to mainstream electronics in which the spin of the electron is ignored. Adding the spin degree of freedom provides new effects, new capabilities and new functionalities. Beyond today's applications to hard discs and memories, the potential of spintronics is very promising for new advances and an important impact on science and technology of the 21st century.

The influence of the spin on the electronic transport properties of ferromagnetic materials has been known for a long time. The existence of spin polarized currents in ferromagnetic metals, first suggested by Mott, has been experimentally demonstrated and theoretically described about thirty years ago, mainly by European researchers (at Orsay, Strasbourg, Eindhoven). In metals like iron or cobalt, the "majority spin" and "minority spin" electrons carry currents that can be different by more than a factor of ten. This spin dependent conduction comes from the splitting of the "majority spin" and "minority spin" energy bands and also from the spin dependent cross section of some defects or impurities.

Everybody has already a spintronic device on their desktop

The first step on the road of the utilization of the spin degree of freedom was the discovery of the Giant Magnetoresistance of magnetic multilayers in 1988 [2]. A magnetic multilayer is a film composed of alternate ferromagnetic and nonmagnetic layers, Fe and Cr for example. The resistance of such a multilayer is lowest when the magnetic moments of ferromagnetic layers are aligned, and highest when they are antiparallel. As the relative change of resistance can be as high as 200%, this effect has been called Giant Magnetoresistance (GMR). The condition required for GMR is a much better conduction through a ferromagnetic layer by the electrons of one of the spin directions, say the majority spin direction for example. When the magnetic moments of all the layers are aligned, half of the electrons are majority spin electrons in all the magnetic layers, and the short circuit effect by this high conduction channel results in a low resistance. In the antiparallel configuration, each electron is alternately a majority and a minority spin electron, the short circuit effect does not exist and the resistance is much higher. In specially designed multilayers, known as spin valves, the magnetic configuration can be switched between parallel and antiparallel configuration by a field of only a few Oersted, so that a large change of resistance can be induced by a very small field. The first spintronic devices have been based on spin valves. Today everybody has already a spintronic device on their desktop, since all modern computers use spin valves for the read heads of the hard disc. Because they can detect very small fields and very small magnetic bits, the spin valve-based read heads have led to an increase of the density of stored information by almost two orders of magnitude. It might however be hard to go beyond the 100 Gbit/in^2 of today's prototypes with conventional spin valves. A further increase of read head sensitivity and information density in hard discs will be probably achieved with other spintronic devices, magnetic tunnel junctions [2] (see next paragraph), patterned multilayers for GMR in the non-conventional geometry where the current is perpendicular to the layers [4] or magnetic nanocontacts presenting a ballistic version of GMR known as BMR [5].

Magnetic tunnel junctions and MRAM

The magnetic tunnel junction (MTJ) [3] is the second type of spintronic device that will have soon important applications. A MTJ (Fig. 1a) is a structure in which two ferromagnetic layers (electrodes) are separated by a very thin insulating layer, commonly aluminum oxide. The electrons can tunnel through the insulating layer and, because the probability of tunneling from a ferromagnetic electrode depends on the spin direction, the resistance of the MTJ is different for the parallel and antiparallel orientations of the magnetic moments of the electrodes [3]. For electrodes of conventional ferromagnetic alloys, the relative change of resistance (Tunnel Magnetoresistance or TMR) can reach 70% at room temperature. MTJ of very small size, below the micron range, can be fabricated by lithographic techniques and an important application of these small size MTJ will be for a new type of computer memory, the MRAM (Magnetic Random Access Memory). As illustrated in the upper part of Fig.1, each junction can store one bit of data, say "0" for the parallel configuration of the magnetic moments of the electrodes, "1" for the antiparallel configuration. The sketch below is a schematic representation of a MRAM with MTJ connected together in a point contact array. The MRAM presently in development are expected to reach similar densities and access times as the current DRAM or SRAM, but their main advantage on these volatile semiconductor-based memories is that they retain data after the power is

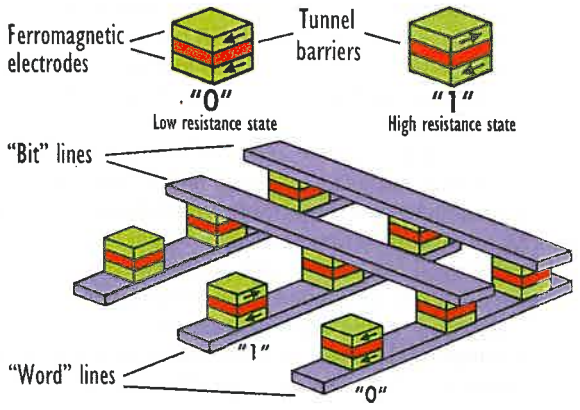

▲ Fig. 1: Top: Memory cells of an MRAM (Magnetic Random Access Memory). Each cell is a submicronic MTJ and the states "0" and "1" of the cell corresponds respectively to the parallel and antiparallel configurations of the magnetic moments of electrodes of the MTJ (low and high resistance states). Central sketch: schematic of an MRAM constructed of MTJ connected together in a point contact array. Conducting wires, "bit lines" and "word lines" permit voltage measurements to read the stored information. They also enable manipulation of the magnetization of the elements (writing) by the magnetic field created by currents in the lines. The main advantage of MRAM over semiconductor-based DRAM or SRAM is their permanent character (for similar density and speed).

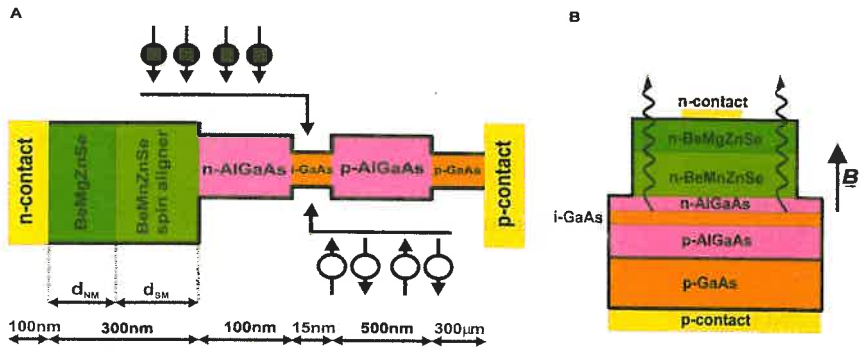

◀ **Fig. 2:** Spin Light Emitting Diode (Spin-LED). A current of spin-polarized electrons is injected from the diluted magnetic semiconductor $Be_xMn_yZn_{1-x-y}Se$ into a GaAs/GaAlAs light-emitting diode A circularly polarized light is emitted from the recombination of the spin polarized electrons with non-polarized holes. An injection efficiency of 90% spin polarized current has been demonstrated by Fiederling *et al.* [10]. As $Be_xMn_yZn_{1-x-y}Se$ is paramagnetic, the spin polarization is obtained only in an applied field and at low temperature.

turned off, possibly eliminating the long boot-up time when the computer is switched on. The MRAM have also an important advantage in terms of speed (a gain of 1000 for the write time) over the permanent memories of Flash type that are used today for mobile electronics. At least two commercial efforts—one by Motorola, the other by IBM and Infineon in Munich—plan to begin production of MRAM in 2004.

Though commercial products using MTJ are expected very soon, the physics of spin dependent tunneling is still far from being clearly understood. In the early research on the MTJ, it was thought that the spin polarization of the tunneling electrons and the TMR were simply reflecting the spin polarization of the electronic density of states at the Fermi level in the ferromagnetic electrodes. It now turns out that the TMR also depends on the insulating material of the tunnel barrier and, more specifically, on the details of the electronic structure at the electrode/barrier interface. The present theories are not really quantitative yet and further theoretical developments are still needed for more reliable predictions. Another important challenge is the research of ferromagnetic materials providing higher spin polarizations than conventional metals like cobalt or iron. A few ferromagnets have been predicted to be half-metallic, that is to present a spin polarization of 100% at their Fermi level. A record TMR ratio of 1800%, corresponding to a spin polarization of 95%, has been found with electrodes of the manganite $La_{2/3}Sr_{1/3}MnO_3$ (LSMO) [6]. However these results are obtained only at low temperature and LSMO cannot be considered for practical devices. Better candidates for room temperature applications seem to be magnetite (Fe_3O_4) and several oxides of double perovskite structure. High TMR ratios might also be obtained with ferromagnetic insulating materials presenting a spin dependent gap and acting as spin filter for the tunneling electrons. Some interesting results have been recently obtained with EuS barriers, but at low temperature only.

Spin transfer to reverse a magnetic moment without applying a magnetic field

In a GMR or TMR device, switching the magnetic configuration changes the electrical current passing through the device. Magnetization reversal by spin transfer is an opposite effect: a spin polarized current is let into a device and the transfer of spin from the current switches the magnetic configuration of the device. This concept of magnetization reversal by spin transfer from a spin-polarized current has been introduced by Slonczewski [7] in 1995 and has been now confirmed by series of experiments (mainly on pillar-shaped multilayers). From the application point of view, reversing a magnetic moment by spin transfer without applying an external applied field can be of great interest to switch spintronic devices, MRAM for example. However the current density needed in the existing experiments is still relatively high, of the order of $10^7 A/cm^2$, and a better understanding of the spin transfer mechanisms seems necessary to obtain a significant reduction ot the current density. Another effect of the same type but probably requiring a smaller current density is the displacement of a domain wall by spin transfer from a spin-polarized current.

Spintronics with semiconductors

Whereas the metallic spin devices just described provide new ways to store and read information in hard discs, tapes or MRAM, semiconductor-based spintronics may offer a greater wealth of possibilities. Why is spintronics with semiconductors interesting? First, semiconductor-based spintronics could combine storage, detection, logic and communication capabilities on a single chip to produce a multifunctional device that could replace several components. For example, it could permit a better integration between MTJ and silicon-based electronics than in the present prototypes of MRAM. The optical properties of the semiconductors are also of particular interest to transform a magnetic information into an optical signal. Finally, because the manipulation of spins presents some advantages in term of speed and required power over the manipulation of charge in conventional electronics, some concepts of device exploiting these advantages have been already proposed.

A first interesting property of the semiconductors for spintronics is the long electron spin lifetime.

A first interesting property of the semiconductors for spintronics is the long electron spin lifetime. Fine time-resolved magneto-optical experiments have been developed at the University of Santa Barbara and have revealed spin lifetimes that can exceed 100 ns for electrons in bulk semiconductors at low temperature [8]. In heterostructures and quantum dots, nanosecond dynamics persist at room temperature [8]. In most of these experiments on spin dynamics, the spin polarization is created by optical excitation. However, for practical applications, it is highly desirable that the injection and detection of spin currents be electrical. The most direct way for spin injection would seem injecting from a classical ferromagnetic metal in a metal/semiconductor heterostructure but this raises difficult problems related to the difference in con-

ductivity and spin relaxation time in metals and semiconductors. Although these problems are now better understood, this has slowed down the progress for spin injection from metals. On the other hand, this has boosted the research on diluted magnetic semiconductors (DMS) [9] that can be associated more easily with nonmagnetic semiconductors for spin injection. GaAs doped with Mn is an archetypal DMS which presents ferromagnetic properties up to 150 K. Some other compounds are promising for room temperature ferromagnetism. We will describe two examples of spin injection from DMS in experiments respectively achieved at the University of Wurzburg [10] and in our team [12].

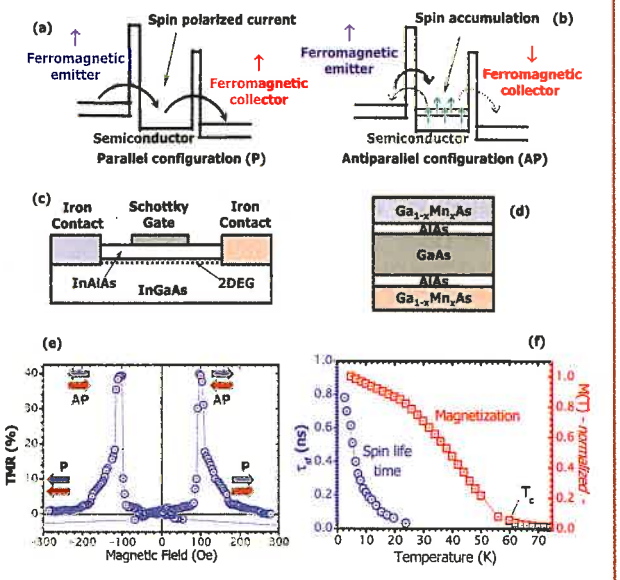

▲ **Fig. 3:** (a,b) Sketches illustrating spin injection from a magnetic spin emitter (metal or semiconductor) into a semiconductor (2D-electron gas channel, Quantum Well, etc.) and spin detection by a magnetic collector (spin analyser). Injection and detection are through tunnel barriers. For a parallel (P) configuration of magnetic moments in the emitter and collector (a), a spin-polarized current (spin up on the figure) is injected and transmitted to the collector. For an antiparallel (AP) configuration (b), spin up electrons are injected and accumulated in the semiconductor (accumulation due to the poor transmission to the collector) and rejected in major part by the spin up accumulation into the emitter. The condition for strong accumulation and large difference between the resistances of the P and AP configurations is that the spin lifetime in the semiconductor be longer than the time spent by the particle in the semiconductor. (c) Lateral heterostructure with metallic spin emitter and spin analyser for spin injection into a 2D Electron Gas (DEG). With a Schottky gate to rotate the spin polarization by the Rashba effect, this device is the Spin Field Effect Transistor proposed by Datta and Das [11]. (d) Vertical heterostructure for injection of spin-polarized holes into a GaAs Quantum Well (QW) in the experiments of Mattana *et al.* [12]. Emitter and analyser are layers of the ferromagnetic semiconductor $Ga_{1-x}Mn_xAs$. (e) Magnetoresistance of a heterostructure of the type of (d) [12]. (f) Temperature dependence of the spin life time in a GaAs QW from magnetoresistnace measurements on a heterostructures of the type of (d).

In the heterostructure of Fig.2, spin-polarized electrons are injected from a paramagnetic DMS ($Be_xMn_yZn_{1-x-y}Se$) into a GaAs/AlGaAs light emitting diode (LED), which leads to emission of circularly polarized light. An injection efficiency of 90% spin polarized current has been demonstrated with this structure [10]. Similar experiments but with smaller polarization have also been performed with spin injection from ferromagnetic GaMnAs and from metals.

Fig.3 illustrates the physics of devices where both injection of spins into the semiconductor and detection of the spin information are electrical. The ideal situation is when the spin lifetime is much longer than the time spent by the carriers in the semiconductor. As illustrated in Fig.1(a,b), a spin-polarized current is then easily transmitted in the parallel configuration of emitter and collector, whereas the antiparallel one leads to spin accumulation and current blockade. In the Datta and Das [11] spin transistor of Fig.3(c), a gate voltage can rotate the spins to switch the device between the two regimes. Fig.3(d) represents an example of vertical version of such an emitter/semiconductor/analyser structure, and, in Fig.3(e), we show the magnetoresistance resulting from the coherent transmission of the spin information in this device [12]. The temperature dependence of the spin lifetime in the GaAs QW derived from this magnetoresistance is shown in Fig.3(f).

The two examples of Fig.2 and 3 show it is now possible to inject spins electrically into a semiconductor heterostructure and to transform the spin information into an optical (Fig.2) or electrical signal (Fig.3). This paves the way for more advanced spintronic devices in which it will be possible to manipulate the spin polarization between emitter and analyser.

In just a dozen of years, we have seen spintronics increasing considerably the capacity of hard disks and now getting ready to enter the RAM of computers. In the next decade, spintronics with semiconductors has the potential to gain an important place in the microelectronics industry. Another perspective, at longer term and out of the scope of this paper, is the exploitation of the truly quantum-mechanical nature of spin and the long spin-coherence time in confined geometry for quantum computing in an even more revolutionary application.

features

References.

[1] For a recent detailed review, see S. A. Wolf *et al.*, Science 294, 1488, 2001.

[2] M. Baibich *et al.*, Phys. Rev. Lett.61, 2472, 1988; Binasch *et al.*, Phys. Rev. B39, 4828, 1989.

[3] M. Jullière, Phys. Lett. 54A, 225, 1975; J. S. Moodera *et al.*, Phys. Rev. Lett.74, 3273, 1995.

[4] J. Bass and W. P. Pratt, J. Mag. Mag. Mat. 200, 274, 1999.

[5] N. Garcia *et al.*, Phys. Rev. Lett. 82, 2923, 1999.

[6] M. Bowen *et al.*, Appl. Phys. Lett. 82, 233, 2003.

[7] J. Slonczewski, J. Mag. Mag. Mat. 159, 1, 1996.

[8] J. M. Kikkawa *et al.*, Science 277, 1284, 1997; Phys. Rev. Lett. 80, 4313, 1998.

[9] T. Dietl *et al.*, Science 287, 1019, 2000.

[10] R. Fiederling *et al.*, Nature 402, 787, 1999.

[11] S. Datta and B. Das, Appl. Phys. Lett. 56, 665, 1990.

[12] R. Mattana *et al.*, Phys. Rev. Lett. 90, 166601, 2003.

EURESCO Conferences

A Programme of the European Science Foundation with the support of the European Commission

2004 PROGRAMME in Physical & Mathematical Sciences

On line at: http://www.esf.org/euresco/

*The EURESCO Programme (European Research Conferences) is run by the European Science Foundation, largely with funding from the Euroconferences Activity of the European Union (except for events marked by *). Each conference consists of a series of meetings, held typically every other year. There are neither written contributions nor proceedings. Unconventional ideas and new approaches, not yet fully explored, are encouraged.*

Mathematics

▪ Symmetries and Integrability of Difference Equations:
EuroConference on Analytic Linear and Nonlinear Difference Equations and Special Functions,
Chair: J. Hietarinta (Turku)
Helsinki, Finland, 19 - 24 June

Physics

▪ Cluster - Surface Interactions:
EuroConference on Cluster Systems and Nanotubes,
Chair: A. Perez (Villeurbanne)
Giens (near Toulon), France, 8 - 13 May

▪ Quantum Optics*:
Quantum Manipulation of Photons, Atoms and Molecules,
Chair: E.A. Hinds (London)
Dates and place to be confirmed

Engineering & Material Sciences

▪ Zeolite Molecular Sieves:
EuroConference on Guest-Functionalised Molecular Sieve Systems,
Chair: F. Marlow (Mülheim a.d. Ruhr)
Hattingen (near Essen), Germany, 20 - 25 March

Chemistry

▪ Molecules of Biological Interest in the Gas Phase*:
Optical Spectroscopy, Mass Spectrometry and Computational Chemistry,
Chair: J.P. Simons (Oxford)
Exeter, United Kingdom, 13 - 18 April

▪ Inorganic Chemistry:
EuroConference on New Theoretical and Spectroscopic Approaches to Inorganic Chemistry Problems,
Chair: C. Mealli (Firenze)
San Feliu de Guixols, Spain, 4 - 9 September

▪ Interfaces and Colloidal Systems*:
Structure and Dynamics of Polymers and Colloidal Systems,
Chair: P. Luckham (London)
Giens (near Toulon), France, 10 - 15 September

▪ Chemistry and Physics of Multifunctional Materials:
From Clever Molecules to Smart Materials EuroConference,
Chair: D. Leigh (Edinburgh)
Tomar, Portugal, 11 - 16 September

Conferences are open to researchers world-wide, whether from industry or academia.
Deadline for applications: 3-4 months before a conference. Participation will be limited to 100.
***Grants** are available in particular for nationals under 35 from EU or Associated States.*

For information & application forms contact:

EURESCO Office, European Science Foundation, 1 quai Lezay-Marnésia, BP 90015, 67080 Strasbourg, France
Fax: +33 (0)388 36 69 87 • E-mail: euresco@esf.org • WWW server: www.esf.org/euresco

EURESCO Conferences

A Programme of the European Science Foundation with the support of the European Commission

Zeolite Molecular Sieves:
EuroConference on Guest-Functionalised Molecular Sieve Systems

Hattingen (near Essen), Germany, 20 - 25 March 2004

Chair: Frank Marlow (MPI für Kohlenforschung, Mülheim a.d. Ruhr, D)
Vice-chair: Mika Lindén (Åbo Akademi University, SF)

Speakers will provisionally include:

G.S. Attard (Southampton, UK); T. Bein (Munich, D); C. Bräuchle (Munich, D); J. Caro (Hannover, D); H. Garcia (Valencia, E); P.J. Grobet (Heverlee, B); H.W. Hillhouse (West Lafayette, US); N. Hüsing (Wien, A); J.C. Jansen (Delft, NL); F.G. Laeri (Darmstadt, D); U. Müller (Ludwigshafen, D); J.-L. Paillaud (Mulhouse, F); C. Sanchez (Paris, F); G. Schulz-Ekloff (Bremen, D); S.A. Schunk (Heidelberg, D); O. Terasaki (Stockholm., S); F. Tihay (Rueil-Malmaison, F); B. Weckhuysen (Heverlee, B); J. Weitkamp (Stuttgart., D); D. Wöhrle (Bremen., D); P. Wright (St. Andrews, UK).

Scope of the conference:

This conference – the second of the series – will deal with the synthesis, characterization, properties and applications of guest-functionalized crystalline or organized porous solids (zeolites, mesoporous solids, macroporous solids).

The aim is an assessment of the relationship between methods of preparation, characterization of the composites and properties of the materials. It should open the way to progress in the synthesis of novel materials and the tailoring of their properties. The development of new applications concepts is also expected. Sessions will focus on:
• Modification • Characterization • Novel Functions.

The scientific programme will include about 13 invited lectures, 8 sessions of short oral presentations of selected posters given by young researchers, 8 discussion sessions, 4 poster sessions and 2 round-table discussions chaired by industrial researchers. There will be no Proceedings and no Book of Abstracts.

Deadline for applications: 19 December 2003

Cluster - Surface Interactions:
EuroConference on Cluster Systems and Nanotubes

Giens (near Toulon), France, 8 - 13 May 2004

Chair: Alain Perez (Université Claude Bernard Lyon I, F)

Speakers will provisionally include:

J.-P. Ansermet (Lausanne, CH); R. Berndt (Kiel, D); X. Blase (Lyon, F); J.-P. Bucher (Strasbourg, F); C. Colliex (Orsay, F); J. Feldmann (München, D); A. Fert (Corbeville, F); A. Gerber (Tel Aviv, IL); A. Li Bassi (Milano, I); L.M. Liz Marzan (Vigo, E); B. Masenelli (Lyon, F); K.H. Meiwes-Broer (Rostock, D); P. Milani (Milano, I); R. Palmer (Birmingham, UK); G. Pastor (Toulouse, F); S. Purcell (Lyon, F); J.-Y. Raty (Liège, B); J. Sloan (Oxford, UK); K. Teo (Cambridge, UK); F. Vallée (Bordeaux, F); T. Vossmeyer (Stuttgart, D); W. Wernsdorfer (Grenoble, F); M. Wolf (Berlin, D).

Scope of the conference:

The rapid developments in the field of clusters, nanoparticles, nanotubes and nanowires physics clearly indicate the vital role which will be played by these systems in future. This conference, instead, is thought to more concentrate on clusters and nanostructures which are governed by quantum effects. This means that the physical and chemical properties might change dramatically with the size or even the geometrical structure of the system. Whereas it is necessary to further investigate the new physics of the nano-objects, the meeting will lay particular effort on the functionality of the clusters, nanotubes and nanowires in appropriate environments. In this general context, the following main topics will be covered:
• Cluster based structures: Magnetism, electronic and optical properties • Functionalized cluster matter • Nanotubes, nanowires • Nanostructured devices.

Emphasis will be put on experimental and theoretical aspects. Poster sessions are planned and time will be allotted to short oral contributions.

Deadline for applications: 17 February 2004

Conferences are open to researchers world-wide, whether from industry or academia.
Participation will be limited to 100. The registration fee covers full board and lodging. Grants are available (EC support from the High Level Scientific Conferences Activity), in particular for nationals under 35 from EU or Associated States.

For information & application forms contact:

EURESCO Office, European Science Foundation, 1 quai Lezay-Marnésia, BP 90015, 67080 Strasbourg, France
Fax: +33 (0)388 36 69 87 • E-mail: euresco@esf.org • WWW server: www.esf.org/euresco

Magnetism in nanocrystals

A.Hernando, Instituto de Magnetismo Aplicado. Complutense University. PO Box 155 Las Rozas, Madrid 28230, Spain

Physics of magnetic materials portends the improvement of the magnetic properties useful for applications. These can be roughly classified in two big groups [1], i) magnetic flux multiplication (magnetic cores) and ii) magnetic storage of either energy (magnets) or information (magnetic recording). There also exist other sophisticated devices as sensors and actuators that, being based on magnetic properties of materials as magnetostriction or giant magnetoresistance, GMR, are widely used in electronic and microelectronics circuits [2]. For flux multiplication soft magnetic materials characterised by low losses and coercivity, H_c, are required; whereas, high H_c and energy product are the relevant properties of hard magnetic materials used for storage. Control of coercivity has been carried out by playing with the parameters that governs the magnetic anisotropy i.e. composition and structure [3]. The possibility of tailoring anisotropy has allowed us to spread nowadays the available spectrum of coercivities over seven orders of magnitude. But what is really remarkable is that the softest materials $Fe_{79}Zr_7B_9$ ($\mu_0H_c=10^{-7}$T) as well as the hardest material $Fe_{79}Nd_7B_9$ ($\mu_0H_c=10$T) known in 2000 are obtained from amorphous alloys with closely related compositions. Notice that only a difference of 7 at. % in content gives rise to a difference of seven orders of magnitude in coercivity. This enormous difference is due to the nanocrystalline structure obtained by partial devitrification of the initial amorphous state. Both types of samples consist of a soup of nanograins embedded in a softer matrix [4]. Therefore, it can be concluded that nanocrystalline materials form an outstanding group of magnetic materials as concerns applied magnetism [5].

In this review the basic definitions and classification of nanocrystalline materials as well as their more remarkable intrinsic characteristic are introduced. Finally two examples of nanocrystalline magnetism related to pure Fe ferromagnetic grains are described. The first example deals with the amazing magnetic behaviour observed at low temperature in nanocrystalline Fe and the second one is related to the anomalous thermal dependence of the spontaneous magnetization in nanosized Fe ribbons embedded in a Cu matrix. It is shown that such anomalous thermal dependence can be explained by taking into account the combined effect of size and shape on the spin wave thermal excitation. These two examples are expected to be useful to illustrate the relevance of nanocrystals not only on technical magnetism but also on more fundamental aspects of magnetism.

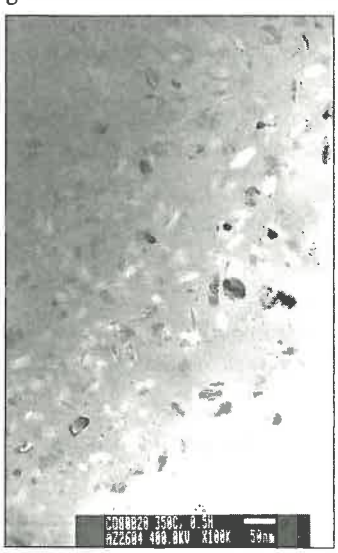

◀ **Fig. 1:** Nanocrystalline system formed by Co nanograins embedded in a Co rich CoB amorphous ribbon as observed by TEM (Zern *et al.* [4])

A polycrystalline solid formed by an isotropic distribution of nanometric sized grains is known as a nanocrystalline material. Figure 1 shows an assembly of Co nanograins embedded in an Co rich amorphous matrix. The structure corresponds to the partial devitrification of amorphous $Co_{80}B_{20}$ obtained after annealing at 630 K for 30 minutes. In general nanocrystals are connected between them by either grain boundaries or a different matrix. In the case of ferromagnetic nanocrystals, the matrix can be magnetic or non magnetic. The strength of the exchange coupling between the magnetization of the adjacent ferromagnetic grains strongly depends on the average thickness, d, and the magnetic nature of the matrix. It is important to remark that the macroscopic properties of nanocrystalline ferromagnetic samples are governed by the nanometric dimensions of the grains and also by the degree of ferromagnetic coupling between grains. Hence, the matrix nature becomes an extremely important parameter.

A polycrystalline solid formed by an isotropic distribution of nanometric sized grains is known as a nanocrystalline material.

The relevance of nanocrystals in magnetic research is associated with the control of the magnetic and magneto-transport (magnetorresistance [6] and tunnel magnetorresistance [7]) properties. Before going into deeper details, let us state the two outstanding physical aspects of nanocrystalline materials. First, is the high value of the ratio, N_s/N_v, between the atoms at the interface, N_s, and the total number of atoms N_v. If we call D the average grain size and a the inter-atomic distance, N_s/N_v varies roughly as a/D that, when D is a nanometric distance, can reach values as high as 30%. Second, there is coincidence between the grain size scale with the exchange correlation length, L_0, or domain wall width of the bulk ferromagnetic materials with the same composition as that of the nanocrystals [8]. In fact L_0 is the distance at which any local disturbance in the collinear ferromagnetic order propagates through the material.

The actual exchange correlation length in the nanocrystalline sample, L, can be either larger or shorter than L_0, depending on the magnetic nature of the matrix interconnecting the grain. Let us restrict the discussion to those nanocrystalline materials with grain size D very close to L_0 and average distance between grains, d of the order or smaller than D. The following two cases, described in Figure 2, can be distinguished

i) First case: L<D. This happens always for L_0<D [9], as, for example, is the case of nanocrystalline $Fe_{79}Nd_7B_9$. But, even if L_0>D, it is also possible that L<D if the matrix does not transmit exchange between grains (non magnetic matrix). For this case the grains are ferromagnetically decoupled and should closely behave as isolated magnetic single domains [10]. In general, the systems for which L<D would exhibit high temperature superparamagnetism, low temperature hard magnetic behaviour

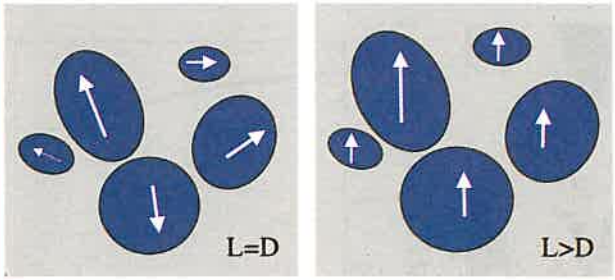

▲ Fig. 2: Schematic magnetization arrangement in A) a decoupled nanocrystalline system (L=D); the magnetic moment of each crystallite align along the easy axis and B) in a coupled system (L>>D) in which the ferromagnetic arrangement is achieved by exchange interactions that overcome anisotropy.

and giant magnetorresistance, GMR [6]. The particles are only coupled through magnetostatic interactions whose strength depends on the particle dilution or average intergrain distance, d [11].

ii) L > D. This case only holds under two independent conditions, a) L_0>D and b) the matrix is a good exchange transmitter (soft ferromagnetic matrix). In this case all the grains contained in L^3 are exchange coupled among them. The magnetization process is collective and the average anisotropy falls from the anisotropy of an isolated nanograin k down to $k^* = k/N^{1/2}$. Under the alignment effect of the exchange interaction between grains,the magnetic moments tend to arrange in a ferromagnetic structure. Since the easy axis fluctuates in orientation from one grain to the adjacent (random anisotropy), the exchange effect is counterbalanced by the misalignment tendency exerted by the anisotropy at each nanograin. When the exchange is stronger than the local anisotropy, k, the average anisotropy, k*, decreases as expected from random walk considerations [12]. Therefore, it can be concluded that the extremely soft magnetic character of nanocrystalline $Fe_{79}Zr_7B_9$ is due to the effect of random anistropy.

In order to illustrate the influence of the nanostructure in the magnetic properties pure iron has been found to be an excellent example. In fact it is somehow amazing that Fe, the oldest known ferromagnetic metal that has been considered the archetype of a ferromagnetic material, exhibits new and singular magnetic properties when it is in the form of nanostructures. Indeed, recent experiments performed on nanocrystalline Fe systems obtained by different methods have shown that intrinsic properties, such as the thermal dependence of the spontaneous magnetization, and technical aspects, as magnetic softness, are strongly modified by the nanometric scale of the Fe grains.

Let us start with the case of pure nanocrystalline Fe in which the contact between grains takes place through the grain boundaries that act as matrix. After measuring the thermal dependence of the magnetization under weak applied fields after field cooling, FC, and zero field cooling, ZFC, processes, a dramatic hardening of the samples was observed for temperatures below 70 K. The hardening was detected by the decrease of the real component of the susceptibility and the dramatic drop of the thermoremanence. It is important to remark that this low temperature anomaly has been observed in nanocrystalline Fe obtained by two very different methods such as ball milling [13] and sputtering [14]. Mössbauer spectroscopy carried out on strongly milled Fe powders with average grain size of 12 nm indicated than 13 at% of the Fe atoms were subjected to an hyperfine field different to that of regular α-Fe, ie. 33 T. This result suggested that 13 at% was the percentage of atoms located at the grain boundaries that, due to fluctuations of interatomic distances and coordination angles, exhibited a broad spectrum of hyperfine fields. Since magnetism is known to be extremely sensitive to short range order, the hardening was suggested to be due to spin disorder being frozen-in within the boundaries at low temperature. Spin disorder must drastically decrease the ferromagnetic exchange connection between grains giving rise to a shortening of L that promotes magnetic hardening. In order to confirm this suggestion electrical resistivity measurements were performed in thin films formed by (110) Fe islands grown by sputtering onto Al_2O_3 (0001) substrates in an ultrahigh vacuum triode sputtering system at 980 K. Figure 3-a shows the structure of the film observed by Atomic Force Microscopy and Figure 3-b illustrates the thermal dependence of resistivity measured during field cooling and zero-field cooling processes. The enormous increase of resistivity observed at low temperature under the zero-field cooling procedure and not observed when the cooling is achieved under a field can be explained by the proposed spin disorder at the boundary that also

Fe, the oldest known ferromagnetic metal... exhibits new and singular magnetic properties

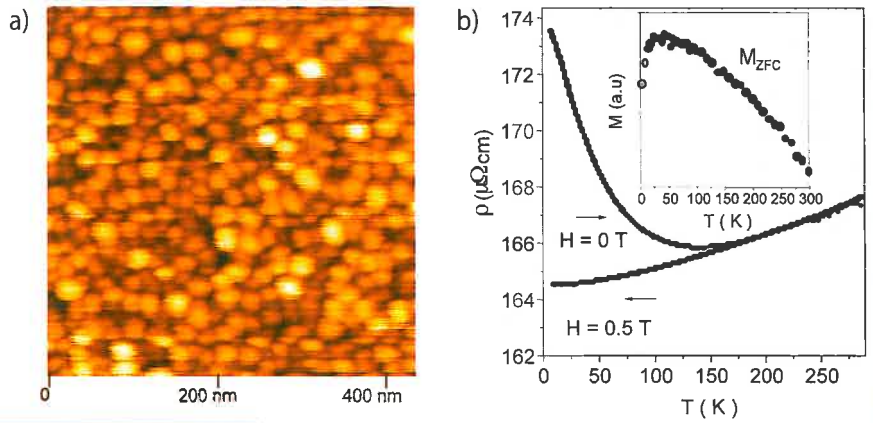

◀ Fig. 3:
a) AFM image of the Fe grains;
b) Electrical resistivity measured during zero-field cooling and field cooling. The dramatic increase of resistivity observed at low T in the zero-field cooling curve is originated by the disorder spin structure frozen in the grain boundaries.

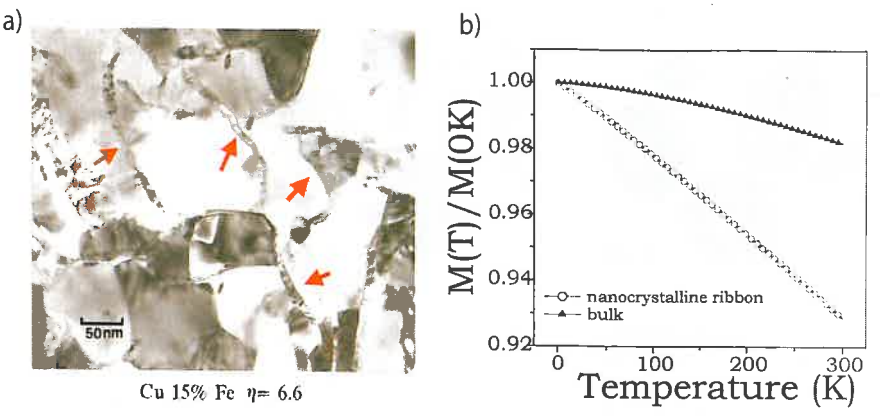

▶ **Fig. 4:**
a) Scanning Electron Microscopy image of the composites. The nano-ribbon of Fe can be observed at the grain boundaries of Cu grain;
b) Thermal dependence of the reduced magnetization for bulk and nanocrystalline ribbon shaped Fe.

contributes to increase the scattering with conducting electrons and therefore to enhance resistivity. Therefore, at low temperatures the exchange correlation length and the electron mean free path are remarkably reduced in nanocrystalline Fe. These effects are consequences of the low temperature disordered distribution of those spins located at the structurally disordered grain boundaries. It is obvious that this effect is not appreciable in polycrystalline Fe for which the percentage of atoms at the boundaries is negligible and the exchange connection between grains does not have any significant influence on the macroscopic magnetic properties.

Finally let us discuss the effect observed in Fe ribbon shaped nanocrystals embedded in a Cu matrix. Wire Cu-15 vol%Fe composite alloys have been produced by heavy working of spray-deposited billets. With the cold working proceeding the spheroidal Fe particles, about 1 μm in size, become drawn into elongated, flattened ribbons with progressively smaller cross section and (1,1,0) texture [15]. Figure 4-a shows the microstructure of the composite and Figure 4-b summarises the experimental thermal dependence of the reduced spontaneous magnetization, M(T)/M(0K), for bulk Fe and that measured in Cu-Fe composites formed by Fe grains with 3.5 nm thickness, 27 nm width and 5×10^3 nm length. The nanocrystalline sample exhibits an almost linear decrease of magnetization with temperature, T, instead of the usual $T^{3/2}$ bahavior predicted by the Bloch law and experimentally observed in bulk samples. This effect can be understood by considering that spin waves with wavelength larger than the nanocrystals dimensions can not be excited. At low temperatures the Planck distribution indicates that only large wavelengths are excited to a considerable extent. Thus, in nanometric spheroidal particles the magnetization is stable at low T up to that T at which spin waves of the sample dimensions are allowed to be excited. However, in the case of ribbon shaped nanocrystals, the spin waves excited at low T can only be those with wave vector oriented along the particle length. But, as is well known, the number of spin waves excited in one dimension diverges in the limit of very large wavelength. Therefore, the number of spin waves excited within the T interval in which all of them are one dimensional is enormous. Such T interval increases with the aspect ratio.

We have shown two examples that illustrate the sensitivity of Fe magnetism to short range order. The spin disorder at grain boundaries of Fe nanocrystals indicates the dependence of the magnetic structure on the topological short-range order. The shape influence, at the nanometric scale, on the spin-wave excitation rate also emphasises the relevance of nanocrystalline structure for controlling the intrinsic magnetic properties of the materials.

References

[1] D.Givord, Europhysics News 34/6, 219 (2003)

[2] M.N.Baibich, J.M.Broto, A.Fert, F.Nguyen van Dau, F.Petroff, P.E.Etienne, G.Creuzet, A.Friedich and J.Chazelas. Phys.Rev.Lett. 61, 2472 (1998).

[3] A.Hernando. J.Phys.Condens. Matter 11, 9455-9482 (1999)

[4] Y.Yoshizawa, S.Oguma and K.Yamauchi. J.Appl.Phys. 64, 6044 (1998). A.Zern, I.Kleinschroth, A.González, A.Hernando and H.Kronmüller. J.Appl.Phys. 85, 7609-7615 (1999)

[5] G.Herzer. Scr.Metall.Mater. 33, 1741 (1995). H.Kronmüller, R.Fischer, M.Seeger and A.Zern. J.Phys. D: Appl.Phys. 29, 2274 (1996). A.Manaf, R.A.Buckley, H.A.Davies and M.Leonowicz. J.Magn.Magn.Mater. 101, 360 (1991). G.Herzer. J.Magn.Magn.Mater. 157/158, 133 (1998)

[6] J.Q.Xiao, J.S.Jiang and C.L.Chien. Phys.Rev.Lett. 68, 3749 (1992). A. E. Berkowitz, J. R. Mitchell, M. J. carey, A. P. Ypung, S. Zhang, F. E. Spada, F. T. Parker, A. Hutten, and G. Thomas. Phys. Rev. Lett. 68, 3745 (1992)

[7] W.H.Butler, X.-G.Zhang, T.C.Schulthess, J.M.MacLaren. Phys.Rev. B 63, 054416 (2001)

[8] G.Bertotti. Hysteresis in Magnetism (London: Academic) 170 (1998)

[9] R.Fischer and H.Kronmüller. Phys.Rev. B 54, 7284 (1996). R.Fischer, T.Schrefl, H.Kronmüller and J.Fidler. J.Magn.Magn.Mater. 153, 35 (1996)

[10] K.Suzuki and J.M.Cadogan. Phys.Rev. B 58, 2730 (1998). A.Slawska-Waniewska, M.Gutowski, H.Lachowicz, T.Kulik and H.Matyja. Phys.Rev. B 46, 14594 (1992). A.Hernando and T.Kulik. Phys.Rev. B 49 7064 (1994).

[11] P.Allia, M.Knobel, P.Tiberto and F.Vinai. Phys.Rev. B 52, 15398 (1995)

[12] R.Alben, J.J.Becker and M.C.Chi. J.Appl.Phys. 49, 1653 (1978)

[13] E.Bonetti, L.del Bianco, D.Fiorani, D.Rinaldi, R.Caciuffo, A.Hernando. Phys.Rev.Lett. 83, 14, 2829-2832 (1999)

[14] Z.Sefroui, J.L.Menéndez, E.Navarro, A.Cebollada, F.Briones, P.Crespo, A.Hernando. Phys.Rev.B 64, 224431-224434 (2001)

[15] C.Biselli and D.G.Morris, Acta mater. 44 (2), 493 (1996). A.Hernando, P.Crespo, A.García-Escorial, M.A.Mu24434 (2001)

Magnetoresistance and magnetostriction in magnetic contacts

N. García, Laboratorio de Física de Sistemas Pequein magnetic contacts, Consejo Superior de Investigaciones Científicas Serrano 144, Madrid 28006, Spain,

Ballistc magnetoresistance in atomic and nanometer size electrodeposited contacts

Ballistic magnetoresistance (BMR) in point atomic contacts with resistances (R) larger than around 1000 Ω exhibits very large values, up to 500% [1-4], while the general trend is that BMR increases when R decreases. This BMR is the resistance that the electric current manifests through a point contact when a magnetic field is applied. The cause of this phenomena is explained in terms of domain wall (DW) scattering in magnetic materials [2,5], assuming that the DW width formed at the contact is of the order of the contact size. If the DW is narrow, strong non-adiabatic scattering with spin conservation at both sides of the contact is predicted by an old theory of Cabrera and Falicov [5], applied to atomic contacts by Tatara *et al.* [2]. The BMR can be expressed by:

$$BMR(\%) = \pi^2/4(\zeta^2/1-\zeta^2)F(\xi) \qquad (1)$$

The factor F is a dynamic term that reduces BMR according to the DW width and shape, and describes the adiabaticity in the spin electron transfer from one side of the contact to the other. The rest of eq. 1 is the ratio of the difference in the density of states between majority and minority spins at the Fermi level in the electrodes at both ends of the contact. This is basically the Julliere formula [6] for two electrodes made of same metal. The resistance is spin ballistic if the contact is small and the spin mean free path (l) is larger than the contact size.

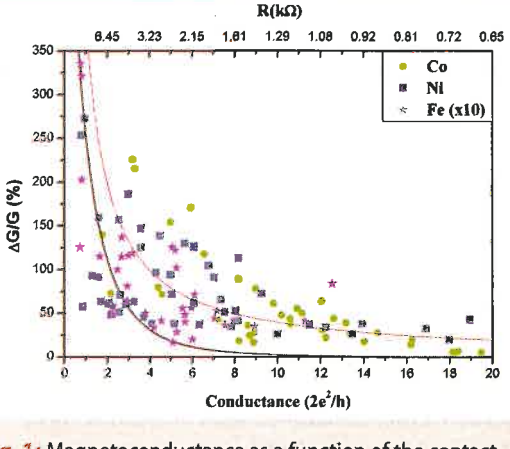

▲ Fig. 1: Magnetoconductance as a function of the contact conductance (bottom x-axis) and the contact resistance (top x-axis) for Ni, Co and Fe contacts. Black and red are the theory line approximations in the limits of a small and large number of conducting channels, respectively.

The resistance can be estimated assuming that one atom at the contact provides a conducting channel, and that one atom takes a surface area of approximately 0.1nm² by:

$$R(\Omega) = 12900\ \Omega / (10\ a^2\ (nm^2)) \qquad (2)$$

where 12900 Ω is the quantum of resistance, and a is the size of the contact in nm. The above formula is basically Sharvin's formula for ballistic transport [7]. The typical values from (l) for the spin mean free path are 30-50nm, and it therefore can be observed from the above formula that the limit for ballistic transport are in R values larger than 1Ω. For much smaller values of R the classical Maxwell formula controls the resistance that becomes non-ballistic. Fig.1 shows BMR values for Ni, Fe, and Co as a function of the conductance expressed in quantum units. The resistance of the contact is obtained simply by dividing the quantum of resistance 12900 Ω by the number of conducting channels (given in the upper x-axis). Fig.1 indicates that, for example, for 20 channels, corresponding approximately to 2 nm² of contact area, the resistance is 600 Ω! By then, the BMR is largely reduced to a 10% value of that for one channel of conductance. This conforms very well with theory, as indicated by the good agreement between the lines (theory) and dots (experiment) in the Fig 1. While this observation may produce very interesting physics from the point of view of theory and experiments, it does not qualify for technological applications because the contacts are unstable and last only a few minutes.

To overcome this problem and improve the stability of the contacts, we have electrodeposited contacts in magnetic and non-magnetic wires and films, forming a "T" configuration. To our surprise, we have observed even larger values of MR; up to 700% in Ni contacts deposited on small gaps between Ni wires [8] with typical R-values of 5-20 Ω. These MR values clearly cannot be explained by DW scattering [9], since the contact sizes are of the order of 10 nm, while the DW scattering [2,5,9] yields BMR values not larger than 10%. Recently, much larger values (many thousands per hundred!) of MR have also been claimed [10,11]. This effect of large BMR values in 10 nm size contacts may be assigned to the formation of a very thin "dead layer" or non- stoicheometric compound (oxide, sulfite, etc), at the nanocontact region that may reconfigure the spin density of states defining the electron transport [11,12]. While the very large values are very difficult to reproduce and to stabilize, we have been able recently [13] to obtain very stable contacts with highly reproducible R(H) curves; i.e., variations of resistance versus applied magnetic field H.

These last recent magnetic contacts were formed with two films of Cu as a substrate, separated by a gap between 100 and 2 μm wide that we can create with electrodeposition techniques, Fig.2a. Once the desired gap is created, we deposit the magnetic contact. This material may be Ni, Fe, Co or whatever as well as binary compounds such as Permalloy $Ni_{85}Fe_{15}$, which is very soft and has a small coercive field. With this procedure we have obtained extremely stable and reproducible R(H) curves that can last for the duration of thousand of loops. As an example, Fig.2b shows the reproducibility of the R(H) curves, for only some tens of the hundreds of curves that have been measured. The reproducibility is astonishing and is encouraging for the development of highly sensitive sensors as magnetic reading heads. At present we can obtain these kinds of results with a yield of 60% out of the thousands of samples we have studied. The BMR values, obtained with the typical reproducibility given in fig.2(b), range between 20% and 300% for contacts of the order of 10 Ω that correspond to contacts of approximately10nm in size.

Magnetoresistance of the deposit controls its morphology and structure

To prove the magnetoresistive effect we have performed electrochemical experiments applying a magnetic field during deposition. The idea goes as follows:

a) We grow Ni by electrodeposition with zero applied fields at several anodic potentials.

b) We, subsequently, make the same experiments with an applied magnetic field using weak fields up to 500 Oe. This field is approximately the coercive field of the Ni electrodeposits as we observed in our BMR experiments on nanocontacts (see Ref.8). This is not, however, to be confused with Fig.2(b) where the coercive fields are much smaller because in the latter case the deposit is permalloy and has a 25 Oe coercive field.

c) The field is applied in the direction perpendicular to the deposit plane in such a way that the cross product $\mathbf{H} \times \mathbf{v} = 0$ ($\mathbf{H}$ and $\mathbf{v}$ being the applied field and the velocity of the ions in the electrochemical solution, respectively). In other words, no Lorentz force exists, and thus no surface smoothing effects are expected [13, 14]. In fact, the only gradient effects that are expected should be weak due to the small fields that were applied, (500 Oe maximum).

d) Under these conditions no important effects were expected [13,14]. We discovered, however, very large effects due to these subtle small fields. We attribute these to the resistance of the deposits without field and with field. This resistance should be small for applied field due to magnetoresistive effects. When the field is applied the DW's are removed- as already discussed- and the resistance decreases.

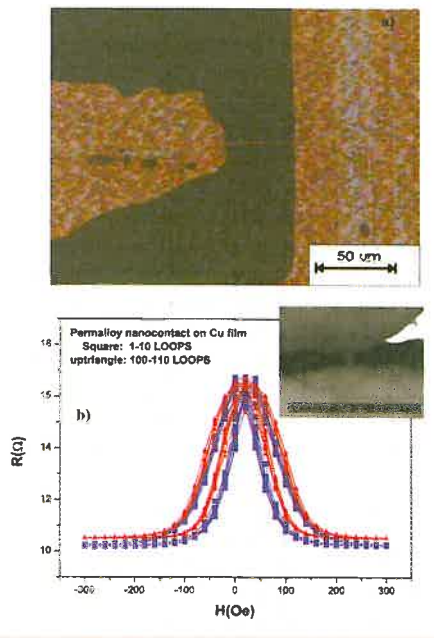

▲ Fig. 2: a) Optical microscope photograph taken near the contact area of the "T" configured Cu film arrangement. b) BMR curves of deposited permalloy contacts on Cu film. We measured the sample twice, taking one hundred loops per measurement. Indicated here are the first ten loops of each measurement: the upward-pointing triangular data points depict loops 1 through 10, while the square data points depict loops 100 through 110. The inserts at the top right of the curve depict SEM scans corresponding to the contacts referred to with the scales shown at the bottom of the photos.

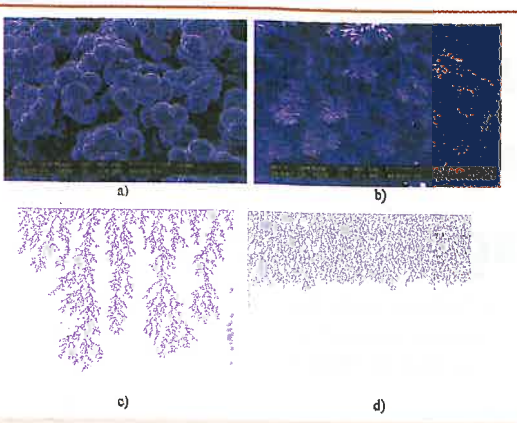

▲ Fig. 3: SEM microphotographs of nickel deposits obtained at a cathodic potential of -1300 mV/SCE from a Watt plating solution with the addition of coumarin: a) without and b) with a perpendicularly oriented magnetic field of 500 Oe; and the result of simulation of a cluster growth on the surface for c) k_1=1 and d) k_1=5.

In Fig.3a we show experiments revealing SEM micrographs of the deposits of Ni on Cu for an anodic potential of –1300mV/SCE with no field. The observed structure here is made of an aggregation of clusters. However, when a field H = 500 Oe is applied in the direction that the ions in the solution move, we observe an arboreous dendritic structure of long branch formations similar to that of sea algae (Fig.3(b)), which is completely different to that of the case when H = 0 (Fig.3a). This is due to the fact that when the field is 500 Oe the resistance is smaller than that for zero field applications, because the DW's have been removed. In the zero field case, on the other hand, DW's are present and contribute to the resistance. The effective anodic potential between the end of the filamentous deposits and the calomel reference electrode is smaller for zero fields due to the larger resistance of the filaments, which does not allow them to grow. Notice that the growth reported here does not have the form of needle-like structures [15], but has the form of a bead-arboreous-dendritic structure; i.e. the filaments have the form of a rosary formed by beads and the filaments do not have any special orientation depending on the applied field. This is at variance with the needle- like structure observed in the deposits of Fe at 2000 Oe fields [15]. In addition, the field does not affect the growth of Cu because this is non-magnetic.

This idea is illustrated by a computer simulation using the diffusion limited aggregation (DLA) model [16,17]. Fig.3c is a simulation considering that the filaments resistance is zero and then an arboreous dendritic structure is obtained for the deposit in agreement with Fig.3b and the discussion above. However, when the resistance of the wires is taken into account the structure is more compact as described in Fig.3d, which correlates well with Fig.3a. These experiments, therefore, show how a subtle magnetic field can provide a gracious and different kind of structure. As in nature, the processes are mostly electrochemical, and it just might be that many natural forms could be influenced by subtleties of the surrounding stray magnetic fields.

Magnetostriction measured with an atomic force

One of the problems raised while measuring the variation of the resistance with the applied magnetic field in small contacts is: *how much variation of the resistance may be due to change of the contact during the application field because of the accumulated magnetoelastic energy or magnetostriction?* This is a difficult problem to solve and in order to do it we have established a new method, that is elegant

and educational at the same time, using a local probe; i.e., scanning tunnelling microscopy (STM), atomic force microscopy (AFM), etc. We illustrate it below with the case where we use an AFM.

To observe magnetostriction under the AFM, we place the sample between the poles of a magnet where we can vary the field without moving the magnet itself. An electromagnet is ideal for this application. A schematic diagram of the set up is shown in Fig.4a. While the tip is scanning the surface (typically an area less than a thousandth of a millimetre), the field is activated by turning on the current to a value corresponding to whatever magnetic field strength we desire. The results are instantaneous, and quite illustrative of the process in action. The sample (typically a wire during our first measurements) was glued to the sample holder on one end, while scanning occurred at the other (see Fig.4b). In this way we could for example observe the change in the wire's length when the direction of scan was aligned with both the direction of the magnetic field and the length of the wire. After consecutive field applications the result would be a picture such as shown in Fig.4c. In this case contraction is movement to the left, and expansion to the right. What is interesting is that depending on the rate of scanning (typically less than a second per line for slow scans), the tip/sample contact is disrupted for a few lines, but then stabilizes immediately after the magnetostriction effect is completed. Even more important, when the field is removed the picture moves precisely back to its original position as if nothing ever happened. We can measure the shift by taking any features immediately before the field is applied and measuring the distance to the same features after field application. Our results invariably agree with other methods of measurement, yet only this technique provides valuable topographic information of the shift itself on the nanoscopic level.

The method is simple, direct and illustrative in a visual manner of a phenomenon only previously measured indirectly, and its potential is endless with applications ranging from nanotechnology and nanocircuitry to the exploration of new magnetic materials and even with possible extensions in biology. Besides technological applications the direct observation of magnetostriction holds the potential to expand the understanding of the relationship between mechanical and magnetic properties of materials, and may even lead to the observation of magneto-mechanical phenomena on the atomic level.

Using this method we have measured the possible displacements or motions of the contacts that give rise to the large BMR depicted in Fig.2b with substantial reproducibility. Within our resolution in the measurement (1 nm), we see no motion whatsoever of the contacts. That implies that if there are displacements they must be much smaller than 1 nm because we do not see any instability whatsoever in the AFM tip when the magnetic field is applied. Therefore, this tends to indicate that the observed values result from magnetoresistance with a high degree of reproducibility. If this is the case, these contact devices clear new ground for very sensitive sensors, especially as reading heads for reading magnetic information compacted in the Terabit/inch^2. At present research is going on in miniaturization and stabilization over weeks of the electrodeposited contacts.

Acknowledgments

This work has been supported by the Spanish DGICyT. I thank my students C. Guerrero, Hao, Cheng, and post-docs A.C. Papageorgopoulos, Hai Wang, N. Nikolic and M. Muñoz.

References:

[1] N. García, M. Muñoz and Y-W Zhao, Phys. Rev. Lett. 82, 2923 (1999).

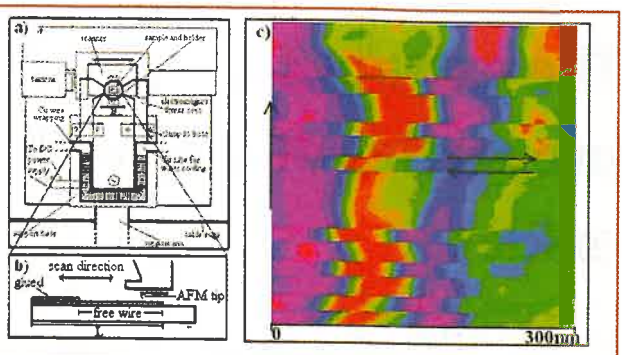

▲ **Fig. 4:** a) Top-view schematic of our setup for the AFM magnetostriction measurement. The sample is depicted in the bold circle between the two poles of the electromagnet and under the scanner. The double arrow marked B indicates the direction of the magnetic field. b) Side-view zoom of the sample configuration, including the AFM tip situated at the bottom of the scanner. The samples were metallic wires, glued on one end, while scanning occurred as close to the free tip of the wire as possible. c) A typical topographic image, of area 300 nm x 300 nm, which results from a tip scan along the length of the wire. The corresponding wire length is from left (toward glued portion) to right on the scan, while the scan itself is moving in the direction of the vertical arrow (bottom to top). The material used is a permalloy (an alloy of nickel and iron), and the length of the wire is about 10 mm. Application of a field causes a linear shift in the whole picture to the left, that indicates contraction, whereas on removal of the field the image moves to the right, and the wire expands back to its original position (see corresponding horizontal arrows). The shift itself was measured at 11 nm for the field strength applied.

[2] G. Tatara, Y-W Zhao, M. Muñoz and N. García, Phys. Rev. Lett. 83, 2030 (1999).

[3] J.J. Verluijs, A.M. Bari and J.M.D. Coey, Phys. Rev. Lett. 87, 026601 (2001).

[4] S. H. Chung, M. Muñoz, N. García, W. F. Egelhoff and R.D. Gomez, Phys. Rev. Lett. 89, 287203(2002).

[5] G. G. Cabrera and L. M. Falicov, Phys. Status Solidi, **B** 61, 539 (1974).

[6] M. Julliere, Phys. Lett. 54A,225(1975).

[7] Yu. V. Sharvin, Zh. Eksp. Teor. Fiz. 48, 984(1965). [Sov.Phys. JEPT 21, 655(1965)].

[8] N. García, M. Muñoz, G. G. Qian, H. Rohrer, I. G. Saveliev and Y.-W. Zhao, Appl. Phys. Lett. 79, 4550 (2001).

[9] V. A. Molyneux, V.V. Osipov and E. V. Ponizowskaia, Phys. Rev. B65,184425(2002).

[10] H. D. Chopra and S. Z Hua, Phys. Rev. **B** 66, 0204403(2002);

[11] Hai Wang, Hao Cheng and N. García arXiv:cond-mat/0207516v1 We should mention here that very large variation of resistance with magnetic field up to practically infinity have been obtained with Ni wires but this needs further understanding in the view of magnetoelastic deformations. The possibilities of magnestostriction effects are discussed below.

[12] N. Papanikolaou, arXiv:cond-mat/0210551v1.

[13] R. Aogaki, J. Electrochm. Soc. 142, 2954(1995)

[14] A. Oliver, J.P.Chopart and J. Douglade, J. Electroanal. Chem., 217, 443 (1987).

[15] S. Bodea, L. Vignon, R. Ballou and P. Molho, Phys. Rev. Lett., 83, 216 (1999).

[16] T.A. Witten and L.M.Sander, Phys. Rev. Lett. 47, 1400 (1981).

[17] E. Louis, F. Guinea and L.M Sander, Phys. Rev. Lett. 68, 209 (1992).

[18] A. C. Papageorgopoulos, Hai Wang, C. A. Guerrero and N. Garcia, *in press in* J. M. M. M.

The extraordinary properties of magnetic oxides

B. Raveau and A. Maignan
Laboratoire CRISMAT, CNRS/ENSICAEN, 6 boulevard du Maréchal Juin, 14050 CAEN cedex 4 – France

The physical properties of transition metal oxides have been currently the object of many investigations, since the discovery in 1986, of superconductivity at high temperature in cuprates. In these chemically complex materials, the electronic configuration of the transition elements, varies with its valency and is susceptible to adopt various spin states. As a result, strongly correlated electron interactions are generated, leading to complex magnetic and metal-insulator transitions. In this respect, magnetic oxides, containing transition elements such as manganese, cobalt or ruthenium exhibit most fascinating properties.

One of the most famous classes of magnetic oxides concerns the manganites with the perovskite structure (Fig. 1a), which exhibit colossal magnetoresistance (CMR) properties. In these oxides of generic formula $Ln_{1-x}A_xMnO_3$ (A = Ca, Sr, Ba), double exchange phenomena take place, which require a hopping of charge carriers from a Mn^{3+} to a Mn^{4+} ion through an oxygen atom. This effect generates a ferromagnetic metallic state at low temperature, and a metal-insulator transition versus temperature, which coincides with a ferromagnetic to paramagnetic (or antiferromagnetic) transition (Fig. 1b). The latter are also coupled with a structural transition, implying the disappearance of the static Jahn-Teller distortion due to Mn^{3+}, in the ferromagnetic state. As a consequence, at the vicinity of the Curie Temperature T_C a large magnetoresistance can be obtained: the resistance of these materials can be decreased by several orders of magnitude by an external magnetic field of some teslas. A part of these manganites, those which contain smaller A cation (Ca^{2+}), exhibit a more complex physical behavior, due to orbital and charge ordering phenomena. In these oxides, the manganese octahedra are occupied by Mn^{3+} and Mn^{4+} species in an ordered way, forming stripes of Mn^{3+}distorted octahedra due to Jahn-Teller effect, which alternate with stripes of quasi-regular Mn^{4+} octahedra. The physics of the latter compounds is then governed by the competition between ferromagnetism and charge/orbital ordering, i.e. the orbital-charge ordered state which is antiferromagnetic and insulating transforms to a metallic ferromagnetic state on the application of a sufficiently high magnetic field, leading also to CMR effect. In these materials, orbital-charge ordering can be destroyed by doping the manganese sites with magnetic cations such as chromium or ruthenium, which by magnetic coupling with adjacent manganese induce ferromagnetism and metallicity, so that spectacular modifications of the magnetic phase diagrams of these systems are obtained. In this way, insulator-metal transitions can be induced and CMR effects are enhanced under much lower magnetic fields.

Another interesting property of these manganites deals with their ability to exhibit a spin glass like behavior, for small A site cations in the composition range close to $CaMnO_3$ ($x \sim 0.8 - 0.9$).

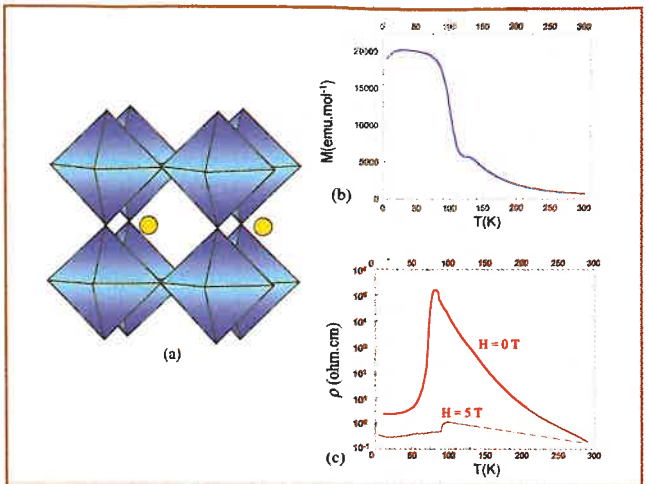

▲ **Fig. 1:** The CMR perovskite manganites $Ln_{1-x}A_xMnO_3$: (a) The perovskite structure built up of corner-sharing MnO_6 octahedra forming cages where Ln^{3+} and A^{2+} cations are located (b) Ferromagnetic to paramagnetic transition, and (c) corresponding insulator to metal transition (H = 0 zero field) and field effect upon resistivity (H = 5T) observed in $Pr_{0.7}Ca_{0.25}Sr_{0.05}MnO_3$.

Moreover at the boundary between this region and charge ordered region, CMR properties are also observed.

In fact, the unusual behavior of the manganites is based on a new phenomenon, the electronic phase separation. It has indeed been observed that charge ordered insulating regions coexist at low temperature with small ferromagnetic regions at a submicrometer scale, in a coherent manner in the same matrix. Thus, the CMR effect for the low T_C manganites results from the percolative conduction through the small ferromagnetic domains embedded in the antiferromagnetic insulating matrix. Such an electronic phase segregation was also predicted from the large magnetostriction effects observed in these materials, and described either as dynamic magnetic polarons, or as static phase segregation. Many other properties of these manganese perovskites are closely relat-

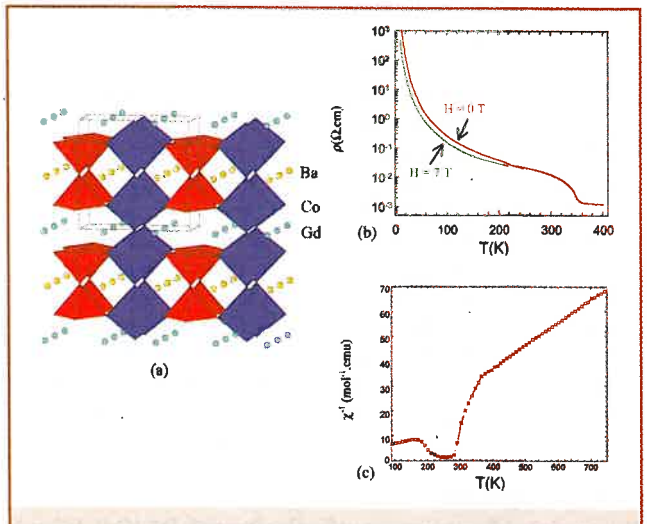

▲ **Fig. 2:** The cobaltites $LnBaCa_2O_{5.5}$: (a) The structure of the ordered oxygen deficient structure built up from rows of CoO_6 octahedra and CoO_5 pyramids, and involving layers of Ln^{3+} and Ba^{2+} cations alternately. (b) The metal to insulator transition of the manganite $GdBaCo_2O_{5.5}$, (c) The corresponding magnetic transition in the paramagnetic regime.

ed to the peculiar double exchange phenomena, such as the photo induced metal-insulator transition, as well as the electrical field induced magnetic transition that have been recently observed. The curious effect of thermal cycling upon the resistivity, and the step like behavior at low temperature of their magnetization, resistivity and specific heat versus magnetic field at low temperature, are also certainly related to the phase separation that exists in these compounds, and suggest a martensitic type mechanism.

The high degree of spin polarisation of the conduction electrons in these oxides is of great interest since it can be used to achieve large low field magnetoresistance, which is of capital importance for magnetic recording, or sensing applications. Artificially prepared grain boundaries in thin films allow indeed promising magnetoresistance values to be reached. Finally it must be emphasized that the 3D perovskites are not the only manganites which exhibit CMR. High magnetoresistance can also be obtained in the 2D Ruddlesden and Popper manganites, such as $Ln_{2-x}A_{1+x}Mn_2O_7$, but the low dimensionality of these oxides strongly damages their Curie temperatures. In the same manner, the perovskite structure is not the only one to exhibit magnetoresistance. Large magnetoresistance has also been discovered in the pyrochlore $Tl_2Mn_2O_7$ which contains only Mn^{4+} species suggesting a different origin of CMR.

Cobalt oxides form also a very important family with extraordinary magnetic properties. This is for instance the case of the compounds $LnBaCo_2O_{5.5}$ (Ln = lanthanide), which exhibit a metal-insulator (MI) transition coupled with a spin transition. These materials are ordered oxygen deficient perovskites, characterized by a layered ordering of the Ln^{3+} and Ba^{2+} cations, so that rows of CoO_6 octahedra alternate with rows of CoO_5 tetragonal pyramids (Fig. 2a). As a result, there exist two sorts of trivalent cobalt in the structure at high temperature ($T>T_{MI}$): the octahedral cobalt has a high spin (HS) $t_{2g}^4e_g^2$ configuration, whereas the pyramidal one has an intermediate spin (IS) $t_{2g}^5e_g^1$ configuration. In contrast to manganites, the metal to insulator transition appears in these oxides at decreasing temperature (Fig. 2b) around 300 – 350K, and coincides with the transition in the paramagnetic susceptibility (Fig. 2c). This strong coupling between magnetism and transport properties is explained by a spin transition of octahedral Co^{3+} species from high spin (HS) $t_{2g}^4e_g^2$ to low spin (LS) t_{2g}^6, the $t_{2g}^5e_g^1$ (IS) pyramidal cobalt being unchanged at the transition. Recent thermoelectric power studies of these oxides, corroborate this viewpoint showing that S changes of sign at the transition from n-type in the metallic state to p-type in the insulating state. Moreover, these cobaltites also exhibit negative giant magnetoresistance at lower temperature. For instance, resistance ratio higher than 10 can be obtained under 7T (Fig. 2b),

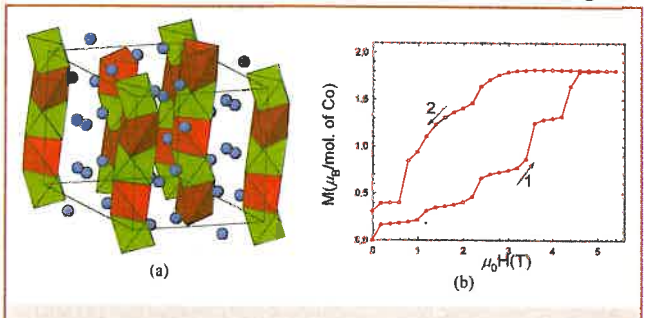

▲ **Fig. 3:** The cobaltite $Ca_3Co_2O_6$: (a) The structure consists of $[Co_2O_6]_\infty$ chains of face sharing CoO_6 octahedra and CoO_6 trigonal prisms forming a triangular array. (b) Magnetization half loop M(H) of this phase registered at T = 2K.

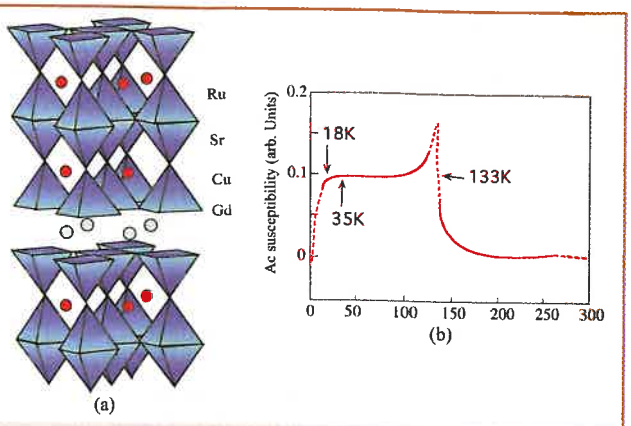

▲ **Fig. 4:** The ferromagnetic superconductor $RuSr_2GdCu_2O_8$: (a) The structure consists of single layers of RuO_6 octahedra sandwiched between layers of CuO_5 pyramids, gadolinium and strontium layers are stacked with a 1-2 order (b) The ac susceptibility curve shows that superconductivity is achieved at 18K (inset at 35K), whereas ferromagnetism appears below 133K according to Chmaissen *et al.*

in the temperature range T < 200K, where a second transition from the paramagnetic to the antiferromagnetic state has been achieved. Note that negative magnetoresistance has also been observed in several other cobaltites: the perovskite $La_{1-x}Sr_xCoO_3$ and the bismuth based cobaltites, $(Bi, Cd)_1Sr_2CoO_5$ with a layered structure similar to the 1201-type cuprate.

Such a coupling of the magnetic and transport properties in the cobaltites is not limited to the oxygen deficient perovskite structure. A metal-insulator transition correlated with a spin state transition of Co^{3+} is also observed at room temperature in the cobaltite $TlSr_2CoO_5$. In the latter oxide, whose 2D structure is an intergrowth of rock salt type layers "$TlSrO_2$" with single perovskite layers "$SrCoO_3$", the metallic state involves strong ferromagnetic interactions, induced by the cooperative spin transition that takes place at lower temperature.

Another example of cobalt oxides is also very attractive for its particular magnetic properties, the one dimensional cobaltite $Ca_3Co_2O_6$. The rhombohedral structure of this phase (Fig. 3a) consists of $[Co_2O_6]$ chains running along the c axis of the hexagonal cell. In each chain, one CoO_6 octahedron alternates with one CoO_6 trigonal prism. The great interest of these compounds deals with the fact that a transition from a ferrimagnetic to a ferromagnetic state is induced on application of a magnetic field. A ferromagnetic intrachain coupling exists along $\vec{c}$, whereas an antiferromagnetic intrachain coupling is obtained in the (a, b) plane. Nevertheless the Co-Co intrachain distances are much larger than the Co-Co interchain distances, so that the magnetism of $Ca_3Co_2O_6$ can be described on the basis of a planar Ising triangular lattice where each chain plays the role of one spin. Thus, the magnetic susceptibility of this phase exhibits two transitions versus temperature at 24K and 12K, which correspond to the setting of the interchain antiferromagnetic coupling and spin freezing (T_f) respectively. In this Ising triangular ferromagnet, AC susceptibility measurements show large shift of T_f from 12 to 16.5K, as the frequency increases by three orders of magnitude. Remarkably, five plateaus can be observed at 2K on the M(H) curve (Fig. 3b), which characteristic magnetic fields are separated by ~ 1.2 T. This feature is reminiscent of the quantum tunneling of mangnetization encountered in high-spin macromolecules.

Ruthenium oxides exhibit also an extremely rich physics from the magnetism viewpoint. Several members of the Ruddlesden

and Popper series $Sr_{n+1}Ru_nO_{3n+1}$, with $n = 1, 2, 3, \infty$ are metallic ferromagnets with T_C ranging from 105K to 165K, whereas the $n = 1$ member Sr_2RuO_4, has often been considered as close to the ferromagnetic order but is in fact a superconductor with a very low critical temperature of ~ 1K. Remarkably, the former compounds, show a Fisher-Langer type anomaly of the conductivity versus temperature at T_C, which is suppressed under a few T. In contrast, the calcium homologous phases which are isostructural, exhibit very different properties: the perovskite $CaRuO_3$ ($n = 1$) is a paramagnetic metal, whereas Ca_2RuO_4 ($n = 2$) is an antiferromagnetic insulator. As a consequence, solid solutions also show complex magnetic properties, as for example the oxides $Ca_{2-x}Sr_xRuO_4$, for which a metal-insulator transition, associated with a structural change and magnetic ordering is observed, for low strontium contents. But the most fascinating properties of ruthenium based oxides have been recently obtained for the ruthenocuprates of the $RuSr_2GdCu_2O_8$ family. The physical behavior of this oxide is unique in that, superconductivity and ferromagnetism coexist within the same matrix. The structure of this phase (Fig. 4a) derives from that of the 92K-superconductor $YBa_2Cu_3O_7$, by replacing the CuO_4 groups by RuO_6 octahedra. It can be described as an oxygen deficient perovskite built up of single octahedral perovskite ruthenium layers sandwiched between pyramidal copper layers, layers of Gd^{3+} and Sr^{2+} being stacked according to a "1-2" order, between the CuO_2 and RuO_2 planes. The remarkable coexistence of superconductivity with a T_c ~ 35K, and of ferromagnetism with a T_C ~ 133K is demonstrated from AC susceptibility measurements (Fig. 4b). Such a behavior shows the important role of the layered architecture of the structure, in order to conciliate these two contradictory properties.

In conclusion, these few examples and those well known on iron oxides show that transition metal oxides represent a vast field of investigation for the discovery of new extraordinary magnetic properties.

References

For manganites:

Colossal Magnetoresistance, Charge ordering and Relation Properties of Manganese Oxides. Edit. C.N.R. Rao and B. Raveau. 1998 – World Scientific.

Ibarra *et al.*, Magnetostriction in mixed valent magnetic oxides: in Modern Trends in Magnetostriction Study and Applications. Edit M.R.J. Gibbs – 2000 – Kluwer Acad. Publi.

For cobaltites:

C. Martin *et al.*, Appl. Phys. Lett. 71, 1421 (1997).

J-C. Burley *et al.*, J. Solid State Chem, accepted 2002.

A.Maignan *et al.*, Eur. Physic. J. B. 15, 657 (2000)

M. Coutanceau *et al.*, Solid State Comm. 96, 569 (1995).

C. Frontera *et al.*, J. Solid State Chem. accepted 2002; Phys. Rev. B 65, 180405 (2002).

M. Respaud *et al.*, Phys. Rev. B, 64, 214401 (2001).

W.S. Kim *et al.*, Solid State Com 116, 609 (2000).

For ruthenates:

O. Chmaissen *et al.*, Phys. Rev. B 61, 6401 (1999).

S. Malo *et al.*, Internal J. of Inorg. Mat. 2, 601 (2000).

G. Cao *et al.*, Phys. Rev. B 56, R 5740 (1197); ibid 56, 321 (1997).

O. Friedt *et al.*, Phys. Rev. B 63, 174432 (2001).

Optical studies of spin injection and detection at ferromagnet / semiconductor interfaces

J.A.C. Bland, S.J. Steinmuller, A. Hirohata, W.S. Cho, Y.B. Xu, C.M. Guertler, G. Wastlbauer, A. Ionescu, T. Taniyama and T. Trypiniotis, Cavendish Laboratory, University of Cambridge, England
S.N. Holmes, Cambridge Research Laboratory, England

Recently, the newly emerging field of spintronics has attracted considerable attention. Significant advances in device performance, in terms of speed, size scaling and power requirements could be achieved by creating spin electronic devices based on the manipulation of spin polarized electrons [1]. Proposed spin analogues to conventional electronic devices have stimulated great interest, *e.g.* the spin polarized field effect transistor (spin FET) [2,3] and the spin polarized light-emitting diode (spin LED) [4,5]. In order to realize such spin electronic devices, spin dependent electron transport needs to be better understood. It is very important to note that efficient spin dependent transport depends on achieving *both* efficient spin injection from a ferromagnet (FM) into a semiconductor (SC) [4-8], *and* efficient spin detection of electrons passing from the SC into the FM. Efficient spin injection has been reported by Fiederling *et al.* [4] and Ohno *et al.* [5] using a magnetic SC but only at low temperature in all SC device structures. Recently, spin injection from a FM metal into a SC has been achieved at room temperature with an efficiency of 2 % [6] and 30 % [7] in Schottky barrier structures, and at 80 K with an efficiency of 9 % in FM/AlO_x barrier/SC structures [8], respectively. The question remains as to whether room temperature efficient operation is possible and also whether strong spin trans-

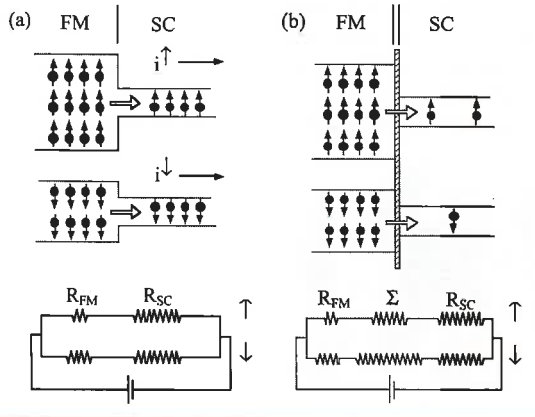

▲ **Fig. 1:** Schematic of spin dependent electron transport at (a) a FM/SC interface and (b) a FM/tunnel barrier/SC interface. A resistor model is also shown for both cases, where R_{FM}, R_{SC} and Σ denote the resistance in the FM and the SC and the tunnel barrier contact resistance, respectively.

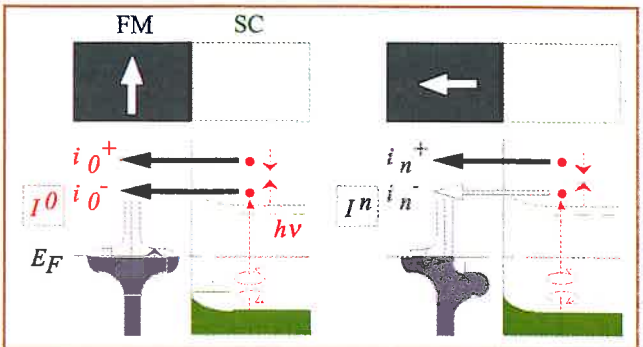

▲ **Fig. 2:** Schematic diagrams illustrating the spin filtering mechanism for electron transport at the FM/Schottky barrier/SC interface. Averaged density of states of FM is shown for the case of I^0 for simplicity.

mission can be achieved between FM metals and SC. Theoretically, it has been suggested that there may be fundamental obstacles to achieving efficient spin transmission across FM metal/SC interfaces via a diffusive electron transport process [9] due to the conductivity mismatch between the FM metal and the SC. In this case the electron transport properties are dominated by the large resistance of the SC, diluting any spin dependent effects at the interface (Fig. 1a). It is expected, however, that spin dependent electron transport can be achieved via electron tunneling at FM/SC interfaces [10]. If the tunneling process is spin dependent and the tunnel barrier contact resistance is larger than the resistance of the SC, spin injection and detection efficiencies of up to 100% can be expected (Fig. 1b). So far very few studies have been conducted on spin detection and further clarification of the mechanisms involved is highly desirable.

We investigated spin filtering across FM/SC Schottky interfaces as a function of FM material, FM layer thickness and applied magnetic field using photoexcitation techniques [11,12]. Polarized photoexcitation in FM/SC structures was employed to create a population of spin polarized electrons in the SC substrate (GaAs). The spin dependent electron transport across the FM/SC interface at room temperature was detected as an electrical response, the strength of which varies according to the configuration of the photon helicity with respect to the FM layer magnetization (inset of Fig. 4). We achieved a change in helicity dependent photocurrent when the magnetization was realigned from perpendicular to parallel to the photon helicity, which is attributed to spin filtering at the FM/SC interface due to the spin split density of states (DOS) in the FM. These spin transport effects increase with increasing FM layer thickness and applied magnetic field. Applying dc measurement techniques, we were furthermore able to quantify the spin polarization of the electrons filtered at the FM/SC interface. Based on our results we discuss a simple model for the spin transport mechanism across the Schottky barrier.

We used ultrahigh vacuum (UHV) deposition techniques to fabricate 2.5, 5.0 and 7.5 nm thick polycrystalline $Ni_{80}Fe_{20}$ and Fe layers directly onto GaAs substrates (Si doped, $n=10^{23}$ m^{-3} and 10^{24} m^{-3} for the NiFe and Fe samples, respectively), capped with 3 nm thick Au layers. An antiferromagnetic Cr sample (5.0 nm, $n=10^{23}$ m^{-3}) was also prepared as a reference. A bias voltage was applied between one Au electrical contact on the surface of the sample and an ohmic contact attached to the back of the substrate. The current flowing through these two pads was measured (both with and without photoexcitation), while the voltage across the sample was also measured using a separate top contact as shown in the inset of Fig. 4 [11]. A circularly polarized laser beam (with photon energy $hv = 1.96$ eV) was used together with an external magnetic field to investigate the spin dependence of the photoexcited electron current at room temperature. The polarization of the beam was modulated from right to left circular using a photo-elastic modulator with 100 % circular polarization at a frequency of 50 kHz.

As discussed above, the process (tunneling, thermionic emission etc.) by which electrons are transported from the SC into the FM is a key issue for the realization of spin detection. Photoexcitation measurements we recently carried out on band gap engineered FM/AlGaAs tunnel barrier/SC structures [13] clearly showed that significant spin filtering can only be expected for tunneling electrons, in good agreement with the theoretical predictions [9,10]. Our discussion of the spin dependent transmission process will therefore focus just on the tunneling of electrons through the Schottky barrier followed by ballistic transport in the FM.

The helicity dependent photocurrent I was measured by modulating the photon helicity from right (σ^+) to left (σ^-). The two helicity values correspond to opposite spin angular momentum values of the incident photons and the helicity gives rise to opposite spin polarizations of electrons photoexcited in the GaAs [14]. The magnetization (M) in the FM is aligned perpendicular or in plane (H=0) using an external field. For $\sigma // M$ (or anti-parallel), the electrons in the FM and the SC share the same spin quantization axis, while for $\sigma \perp M$, on the other hand, the two possible spin states created by the circularly polarized light are equivalent when projected along the magnetization direction in the FM (Fig. 2). Consequently, in the remanent state ($\sigma \perp M$), since M is orthogonal to the photoexcited spin polarization, both up and down spin polarized electrons in the SC can flow into the FM, opposing the electron current from the FM. At perpendicular saturation ($\sigma // M$), on the other hand, the up spin electron current from the SC is filtered due to the spin split DOS in the FM. This means that a greater net negative current now flows with $\sigma // M$ than that for $\sigma \perp M$, since the current from the metal to the SC is largely independent of the magnetization configuration. Spin filtering is therefore turned on or off by controlling the relative axes of σ and M, and is detected as the helicity dependent photocurrent I. With $\sigma \perp M$, there is no spin filtering, while spin filtering is turned on by rotating to $\sigma // M$. The helicity dependent photocurrents I^0 and I^n correspond to the magnetization configurations $\sigma \perp M$ (Fig. 2, left) and $\sigma // M$ (Fig. 2, right), respectively. I^0 and I^n are

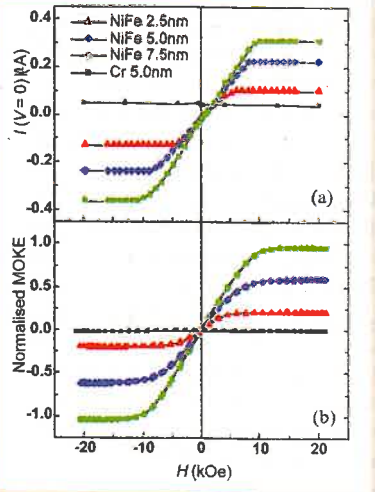

◀ **Fig. 3:** Applied magnetic field dependence of (a) I and (b) MOKE signal for NiFe/GaAs (t=2.5, 5.0 and 7.5 nm) and Cr (5.0 nm)/GaAs samples.

features

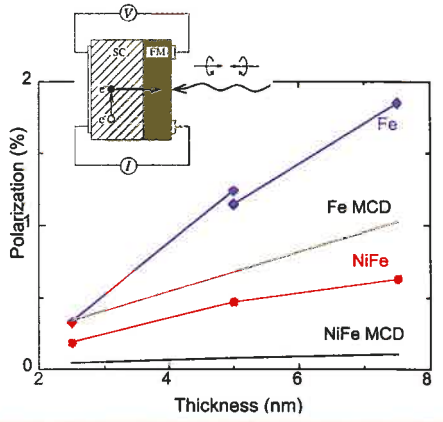

▲ **Fig. 4:** Thickness dependence of spin polarization across the FM/GaAs interface for the case of both NiFe and Fe as the FM. The magnitude of the calculated MCD effects is also shown as positive values. In the inset a schematic of the experimental set up is shown.

proportional to the difference between the current components for right and left circularly polarized light for each magnetization configuration: $I^0 \propto i_0^+ - i_0^-$ and $I^n \propto i_n^+ - i_n^-$. As shown in Fig. 2, $i_0^+ = i_0^-$ is expected for the case of the remanent state, while $i_n^+ \neq i_n^-$ is expected for the case of perpendicular saturation. Due to our experimental geometry, where the light enters the SC through the FM layer, we can expect a contribution from magnetic circular dichroism (MCD, i. e. the different absorption of right and left circularly polarized light in a magnetic material) to I.

The magnetic field dependence of the helicity dependent photocurrent at zero applied bias for the three permalloy samples is shown together with the corresponding polar magneto-optical Kerr effect (MOKE) measurements in Fig. 3 (a) and (b), respectively. The MOKE signal is proportional to the magnetic moment of the FM film and therefore provides a qualitative measure of the FM magnetization. As can be seen in Fig. 3, the field dependence of the helicity dependent photocurrent matches that of the MOKE signals, showing the magnetic nature of the effect. Similar results were obtained for the Fe samples. We can therefore conclude from this observation that there are no significant background effects due to Zeeman splitting in the GaAs. Although the Cr sample shows a small offset, the signal does not possess any field-dependence (due to a possible SC-related background), confirming that the Zeeman splitting effect is negligible in our measurement.

In order to study the spin filtering effect quantitatively, we performed dc photoexcitation measurements. Circularly polarized light was generated using a λ/4 plate, and the dc helicity dependent photocurrent was observed for both right (I^+) and left circular (I^-) configurations. The spin polarization of the spin filtering effect was estimated as $P = (I^+ - I^-)/(I^+ + I^-)$. Figure 4 shows the thickness dependence of both the estimated spin polarization and the magnitude of the MCD effect for both NiFe and Fe samples. The spin polarization increases with the FM layer thickness t and is larger than the calculated MCD effect as shown in Fig. 4. A similar thickness dependence of the spin polarization has been reported by van't Erve *et al.* [15], suggesting that spin filtering occurs in the ballistic regime. It should be noted that the signs of spin polarization for spin filtering are the same for both NiFe and Fe but that the sign of MCD is expected to be opposite for NiFe and Fe.

In conclusion spin polarized electron transport across FM/SC hybrid structures has been investigated for different FM materials (NiFe and Fe), FM layer thicknesses and applied magnetic fields. At room temperature, we observed a clear difference in the helicity dependent photocurrent through the FM/GaAs interface according to the orientation of the sample magnetization with respect to the helicity. This difference in photocurrent corresponds to a measure of the spin polarized photocurrent passing from the SC into the FM. The crucial transport mechanism in this spin filtering process is the tunneling of photoexcited electrons through the Schottky barrier. Antiferromagnetic Cr/GaAs shows no spin dependence as expected and provides an important test of the validity of our experiments. The spin polarization increases with the FM layer thickness, which provides further support of the view that spin filtering is associated with ballistic transport in the metal. Our combined results unambiguously indicate that spin polarized electrons are transmitted from the SC to the FM with high efficiency.

Acknowledgments

We are grateful to Ken Cooper for his help with the sample fabrication. The support of EPSRC, EU (Esprit programme) and ETRI (Korea) is also acknowledged. S.J.S. gratefully acknowledges the financial support of ABB (Sweden). A.H. would like to thank the Toshiba Europe Research Limited and the Cambridge Overseas Trust for their financial support. W.S.C. is supported by postdoctoral fellowship program from Korea Science & Engineering Foundation (KOSEF). G. W. would like to thank the Austrian Academy of Sciences and the Wilhelm-Macke-Stipendienprivatstiftung (Austria) for their financial support. A.I. thanks the Cambridge European Trust and Nordiko Ltd. for their funding. T.T. expresses his gratitude to the Cambridge Commonwealth Trust for their financial support.

References

[1] S. A. Wolf, D. D. Awschalom, R. A. Buhrman, J. M. Daughton, S. von Molnár, M. L. Roukes, A. Y. Chtchelkanova, and D. M. Treger, Science **294**, 1488 (2001)

[2] S. Datta and B. Das, *Appl. Phys. Lett.* **56**, 665 (1990).

[3] M. Johnson, *Phys. Rev. B* **58**, 9635 (1998).

[4] R. Fiederling, M. Keim, G. Reuscher, W. Ossau, G. Schmidt, A. Waag and L. W. Molenkamp, *Nature* **402**, 787 (1999).

[5] Y. Ohno, D. K. Young, B. Beschoten, F. Matsukura, H. Ohno and D. D. Awschalom, *Nature* **402**, 790 (1999).

[6] H. J. Zhu, M. Ramsteiner, H. Kostial, M. Wassermeier, H.-P. Schönher and K. H. Ploog, *Phys. Rev. Lett.* **87**, 016601 (2001).

[7] A. T. Hanbicki, B. T. Jonker, G. Itskos, G. Kioseoglou and A. Petrou, *Appl. Phys. Lett.* **80**, 1240 (2002).

[8] V. F. Motsnyi, J. De Boeck, J. Das, W. Van Roy, G. Borghs, E. Goovaerts, and V. I. Safarov, *Appl. Phys. Lett.* **81**, 265 (2002).

[9] G. Schmidt, D. Ferrand, L. W. Molenkamp, A. T. Filip and B. J. van Wees, *Phys. Rev. B* **62**, R4790 (2000).

[10] E. I. Rashba, *Phys. Rev. B* **62**, R16267 (2000).

[11] A. Hirohata, Y. B. Xu, C. M. Guertler, J. A. C. Bland and S. N. Holmes, *Phys. Rev. B* **63**, 104425 (2001).

[12] A. Hirohata, S. J. Steinmueller, W. S. Cho, Y. B. Xu, C. M. Guertler, G. Wastlbauer, J. A. C. Bland and S. N. Holmes, *Phys. Rev. B* **66**, 035330 (2002).

[13] S. E. Andresen, S. J. Steinmuller, A. Ionescu, C. M. Guertler, G. Wastlbauer and J. A. C. Bland, *Phys. Rev. B* **68**, 073303 (2003).

[14] D. T. Pierce and F. Meier, *Phys. Rev. B* **13**, 5484 (1976).

[15] O. M. van't Erve, R. Jansen, S. D. Kim, F. M. Postma and J. C. Lodder, *The 46th Conference on Magnetism and Magnetic Materials*, GD-04

Strong electron correlations in magnetic systems

F.Steglich, MPI for Chemical Physics of Solids, Dresden, Germany

Heavy-Fermion Metals

Strongly correlated electron systems can be well studied with certain rare-earth—or actinide-based intermetallics. At high temperatures, independent local magnetic moments are formed due to the strong repulsive Coulomb force between electrons on the partially filled *4f*/*5f*-shells of these materials. This local interaction competes with the (upon cooling increasingly strong) coupling between the localized *f*-electrons and the delocalized ligand states. As a result, the local *f*-moments become progressively screened below the characteristic Kondo-lattice temperature T_K, a process that causes the formation of strongly renormalized ("composite-fermion") quasiparticles, consisting of a local *f*-part and some admixture of itinerant conduction-electron contributions. These "heavy electrons" or "heavy fermions" (HFs) exist in extended regions of parameter space and resemble the conduction electrons of simple metals. However, because of the strong intra-atomic Coulomb correlations, they acquire huge effective carrier masses m* ($\approx 100 - 1000\ m_{electron}$) [1].

Most of the HF metals adopt a symmetry-broken ground state, either a superconducting (SC) or an antiferromagnetically ordered one [1]. In some of the U-based HF metals, like UPt_3 and UPd_2Al_3, superconductivity is found to coexist with long-range antiferromagnetic (AF) order (sec.2). On the other hand, for several Ce-based materials superconductivity has been observed to form in the vicinity of an AF instability, at which the Néel temperature, T_N, vanishes continuously as a function of a control parameter like external or internal pressure. Exemplary systems are the pressure-induced superconductors $CePd_2Si_2$ and $CeIn_3$ [2] as well as $CeCu_2Si_2$, the first HF metal for which superconductivity at ambient pressure was observed in 1979 [3] (sect. 2). The low-temperature normal (n)-state properties of these latter materials are displaying pronounced non-Fermi-liquid (NFL) phenomena commonly related to critical fluctuations associated with a quantum phase transition between the antiferromagnetically ordered and a disordered (spin-liquid) state [4]. When applying a sufficiently strong magnetic field, NFL properties usually give way to those of a heavy Landau Fermi liquid (LFL). To study NFL phenomena in more detail, it is highly desirable to search for an AF-QCP in low magnetic fields, i.e., *in the absence* of HF superconductivity. This appears to be realized in both $CeCu_{5.9}Au_{0.1}$ [5] and $YbRh_2(Si, Ge)_2$ [6] (sec. 3).

Superconductivity

The discovery of superconductivity in the tetragonal compound $CeCu_2Si_2$ containing, at $T > T_K \approx 15$ K, a dense lattice of local magnetic Ce^{3+} moments came as a big surprise, given the antagonistic nature of superconductivity and magnetism. On the other hand, it was found that HF superconductivity is phenomenologically related to the superfluidity of ^3He and cannot be explained by the conventional electron-phonon pairing mechanism [3]. In fact, evidence for a magnetic, rather than phononic, Cooper pairing was provided ten years later by inelastic neutron scattering (INS) experiments on UPt_3 where AF order with an extremely small moment ($0.02\mu_B$/U) forms below $T_N \approx 5$ K [7].

For the hexagonal compound UPd_2Al_3 which enters an antiferromagnetically ordered state with a large saturation moment $\mu_s = 0.85\mu_B$/U at $T_N = 14.3$K, HF superconductivity forms and homogeneously coexists with magnetic order below $T_c = 2$K. UPd_2Al_3 may be called a "magnetic HF superconductor", in which magnetism derives from *localized* 5*f* states while Cooper pairs are formed by more hybridized (*delocalized*) 5*f* states, i.e., heavy (composite) fermion quasiparticles. Based upon quasiparticle tunneling [8] and INS [9] work, the acoustic magnon at the center of the Brillouin zone with an excitation energy $\omega_E \approx 1$ meV could be identified [9] as the "exchange boson" forming Cooper pairs in this strong-coupling HF superconductor. This magnon, which, because of the induced singlet-ground-state type of AF order is called "magnetic exciton", may be viewed as a local crystal-field excitation propagating through the U-lattice via inter-site interactions. It thus replaces the optical phonons in classical strong-coupling superconductors like Pb. Thus, UPd_2Al_3 is the first and so far only superconductor for which a non-phononic pairing mechanism could be demonstrated by the same experimental means as the phononic counterpart in Pb.

> The discovery of superconductivity in the tetragonal compound... came as a big surprise

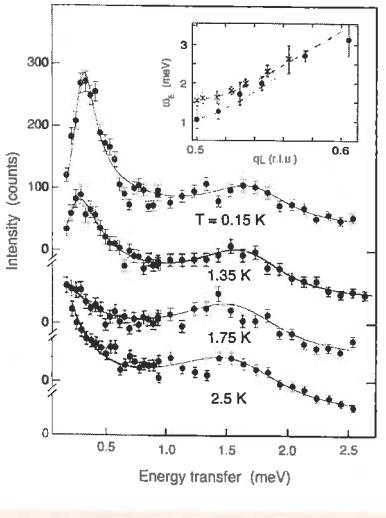

▲ **Fig. 1:** T-evolution of the INS spectra for a UPd_2Al_3 single crystal at the AF ordering wave vector $\vec{Q}_0 = (0,0,q_L=0.5)$ through $T_c = 1.8$ K. Solid lines represent fits using the microscopic "two-component" model described in Ref. 9. This procedure may be repeated for other wave vectors $\vec{q}$ close to $\vec{Q}_0$. There is only one fit parameter at given values of T and $\vec{q}$: The magnetic exciton energy $\omega_E(\vec{q})$ shown in the inset for T = 2.5 K (crosses) and 0.15 K (circles). The low-energy peak, inelastic at $T < T_c$ and quasielastic at $T > T_c$, is related to the itinerant HF quasiparticles, the broad hump at higher energies to the magnetic exciton.

features

The generic phase diagram of $CeCu_2Si_2$ presented in Fig. 2a contains, at small 4*f*-conduction electron coupling constant g, a low-moment spin-density-wave (SDW) or "A"-phase [10] which coexists in a homogeneous way with weak HF superconductivity below $T_c < T_A$, the magnetic ordering temperature. At moderate coupling, the A-phase is fully replaced by strong HF superconductivity, but can be recovered if superconductivity is suppressed by applying an overcritical magnetic field. Beyond a critical coupling constant g_c, at which T_A vanishes continuously characterizing the QCP of this material, pronounced NFL effects were found in the low-temperature n-state properties of "S-type" single crystals [11].

Fig. 2b displays the unusual pressure dependence of the superconducting critical temperature of $CeCu_2Si_2$, highlighting a maximum value of 2.3 K at $p \approx 2.5$ GPa. By deliberately shortening the quasiparticle mean free path through moderate Ge-substitution for Si, Yuan *et al.* could clearly separate two different SC regimes [12]. The low-pressure dome (corresponding to the low-pressure plateau in Fig. 2b) is centered around the AF-QCP, where virtual (high-frequency) fluctuations of the staggered magnetization of the A-phase might be the source to forming massive Cooper pairs [13]. On the other hand, the high-pressure dome (around the maximum T_c in Fig. 2b) appears to coincide with a weak first-order $Ce^{3+} \rightarrow Ce^{3+\delta}$ valence transition [12], giving rise to speculations about charge-fluctuation mediated superconductivity.

Quantum Criticality

Most of the unconventional properties of the low-T n-state not only of $CeCu_2Si_2$ [11], but also of, e.g., $CeNi_2Ge_2$ [14] and UBe_{13} [15] can be explained by low-frequency, spatially extended spin-fluctuations which exist in a nearly AF Fermi liquid forming in the vicinity of a 3D-SDW QCP [4]. On the other hand, thorough INS experiments on the quantum critical material $CeCu_{6-x}Au_x$ ($x = 0.1$) have highlighted [5] the importance of *local* (rather than *extended*) quantum critical fluctuations which are addressed by

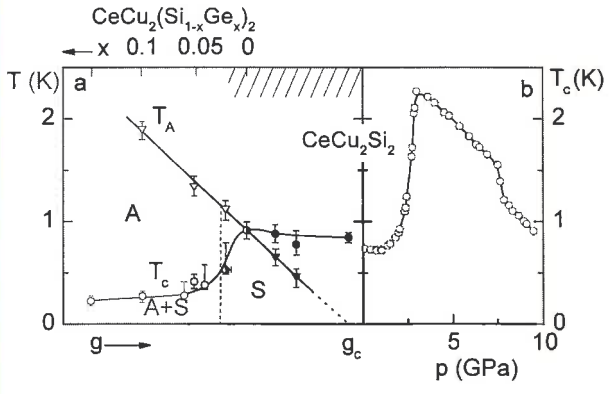

▲ **Fig. 2:** a. Generic phase diagram of $CeCu_2Si_2$ combining data obtained with undoped polycrystals from the homogeneity range of the ternary chemical phase diagram (hatched) and from Ge-doped ones, $CeCu_2(Si_{1-x}Ge_x)_2$. Since the temperature T_A of the SDW transition increases linearly with the Ge-concentration x, the 4f-conduction electron coupling constant g was assumed to be linear in (1-x), i.e., $(1-T_A)$. b. Pressure dependence of T_c up to p = 8.5 GPa for $CeCu_2Si_2$, see Ref. 12. The different T_c values at p = 0 in a and b relate to two polycrystalline samples with slightly different stoichiometry (Cu content).

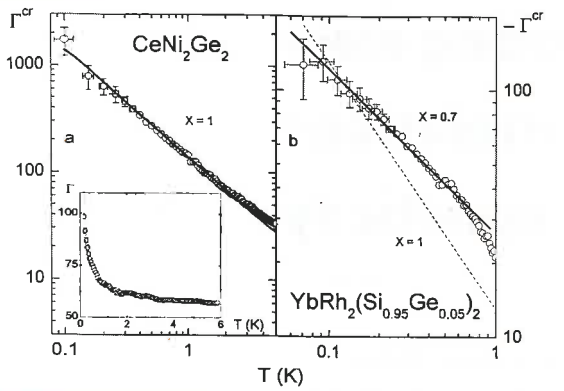

▲ **Fig. 3:** Critical Grüneisen ratio $\Gamma^{cr} = (V_m/\kappa_T)(\beta^{cr}/C^{cr})$, as $(-)\Gamma^{cr}$ vs T in double-logarithmic plots for $CeNi_2Ge_2$ (a) and $YbRh_2(Si_{0.95}Ge_{0.05})_2$ (b) [V_m: molar volume; κ_T: isothermal compressibility; $\beta^{cr} = \beta(T)$-bT and $C^{cr} = C(T) - (\gamma T + \delta/T^2)$ are the critical components to the volume thermal expansion and specific heat, respectively, cf. Ref. 18]. Inset shows $\Gamma(T) \sim \beta(T)/C(T)$ as measured (on linear scales) for $CeNi_2Ge_2$.

new theories of a *local-moment* QCP [16]. Recently, Zhu *et al.* [17] proposed that measurements of the Grüneisen ratio $\Gamma \sim \beta/C$ (where β and C are the volume thermal expansion and specific heat, respectively) may well be suited to distinguish between different QCP scenarios. As these authors argue, $\Gamma(T)$ must diverge at any QCP [17]. This has indeed been observed [18] for both paramagnetic $CeNi_2Ge_2$ (inset of Fig. 3a) and the isostructural weakly antiferromagnetically ordered compound $YbRh_2Si_2$ ($T_N = 70$ mK). In the main part of Fig. 3a the critical Grüneisen ratio, $\Gamma^{cr}(T)$, as given by the singular parts of both $\beta(T)$ and C(T), is shown to diverge $\sim T^{-x}$ with $x = 1$ for $CeNi_2Ge_2$. This agrees well with the prediction for the 3D-SDW scenario [17]. By contrast, recent investigations of $YbRh_2Si_2$ revealed $\Gamma^{cr}(T) \sim T^{-x}$ with $x = 0.7$ [18] as expected in the presence of *local* AF quantum critical fluctuations (Fig. 3b).

A QCP at zero can, in principle, be approached by moderate volume expansion of $YbRh_2Si_2$. In fact, in the case of a slightly doped $YbRh_2(Si_{1-x}Ge_x)_2$ single crystal with a nominal Ge-concentration $x = 0.05$, the Néel temperature was found to be as low as $T_N = 20$ mK [19]. By tuning the system away from its QCP, i.e., through applying a magnetic field ($\perp c$) larger than $B_c \approx 0.027$ T necessary to suppress the weak AF order in this Ge-doped crystal, the field dependences of both the electronic specific heat, $C_{el}(T,B) = \gamma_0(B)T$, and the electrical resistivity, $\Delta\rho(T,B) = A(B)T^2$, could be attributed to the field-induced low-T LFL state. From the divergences of both the Sommerfeld coefficient $\gamma_0(B)$ and the resistivity coefficient A(B) as $B \rightarrow B_c^+$, as well as from those of $C_{el}(T)/T$ and $A(T) = \Delta\rho(T)/T^2$ as $T \rightarrow 0$ at $B = B_c$ it was concluded [19] that field (temperature) acts as the only relevant energy scale at low temperature (field). Two striking observations made with such $YbRh_2(Si, Ge)_2$ single crystals are worth mentioning:
(i) Correlated, but unscreened large paramagnetic Yb^{3+} moments are observed in the static bulk susceptibility (inset of Fig. 4a) as well as in the low-temperature electron-spin resonance [20].
(ii) The temperature dependences of $\gamma_0(T) = C_{el}(T)/T$ and $\Delta\rho(T)$ taken at $B \lesssim B_c(0)$ behave *disparately*: $\gamma_0(T) \sim (-\log T)$ and $\Delta\rho \sim T$ are observed upon cooling from $T \approx 10$ K down to $T \approx 0.3$ K. While the linear T-dependence of the resistivity can be followed all the way down to 10 mK, the lowest temperature of the experi-

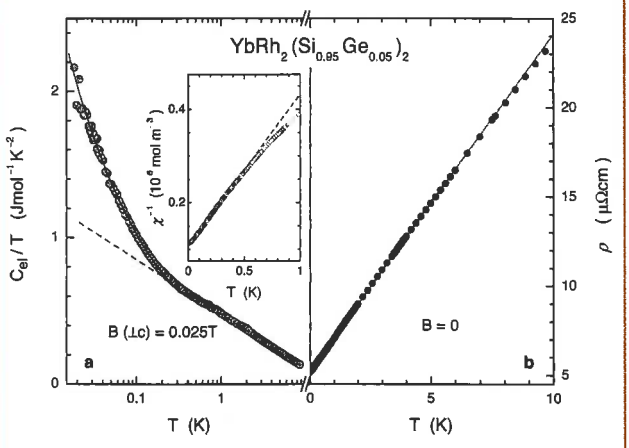

▲ Fig. 4: Electronic specific heat divided by T as a function of T (on a logarithmic scale) measured at a field (⊥c) of 0.025 T, close to $B_c(0) = 0.027$ T (a) and electrical resistivity ρ vs T (on a linear scale) measured at B = 0 (b) for a $YbRh_2(Si_{0.95}Ge_{0.05})_2$ single crystal. Dashed [solid] line in a represents $C_{el}/T \sim (-\log T)$ [$\sim T^{-(0.4\pm0.03)}$], solid line in b represents $\rho - \rho_0 = aT$ with $\rho_0 \approx 5$ μΩcm. Inset displays the zero-field ac-susceptibility as χ^{-1} vs T for the same crystal. In the same T-range ($T < 0.3$ K) where C_{el} (T)/T deviates from –logT, χ(T) follows a Curie-Weiss law, $\chi^{-1} \sim (T - \Theta)$ with $\Theta \approx -0.3$ K. From the slope a large paramagnetic moment, $\mu_{eff} \approx 1.4\ \mu_B/Yb^{3+}$, is derived.

ment (Fig. 4b), γ(T) at $T \leq 0.3$ K is found to diverge stronger than logarithmically, i.e., $\sim T^{-\varepsilon}$, $\varepsilon = 0.4 \pm 0.03$ (Fig. 4a). This disparity hints at a break-up of the composite fermions on the approach to the QCP.

Epilogue

Strong electronic correlations on partially filled localized 4*f* or 5*f* shells, weakly hybridized with the itinerant ligand states, cause the formation of extremely heavy quasiparticles composed of a local spin part and delocalized charge-carrier contributions. They may form Cooper pairs, the SC glue presumably being of magnetic origin, at least in most cases. This could be convincingly demonstrated with the aid of tunneling and neutron scattering experiments on UPd_2Al_3.

In case of a number of Ce-based HF metals, superconductivity was found to be intimately related to the existence of an AF instability, most likely of the 3D-SDW type [4]. On the other hand, the QCP in slightly Ge-doped $YbRh_2Si_2$ appears to be of the *local-moment* variety [16], although already in undoped $YbRh_2Si_2$ the ordered moments below $T_N = 70$ mK are extremely small, in contrast to the large paramagnetic moments, cf. inset of Fig. 4a. Interestingly enough, superconductivity could not be observed in this material. To find out whether a *local-moment* QCP is indeed unfavorable for HF superconductivity has to be left for future work.

Acknowledgments

Fruitful discussions with P. Coleman, J. Custers, P. Gegenwart, C. Geibel, F.M. Grosche, R. Küchler, K. Miyake, C. Pépin, N.K. Sato, G. Sparn, Q. Si, O. Stockert, P. Thalmeier, S. Wirth, H.Q. Yuan and G. Zwicknagl as well as partial support by the Fonds der Chemischen Industrie (FCI) are gratefully acknowledged.

References

[1] see, e.g., N. Grewe, F. Steglich in: Handbook on the Physics and Chemistry of Rare Earths, Vol. 14, edited by K.A. Gschneidner, Jr. and L. Eyring (North Holland, Amsterdam 1991), p. 343.

[2] N.D. Mathur, F.M. Grosche, S.R. Julian, I.R. Walker, D.M. Freye, R.K. Haselwimmer, G.G. Lonzarich, Nature **394**, 39 (1998).

[3] F. Steglich, J. Aarts, C.D. Bredl, W. Lieke, D. Meschede, W. Franz, H. Schäfer, Phys. Rev. Lett. **43**, 1892 (1979).

[4] see, e.g., S. Sachdev, Science **288**, 475 (2000).

[5] A. Schröder, G. Aeppli, R. Coldea, M. Adams, O. Stockert, H. von Löhneysen, E. Bucher, R. Ramazashvili, P. Coleman, Nature **407**, 351 (2000).

[6] O. Trovarelli, C. Geibel, S. Mederle, C. Langhammer, F.M. Grosche, P. Gegenwart, M. Lang, G. Sparn, F. Steglich, Phys. Rev. Lett. **85**, 626 (2000).

[7] G. Aeppli, D. Bishop, C. Broholm, E. Bucher, K. Siemensmeyer, M. Steiner, N. Stüsser, Phys. Rev. Lett. **63**, 676 (1989).

[8] M. Jourdan, M. Huth, H. Adrian, Nature **398**, 47 (1999).

[9] N.K. Sato, N. Aso, K. Miyake, S. Shiina, P. Thalmeier, G. Varelogiannis, C. Geibel, F. Steglich, P. Fulde, T. Komatsubara, Nature **410**, 340 (2001).

[10] T. Tayama, M. Lang, T. Lühmann, F. Steglich and W. Assmus, Phys. Rev. B **67**, 214504 (2003).
O. Stockert, E. Faulhaber, G. Zwicknagl, N. Stüßer, H. Jeevan, R. Borth, R. Küchler, M. Loewenhaupt, C. Geibel, F. Steglich (to be published).

[11] P. Gegenwart, C. Langhammer, C. Geibel, R. Helfrich, G. Sparn, F. Steglich, R. Horn, L. Donnevert, A. Link, W. Assmus, Phys. Rev. Lett. **81**, 1501 (1998).

[12] H. Yuan, F.M. Grosche, M. Deppe, C. Geibel, G. Sparn, F. Steglich (to be published).

[13] In an alternative scenario a mean-field model for a SDW ground state is assumed to compete with d-wave superconductivity. Using a two-dimensional tight-binding band structure, one can then qualitatively explain the phase diagram of Fig. 2a: Here, a SDW order parameter and a SC order parameter with d_{xy}-symmetry can coexist on different parts of the Fermi surface, cf. F. Steglich *et al.* in: More is Different – Fifty years of condensed matter physics, edited by N.P. Ong and R.N. Bhatt (Princeton University Press, 2001) p. 191.

[14] P. Gegenwart, F. Kromer, M. Lang, G. Sparn, C. Geibel, F. Steglich, Phys. Rev. Lett. **82**, 1293 (1999).

[15] F. Steglich, P. Gegenwart, R. Helfrich, C. Langhammer, P. Hellmann, L. Donnevert, C. Geibel, M. Lang, G. Sparn, W. Assmus, G.R. Stewart, A. Ochiai, Z. Phys. B **103**, 235 (1997).

[16] Q. Si, S. Rabello, K. Ingersent, J. L. Smith, Nature **413**, 804 (2001). P. Coleman, C. Pépin, Physica B **312**, 383 (2002).

[17] L. Zhu, M. Garst, A. Rosch, Q. Si, Phys. Rev. Lett. **91**, 066404 (2003).

[18] R. Küchler, N. Oeschler, P. Gegenwart, T. Cichorek, K. Neumaier, O. Tegus, C. Geibel, J.A. Mydosh, F. Steglich, L. Zhu, Q. Si, Phys. Rev. Lett. **91**, 066405 (2003).

[19] J. Custers, P. Gegenwart, H. Wilhelm, K. Neumaier, Y. Tokiwa, O. Trovarelli, C. Geibel, F. Steglich, C. Pépin, P. Coleman, Nature **424**, 524 (2003).

[20] J. Sichelschmidt, V.A. Ivanshin, J. Ferstl, C. Geibel, F. Steglich, Phys. Rev. Lett. **91**, 156401 (2003).

Magnetoelectrochemistry

J.M.D. Coey,
Physics Department, Trinity College, Dublin, Ireland

At first sight, magnetism and electrochemistry seem an odd couple. The energies involved in chemical reactions are of order 1 electron volt (eV), a fact affirmed by countless plots of electrochemical data where the abscissae are on a scale of volts relative to the potential of a reference electrode. Yet magnetic energies in laboratory fields are orders of magnitude smaller; the Zeeman splitting of the spin up ↑ and spin down ↓ states of an electron in a field of 1 tesla (T), for example, is 1.2 10^{-4} eV. Where then is the connection between electrochemistry and magnetism?

There are at least two answers. The first is that electrodeposition is a remarkably versatile (and inexpensive) method of preparing metallic films and nanostructures, including those made of ferromagnetic metals and alloys (Figure 1). A monolayer of atoms can be deposited from a bath containing a solution of metallic cations onto a centimeter-square working electrode in an electrochemical cell from a bath containing a solution of metallic cations by passing a current of 1 milliamp for about a second (Figure 2). It can be removed just as easily by reversing the polarity of the electrodes and runniing the current in the opposite direction. Electrodeposition of permalloy ($Fe_{19}Ni_{81}$) from a bath containing Fe^{2+} and Ni^{2+} ions is an established industrial process. The problem of obtaining smooth, uniform films is solved by a combination of clever electrode design, flow control and judicious use of the chemical additives that make electrochemistry seem as much an arcane art as an exact science. Permalloy films a few microns in thickness were for long used as cores of the thin-film electromagnets that form the write heads for high-density magnetic recording [1]. These have recently been superseded by thinner films of soft nanocrystalline Fe-Co-Ni or Fe-Co alloys which have a polarization in excess of 2 T [2], twice as large as permalloy. Weak uniaxial anisotropy needed to control the magnetization reversal process is induced by depositing the alloys in a magnetic field.

Besides alloys, it is also possible to deposit binary multilayers from a single bath by exploiting the fact that the deposition rates for different metals depend both on the concentrations of the ions in solution, and on the potential used for deposition.

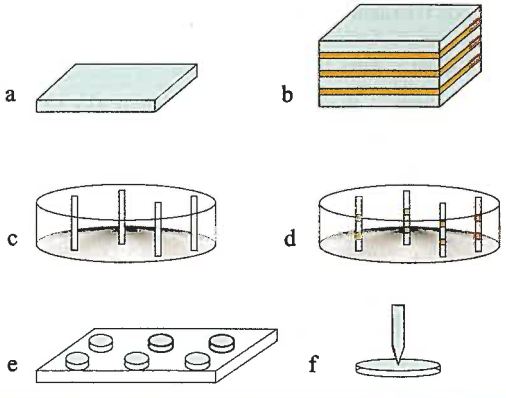

▲ **Fig. 1:** Some magnetic nanostructures produced by electrodeposition a) metal or alloy thin film, b) multilayer, c) nanowires d) multilayer nanowires, e) dot array f) nanocontact.

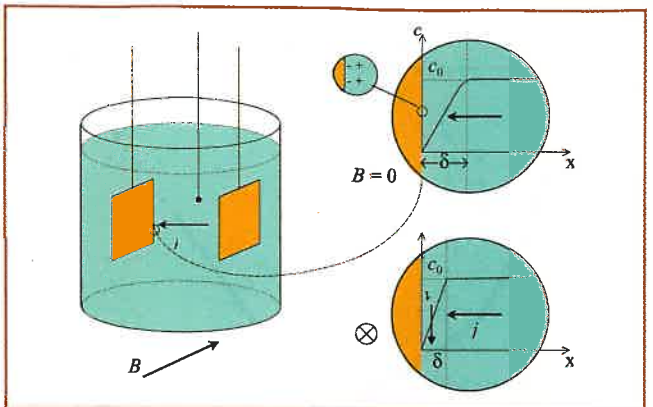

▲ **Fig. 2:** A simple electrochemical cell with working electrode, reference electrode and counter electrode. The enlargements show the concentration gradient of ionic species in the electrolyte near the cathode. An applied magnetic field sets up a convective flow parallel to the electrode surface, which has the effect of narrowing the diffusion layer δ.

Copper/cobalt multilayers for spin valves, for example [3] can be plated from a bath containing a 10^{-3} molar solution of $CuSO_4$ and a 0.1 molar solution of $CoSO_4$ by toggling the cathode potential between −0.3 V (relative to the hydrogen reference electrode) where pure Cu is deposited and −1.0 V where Co with a trace of Cu is deposited. Layer thickness is controlled by varying the time for each step. Magnetic nanowires, which may be made of a single metal like nickel, or a multilayer like Co/Cu are obtained by plating into fine pores in membranes [4]. Nanocontacts (some of which exhibit huge magnetoresistance [5]) can be produced by electrochemical growth across a gap between a fine wire and a substrate, or onto a lithographically-defined metal pattern. Patterns themselves can be written by using a scanning point anode, a method known as dip-pen nanolithography.

The second answer is that application of a magnetic field during electrodeposition can influence the process in unexpected ways. Consider the high-school experiment of copper plating from a $CuSO_4$ bath. According to whether its potential is less than or greater than 0.34 V relative to a standard hydrogen reference electrode, copper is either plated onto or dissolved off the copper working electrode. This information is summarized in the current-voltage characteristic of the cell, the voltamogram shown in Figure 3 [6]. Remarkably, the plating or dissolution rates can be doubled by applying a field of about 1 T,. They increase as $B^{1/3}$. In seeking an explanation of this behaviour, it is instructive to consider the magnetic forces that act on the Cu^{2+} cations in an applied field B. One is the Lorentz force $F_L = j \times B$ newtons per cubic meter (N m^{-3}) acting on the ion currents that constitute the local current density j amps per square meter (A m^{-2}). Other forces are derived from the magnetic energy

$$E = -(1/2)M \cdot B,$$

where $M = \chi_m cB/\mu_0$ is the induced magnetization of the ions with molar concentration c and molar susceptibility χ_m. Since $F = -\nabla E$, there are two force terms:

$$F = (1/2\mu_0)\,\chi_m B^2 \nabla c + (1/\mu_0)\,\chi_m cB \nabla B$$

The first of these F_c depends on the concentration gradient ∇c, the second F_B depends on the field gradient ∇B. Finally, whenever

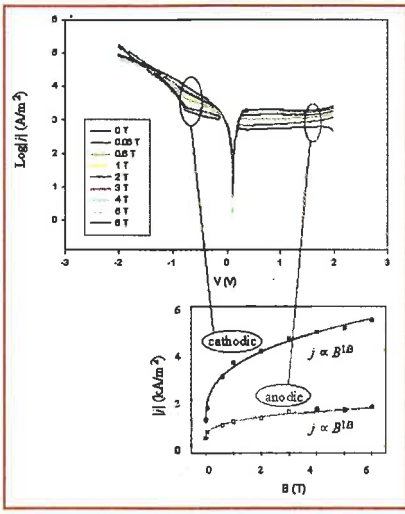

◀ **Fig. 3:** Voltamograms (polarization curve) for copper, showing the effect of applied magnetic field on the cathodic and anodic branches. The magnitude of the current density |j| is plotted on a log scale against the potential of the working electrode.

there is convective movement in the cell, there is also a damping term $F_d = \sigma v \times B \times B$ which depends on σ, the conductivity of the electrolyte, and its velocity v.

With some care, field gradients may be eliminated over the volume of an electrochemical cell, but the concentration gradients cannot be removed. Indeed they are essential to drive the diffusion of ions towards the cathode, which is the current-limiting process at most potentials used in the plating process (Figure 3). The electric field in the cell is largely screened by the supporting electrolyte, and most of the potential drop in the cell occurs at the charged double layer which is established within a few nanometers of the cathode surface, where the reduction of the metal cations occurs. A concentration gradient is established in a diffusion layer near the electrode, as indicated in Figure 2. If this layer has thickness δ, the diffusion equation $\partial c/\partial t = -D\nabla c$ gives a limiting current

$$j_l \approx nFDc_0/\delta$$

where F = 96,485 coulombs is the molar charge and c_0 is the ionic concentration in the bulk of the solution. Typically, the diffusion coefficient $D \approx 10^{-9}\,m^2s^{-1}$ for ions in solution, so the diffusion layer thickness for typical current densities in the diffusion-limited region is ≈ 100 μm. Close to the rest potential, where little current flows in the cell, the currents are limited by the kinetics of the $Cu^{2+} \leftrightarrow Cu^{+} \leftrightarrow Cu^{0}$ reduction reaction. There is no field effect here. The influence of the field appears to be restricted to the diffusion-limited regions. It is now appreciated that the $B^{1/3}$ variation arises from the Lorentz force, which creates a convective flow parallel to the surface whenever the field is not parallel to the current [8]. This in turn reduces the thickness δ of the diffusion layer, and enhances the current j, as originally proposed by Aogaki. Convincing evidence of the hydrodynamic nature of the effect is that a similar enhancement can be achieved by gentle stirring, and the field effect is progressively eliminated by increasing the viscosity of the electrolyte [6].

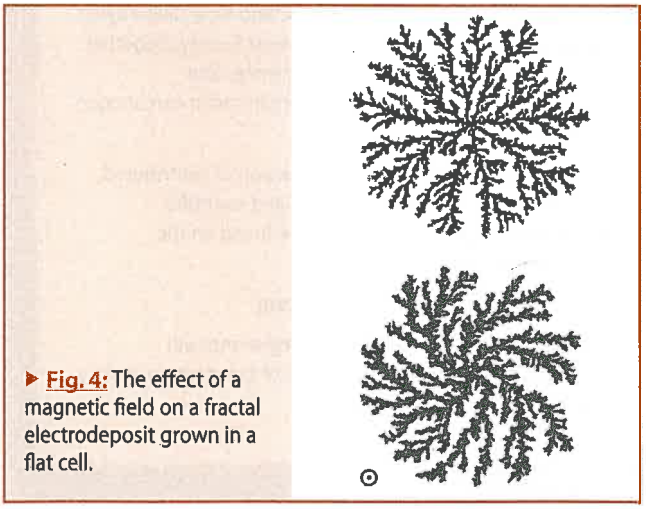

▶ **Fig. 4:** The effect of a magnetic field on a fractal electrodeposit grown in a flat cell.

▼ **Table 1:** Magnetic forces acting in a typical electrochemical cell [8].

Force		Expression	Typical magnitude (N m^{-3})
Lorentz force	F_L	$j \times B$	10^3
Field gradient force	F_B	$(1/\mu_0)\,\chi_m c B \nabla B$	10^2
Paramagnetic force	F_c	$(1/2\mu_0)\,\chi_m B^2 \nabla c$	$4\,10^4$
Damping force	F_c	$\sigma v \times B \times B$	10

[Typical values; $j = 10^3$ A m^{-2}, $B = 1$ T, $\chi_m = 10^{-8}$ m^3 mol^{-1}, $c_0 = 10^3$ mol m^{-3} (1 M), $\nabla B = 10$ T m^{-1}, $\sigma = 100$ S m^{-1}, $v = 0.1$ m s^{-1}, $\delta = 100$ μm]

A glance at Table 1 shows that the Lorentz force is *not* the largest magnetic force in the copper cell. The Cu^{2+} ions have a paramagnetic $3d^9$ configuration, and there is a force associated with the concentration gradient in the diffusion layer. The paramagnetic gradient force F_c is forty times greater in magnitude than the Lorentz force, yet it is ineffectual in influencing diffusion! The reason for this apparent paradox is that diffusion is driven by the entropic force $RT\nabla c$ which is enormously greater than F_c ($\approx 2\,10^{10}$ N m^{-3}), and in the same direction. The Lorentz force is effective precisely because it acts in the direction *perpendicular* to the concentration gradient where it can induce convection. It should be noted that modest field gradients of order 100 T m^{-1}, like those produced by a small permanent magnet, can produce similar effects to the Lorentz force on the flow pattern in the cell. The gravitational force $\Delta\rho g$ that drives natural convection is $\approx 10^2 - 10^3$ N m^{-3}.

The field gradient and Lorentz forces can be deliberately enhanced by using electrodes with microscale or even nanoscale features. The current density is augmented around these features, and particular patterns of vortex flow are induced by a magnetic field [9]. When the electrode itself is ferromagnetic, field gradients of up to 10^5 T m^{-1} or more can be created by patterning or surface roughness. These gradients are similar to those used in high-gradient magnetic separation [10]. They will attract paramagnetic species such as Cu^{2+} or O_2, and repel diamagnetic species such as Zn^{2+} or CO_2; the altered concentrations can influence reaction rates via the thickness of the double layer. It has recently been shown that the oxygen reduction reaction $4H^+ + 4e + O_2 \rightarrow 2H_2O$ which is a limitation in solid polymer electrolyte fuel cells can be significantly increased by magnetic field gradients produced by including hard magnetic particles in the cathode catalyst layer to concentrate oxygen in the vicinity [11].

Other effects of a magnetic field have been seen on the morphology of the ramified fractal electrodeposits grown in flat electrochemical cells with a central cathode and a ring anode [12]. A magnetic field induces chirality when applied perpendicular to the cell, and axial asymmetry when applied in-plane, effects which can again be explained by the field-induced flow patterns in the

cell [13]. At present it seems that all the various effects of magnetic fields in electrochemistry are somehow related to mass transport.

Magnetoelectrochemistry offers opportunities to investigate unexplained phenomena, such as the field-induced shift in rest potential associated with ferromagnetic electrodes [14], or the enhanced dissolution rate of certain crystals [15]. New magnetic nanostructures can be produced using electrochemical scanning probe methods and a new level of control may be exerted over industrial catalytic and electroplating processes by appropriately designed field patterns. Challenges include the deposition of films of hard magnetic rare-earth alloys. The odd couple has given birth to an exciting new area of magnetism, which is sure to turn up surprises, insights and new practical knowledge. Just as in other cross-disciplinary fields, there are rewards for those willing to play with a child.

References

[1] R. L. Comstock, *Introduction to Magnetism and Magnetic Recording*, Wiley – Interscience, New York 1999

[2] T. Osaka, M. Takai, K. Hayashi, K. Ohashi, M. Saito and K. Yamada, Nature **392** (1998) 796

[3] K. Attenborough, H. Boeve, J. de Boeck, G. Borghs and J. P. Celis, Appl. Phys Letters **74** (1998) 2206

[4] A, Fert and L. Piraux, J. Magn.Magn. Mater, **200** (1999) 338

[5] N. Garcia, H. Rohrer, I. G. Saveliev and Y-W Zhao, Phys. Rev. Letters, **85** (2000) 3053

[6] G. Hinds, F. E. Spada, J. M. D. Coey, T. R. Ni Mhiochain and M. E. G. Lyons J. Phys. Chem. B **105** (2001) 9487

[7] G. Hinds, J. M. D. Coey and M. E. G. Lyons, Electrochem. Commun. **3** (2001) 215

[8] R. Aogaki, K. Fueki and T. Mukaibo, Denki Kagaku, **43** (1975) 509; see also O. Aaboubi, J-P Chopart, J.Dougdale, A. Olivier, C. Gabrielli and B. Tribollet, J. Electrochem. Soc. **137** (1990) 1796

[9] K. M. Grant, J. W. Hemmert and H.S. White, J. Amer. Chem. Soc. **124** (2002) 462

[10] R. Gerber in *Applied Magnetism*, Kluwer, Dordrecht (1994) p. 165

[11] T. Okada, N. I. Wakayama, L-B Wang, H Shingu, J Ojano and T Ozawa, Electrochemica Acta, **48** (2003) 531

[12] I. Mogi and M. Kamiko, J. Cryst. Growth, **166** (1966) 276

[13] T. R. Ni Mhiochain and J. M. D. Coey, Magnetohydrodynamics, **37** (2001) 169

[14] M. Waskaas and Y. I. Kharkats, J. Electroanal. Chemistry, **52** (2001) 51

[15] K. Shinohara and R. Aogaki, Electrochemistry **67** (1999) 267

IBA–Europhysics Prize 2004

The Nuclear Physics Board of the EPS invites nominations for the year 2004 for the IBA-Europhysics prize. The award will be made to one or several individuals for outstanding contributions to Applied Nuclear Science and specially Nuclear Methods and Nuclear Researches in Medicine.

The Board would welcome proposals which represent the breath and strength of Applied Nuclear Science and Nuclear Methods in Medicine in Europe.

Nominations should be accompanied by a filled nomination form, a brief curriculum vitae of the nominee(s) and a list of major publications. Letters of support from authorities in the field which outline the importance of the work would also be helpful.

Nominations will be treated in confidence and although they will be acknowledged there will be no further communication. Nominations should be sent to:

Selection Committee IBA Prize:
Chairman Prof. Ch. Leclercq-Willain,
Department of Theoretical Nuclear Physics – PNTPM – CP 229
Université Libre de Bruxelles
Bvd du Triomphe, B1050 Bruxelles , Belgium
Phone: +32 (0)26505560; Fax: +32 (0)26505045
E-mail: cwillain@ulb.ac.be

For a nomination form and more detailed information see the web site of the Nuclear Physics Division: www.kvi.nl/~eps_np and the web site of the EPS: www.eps.org (EPS Prizes, IBA-Europhysics Prize)

The deadline for the submission of the proposals is 10.01.2004.

ECAMP VIII

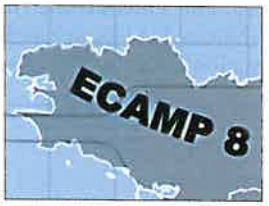

The Eighth European Conference on Atomic and Molecular Physics (ECAMP VIII) will be held 6–10 July 2004 at the University of Rennes. Conference topics will include all aspects of atomic and molecular spectroscopy, interactions and collisions between ions, atoms, molecules, electrons, positrons and photons and other related areas of atomic and molecular physics.

The scientific programme of ECAMP VIII will consist of sessions of invited plenary lectures, review lectures, progress reports, "hot topic" talks, and poster contributions.

Other meetings, such as EGAS36 (European Group for Atomic Spectroscopy) and PAMO2004 (Atomic and Molecular Physics and Optics Division of the French Physical Society), together with symposia on Astrophysics, Life Sciences and Environmental Sciences will also be organized in conjunction with ECAMP VIII.

Details concerning registration, submission of contributed papers, travel, accommodation, social and scientific programmes and other matters can be found on the conference web page:

www.ecamp8.org

Pre-registration is now open and all registrants will automatically be sent updated details of the meeting as they develop.

europhysics news recruitment
Contact **Susan Mackie** • EDP Sciences • 250, rue Saint Jacques • F-75005 Paris • France
Phone +33 (0)1 55 42 80 51 • fax +33 (0)1 46 33 21 06 • e-mail mackie@edpsciences.org

The Hahn-Meitner-Institut Berlin (HMI)
Member of the Hermann von Helmholtz-Gemeinschaft Deutscher Forschungszentren e.V.
and the
Humboldt-Universität zu Berlin (HU)
seek applications for a joint appointment in the field

"Photovoltaics"

as

Head of Department "Silicon Photovoltaics"

within the Division of Solar Energy Research at the HMI
and

Full Professor (Bes.Gr.C4)

at the Faculty of Mathematics and Natural Sciences I – Department of Physics
at the Humboldt-Universität zu Berlin.

The Hahn-Meitner-Institut (HMI) is a scientific research center with approximately 800 employees located in Berlin-Wannsee and Berlin-Adlershof. Structural and solar energy research constitute the main focus of research activities. Solar energy research at the HMI concentrates on thin film photovoltaics, with an emphasis on targeted basic and material research leading to the development of solar cells and modules.

Presently, research at the Department of Silicon Photovoltaics is aimed at the development of the scientific and technological foundations of crystalline silicon thin film solar cells on foreign substrates. These aims are to be achieved using low temperature technologies with special consideration of the fundamental problems of material science.

With the new appointment our goal is to secure the continuation of the work on silicon thin film technologies, as well as to extend and renew the scientific spectrum. We would specifically welcome an expansion of research topics in the area of new materials and solar cell concepts that could eventually lead to alternatives to the traditional thin film technologies.

We are seeking internationally known candidates holding a PhD in physics with outstanding scientific and technological reputation and experience in the field of solid state physics, in particular in semiconductor physics and photovoltaics. The successful candidate is expected to strengthen the curriculum of the Humboldt-Universität zu Berlin in the fields of condensed matter (semiconductor physics, semiconductor devices, spectroscopy). He or she should also enhance the curriculum with classes on renewable energies, especially photovoltaics.

Important for the success of the new Head of Department is the ability to lead a large department and the readiness to fulfill interdepartmental managerial duties.

The HMI and the HU strive to increase the number of female scientists in their institutions. Therefore, women are especially encouraged to apply. Handicapped applicants will be given preference over others of equal qualification. The legal requirements according to § 100 BerlHG must be satisfied.

Application deadline: 6 weeks after publication

Address applications to Prof. Dr. Michael Steiner, Scientific Director HMI, Glienicker Straße 100, D-14109 Berlin. Prof. Dr. Steiner can be reached for further information by telephone at (+49 (0) 30 8062 2762) or e-mail (steiner@hmi.de).

UNIVERSITÉ DE GENÈVE

The Faculty of Sciences, University of Geneva, Switzerland, has an opening for a position as

Full Professor or Associate Professor
in experimental condensed matter physics
(Professeur ordinaire ou Professeur adjoint)

Responsibilities: Full time appointment comprising at least 6 hours of teaching per week and research activities in the area of condensed matter physics. The successful candidate is expected to conduct a vigorous research in experimental condensed matter physics. The Department is particularly interested in developing local probe studies, as well as novel spectroscopies, applied to metals and strongly interacting electron systems in general. Candidates active in these fields are especially encouraged to apply.

Degree of requirements: Ph.D. or equivalent

Starting date: October 1st 2004 or as agreed

Applications, including curriculum vitae, a list of publications and a short research plan are to be sent before March 15th, 2004 to the

Dean of the Faculty of Sciences
30, quai Ernest-Ansermet, CH-1211 Genève 4, Switzerland

where further information concerning the job description and working conditions may be obtained.

In an effort to involve both men and women in teaching and research, the University encourages applications from women.

UNIVERSITÉ DE GENÈVE

The **Department of Condensed Matter Physics** (DPMC) of the University of Geneva, Switzerland, invites applications for a

POST-DOC POSITION

Institution: University of Geneva. Work place: University of Geneva. Job title: Post-Doc position, crystal growth and characterisation. Description: The project concerns the growth of single crystals of superconducting materials and other perovskites by using various techniques (Travelling Solvent Floating zone, self-flux, crystal pulling...). The project will address to the study of the growth conditions of crystals of such novel materials, as well as the structure characterisation and their electrical and magnetic properties. Profile: The applicant should have a background in material science and in solid state chemistry, possibly in single crystal growth. A background in crystallography is an asset. Moreover, good English and/or French skills are necessary. The position is available immediately, and will remain open until it has been filled. Job start: Immediately. Keywords: Crystal growth, superconductivity. Contacts: Candidates are invited to send a CV with references, list of publications and contact address to: Prof. René Flükiger DPMC - Université de Genève 24 Quai Ernest-Ansermet CH-1211 Genève 4 Switzerland.
Email: rene.flukiger@physics.unige.ch
Links: http://dpmc.unige.ch/gr_flukiger/index.html
http://dpmc.unige.ch/

EC-Human Potential Programme (HPP)
Transnational Access to Major Research Infrastructures
EU Contract No HPRI-CT-2001-00122

CALL FOR PROPOSALS

for the time period March 2004 to February 2005.

Researchers in the European Union and associated states are offered access to the research facilities at the Institute for Storage Ring Facilities (ISA) through the Human Potential Programme of the European Commission. Access is offered to **the synchrotron-radiation beamlines and associated experimental equipment at ASTRID (2-1000 eV)**

For a detailed description of the facilities, please visit our web site.

Project proposals are evaluated on the basis of scientific merit by an independent panel.

Approved projects will receive access and support free of charge. Travel expenses and subsistence for eligible users will be reimbursed.

Application forms can be obtained from ISA at the address below, or from our web site. Forms must reach ISA no later than December 19, 2003.

As of March 31, 2004 support will be subject to a contractual agreement with the European Commission.

For further information, please contact:

ISA, Aarhus University,
DK-8000 Aarhus C, Denmark.
Tel.: +45 8942 3778 Fax: +45 8612 0740
Email: fyssp@phys.au.dk
Web site: http://www.isa.au.dk

EU-Contract Manager: Søren Pape Møller

Astronomy & Astrophysics

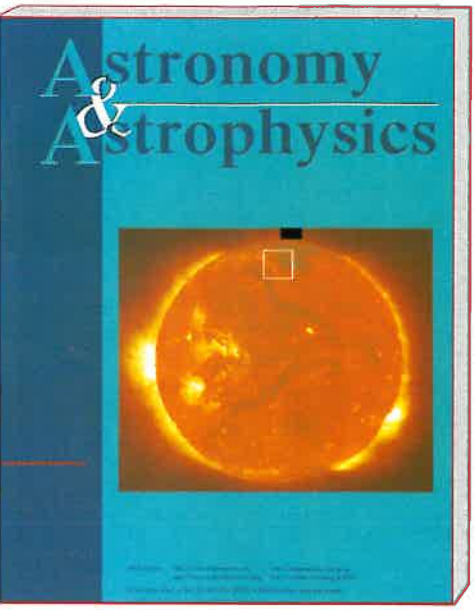

SUBSCRIPTION INFORMATION

ISSN (print edition): 0004-6361.
ISSN (electronic edition): 1432-0746.
2003: Volumes 397-412 (3 issues each).

For Institutions:

• France + EU: (VAT included)	3 205 €
• Rest of the world: (without VAT)	3 205 €

For individuals:

• France + EU: (VAT included)	497 €
• Rest of the world: (without VAT)	497 €

Those prices include access to the electronic version on EDP sciences site

http://www.edpsciences.org

Recognized by the European Physical Society

BOARD OF DIRECTORS:

Chairman: **Aa. Sandqvist** (Sweden)
Vice Chairman: **A. G. Hearn** (The Netherlands)

EDITORIAL BOARD:

- **C. Bertout** (Editor-in-chief) & **A. Jones** (Deputy Editor) - e-mail: aanda@obspm.fr
- **H. J. Habing** (Editor-in-chief) & **J. K. Katgert-Merkelijn** (Deputy Editor) - e-mail: aanda@strw.leidenuniv.nl
- **P. Schneider** (Letter Editor) - e-mail: aal@aanda.astro.uni-bonn.de

ASTRONOMY & ASTROPHYSICS, a European Journal, publishes papers on all aspects of astronomy and astrophysics: theoretical, observational and instrumental, independently of the techniques used to obtain the results.

The sections are :

1. Letters
2. Cosmology
3. Extragalactic astronomy
4. Galactic structure and dynamics
5. Stellar clusters and associations
6. Formation, structure and evolution of stars
7. Stellar atmospheres
8. Formation and evolution of planetary systems
9. Diffuse matter in space
10. The Sun
11. The solar system
12. Celestial mechanics and astrometry
13. Physical and chemical processes
14. Atomic and molecular data
15. Instruments, observational techniques and data processing
16. Computational methods

ASTRONOMY & ASTROPHYSICS is divided as follows:

- New important results which deserve faster publication should be submitted as **LETTERS**, provided they are not more than four printed pages.
- **REGULAR PAPERS** which, though making large use of references, should be self-explanatory, in particular with an introduction sketching its place in its field and its purpose.
- **RESEARCH NOTES** which are short papers that contain either new results as an extension of work reported in a previous paper, or limited observations not urgent enough to be published as a Letter, or useful calculations that have no definite immediate astrophysical applications.

INDEXED / ABSTRACTED IN:

Astronomy and Astrophysics Abstracts, ADS, CAS, CDS, Current Contents, INIST, Inspec, Physics Abstracts, Science Citation Index, and Zentralblatt MATH.

SUBSCRIBE THROUGH YOUR AGENCY or directly to EDP Sciences:
17 av. du Hoggar • B.P. 112 • 91944 Les Ulis Cedex A • France
Tel. 33 (0)1 69 18 75 75 • Fax 33 (0)1 69 86 06 78 • subscribers@edpsciences.org

EDP SCIENCES

Journals Physics & Engineering

http://www.edpsciences.org

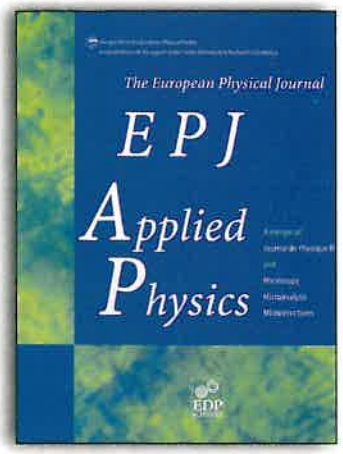

ISSN 1286-0042 • 12 issues

ISSN 1434-6028 • 24 issues

ISSN 1434-6060 • 12 issues

ISSN 1292-8941 • 12 issues

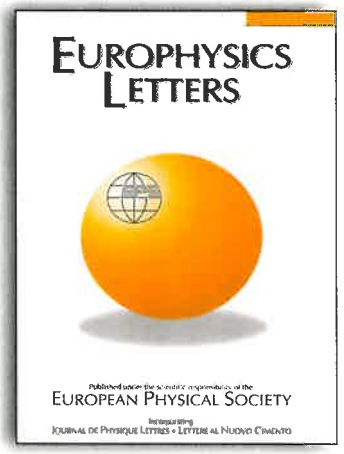

ISSN 0295-5075 • 24 issues

ISSN 0531-7479 • 6 issues

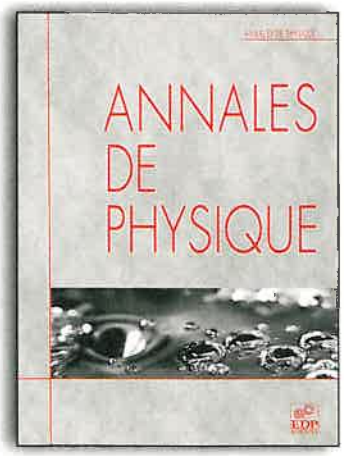

ISSN 0003-4169 • 6 issues

ISSN 1265-6534 • 11 issues

ISSN 1155-4339 • 10 to 12 issues

To order please contact your subscription agent or **EDP Sciences**

17, av. du Hoggar • P.A. de Courtabœuf • F-91944 Les Ulis Cedex A • France

Tel. 33 (0)1 69 18 75 75 • Fax 33 (0)1 69 86 06 78 • **subscribers@edpsciences.org**